CHEMOENZYMATIC APPROACHES TO MONOTERPENOIDS

by

Fathima Zulfa Yoosuf Aly

A thesis submitted to
Cardiff University
for the degree of
DOCTOR OF PHILOSOPHY

School of Chemistry
Cardiff University
October 2014

Abstract

Terpenoids are the largest and structurally most diverse family of natural product. α-pinene, a monoterpene found in turpentine, is a precursor to several high-value mono-oxygenated terpenoids such as verbenone. It is produced naturally through the Mg^{2+}-dependent transformation of geranyl diphosphate (GDP) catalysed by (+)-α-pinene synthase (APS).

Heterologous expression, purification and characterization of recombinant (+)-α-pinene synthase were performed. Several expression conditions and many purification methods were tried in order to get optimum results. After optimisation of His tagged α-pinene synthase (HAPS), chemoenzymatic synthesis of a simple two-step, one pot asymmetric synthesis from GDP of (+)-verbenone, an oxidation product of the monoterpene (+)-α-pinene, that is used to control attacks of pine trees by bark beetles is described. This method generates (+)-verbenone from GDP in good yield and without the need to isolate the intermediate (+)-α-pinene.

Then, synthesis of some chemically modified GDP analogues to obtain (+)-α-pinene analogues was performed. These engineered (+)-α-pinene analogues may display enhanced biological activities due to the potential improvement of their physical properties.

Finally, site directed mutagenesis strategy was employed to HAPS to examine the potential catalytic role of several aromatic amino acids, in stabilizing the carbocationic intermediates generated in the active site of HAPS during the natural conversion of GDP to the monoterpene (+)-α-pinene.

Acknowledgement

I would like to thank my supervisor Prof. Rudolf Allemann for giving me the opportunity of join his group and work on this research project, supporting me all the way along and for getting the best out of me. Thanks to Dr. Mahmoud Akhtar for all his invaluable help. Furthermore I would like to thank Prof. Gerald Richter and Dr. James Redman for their suggestions and support during *viva* and reading reports.

I would like to express my deep appreciation and sincere gratitude to Dr. Juan Faraldos and Dr. David Miller for their assistance, scientific guidance and proof reading this work and giving stimulating suggestions. Extended thanks to Dr. Veronica Gonzalez for assisting me in the bio lab through my first year. I am sincerely grateful to Dr. Sabrina Touchet for all her help with many aspects of this thesis and have always been my first port of call.

Thanks to Dr. Joel Loveridge and Dr. Robert Mart for sharing their views and giving advice related to the project. Special thanks go to Dr. Enas Behiry and Dilruba Meah for their moral support and spending so much quality time. I would like to thank all the members of the Allemann group. Thank you Dr. Amang Li, Dr. Louis Luk, Dr. Sarah Adams, Dr. Naeema Owaid, Dr. Seni Chanapai, Dr. Willaim Dawson, Oscar Cascon, Melodi Demiray and Daniel Grundy.

Special thanks to the technical staff in the school of chemistry, especially Dr. Rob Jenkins, Dave Walker and Robin Hicks for the help on GC-MS service and also specially Moira Northam for all her help.

I would like to thank my parents for all their unconditional support and encouragement. Special thanks goes to my grandparents, my sister and my aunts for being there for me. Finally, I would like to thank my husband for his support, sacrifices and great patience at all times. It would not been possible to write my thesis without his help. Thanks for our fabulous children Aakif and Arham.

Table of Contents

CHAPTER 1 **1**

Introduction **1**

1.1 General Introduction 2
1.2 The biological and ecological functions of terpenes 4
1.3 Biosynthesis of terpenes 10

1.3.1 Mevalonic acid (MVA) pathway 11
1.3.2 Non-mevalonate pathway 12

1.4 Terpene synthases 15

1.4.1 Crystal structures of terpene synthases 17

1.5 Monoterpene synthases: Reaction mechanisms 22

1.5.1 Ionisation and isomerisation of GDP 24
1.5.2 (+)-α-Pinene synthase 26

1.6 Aim of the project 29

CHAPTER 2 **30**

Heterologous expression, purification and characterization of recombinant (+)-α-pinene synthase **30**

2.1 Introduction 31
2.2 Transformation and purification of the cDNA of α-pinene synthase (APS) 32
2.3 Heterologous (large) expression of APS in *E. coli* 33

2.4 Isolation of Recombinant APS 35
2.5 Enzyme Purification 36

2.5.1 Ion exchange chromatography 36
2.5.2 Ammonium sulphate precipitation 40
2.5.3 Hydrophobic interaction chromatography (HIC) 41
2.5.4 Size exclusion chromatography 42
2.5.5 Affinity Column Chromatography 45

2.6 Product profile of purified (+)-HAPS. 48

2.6.1 Chiral GC analysis of (+)-α-pinene 52

2.7 Optimisation of (+)-APS catalysed production of α-pinene 52

2.7.1 Optimum Mg^{2+} concentration 53
2.7.2 Optimum pH 53
2.7.3 Optimum temperature 54

2.8 Kinetic studies 55

2.8.1 Time optimisation 55
2.8.2 Enzyme concentration optimisation 56
2.8.3 Magnesium concentration optimisation 56
2.8.4 Temperature optimisation 57
2.8.5 Determination of Kinetics parameters for HAPS 58

CHAPTER 3 59

Chemoenzymatic synthesis of the alarm pheromone (+)-verbenone from geranyl diphosphate (GDP) 59

3.1 Introduction 60

3.2 Existing methods for the conversion of α-pinene to verbenone 62
3.3 (+)-α-Pinene synthase (HAPS) 65

3.3.1 Calibration of α-pinene concentration 66
3.3.2 Analytical incubation of HAPS with GDP (4) 67

3.4 Synthesis of verbenone from (±)-α-pinene 67
3.5 Development of a protocol towards production of verbenone (13) from enzymatically produced α-pinene (12) 68
3.6 Preparative Scale synthesis of (+)-verbenone from GDP 70
3.7 Chiral GC analysis of (+)-verbenone 72
3.8 Conclusion 73

CHAPTER 4 74

Site-directed mutagenesis study of four aromatic residues potentially involved during catalysis by HAPS 74

4.1 Introduction 75
4.2 Homology model of HAPS 76
4.3 Selection of potential carbocation stabilising amino residues 77
4.4 Conclusion 82

CHAPTER 5 83

Synthesis and incubations of some chemically modified GDP analogues 83

5.1 Introduction 84
5.2 Preparation of pyrophosphate salts 84

5.2.1 Synthesis of neryl diphosphate (NDP) 86

5.3 Synthesis of 8-methyl GDP 86

5.3.1 Allylic oxidation of geranyl acetate (84) with selenium dioxide and tert-butyl hydroperoxide 88
5.3.2 Wittig olefination of 85 to form 87 89
5.3.3 Hydrogenation of 96 using Wilkinson's catalyst to give 97 90
5.3.4 Pyrophosphorylation of alcohol 98 to the 8-methyl GDP (100) 91

5.4 Synthesis of (*E*)-7-vinyl GDP (103) 91
5.5 Synthesis of 10-methyl GDP (114) 92
5.6 Synthesis of (*Z*)-7-vinyl GDP (117) 94
5.7 Incubation of GDP analogues with HAPS 94

5.7.1 Incubation results for 8-methyl GDP 95
5.7.2 Incubation results for (*E*)-7-vinyl GDP (103) 97
5.7.3 Incubation results for 10-methyl GDP (114) 99
5.7.4 Incubation results for (*Z*)-7-vinyl GDP (117) 100

5.8 Conclusions 102

CHAPTER 6 **104**

General conclusions and future works **104**

CHAPTER 7 **107**

Materials and methods **107**

7.1 Materials 108

7.1.1 Primers for inserting TEV cleavage site to his-tagged protein 109
7.1.2 Primers for site-directed mutagenesis 109

7.2 Growth media 111

7.2.1 LB and YT media 111
7.2.2 LB agar plates 111

7.3 *E. coli* strains 111

7.3.1 Cloning strains 111
7.3.2 Expression strains 111

7.4 Preparation of Buffers 112

7.4.1 Lysis buffer 112
7.4.2 Dialysis Buffer 112
7.5.1 Insertion of a TEV cleavage site into the hexahistidine-tag protein using PCR 112
7.5.2 Ligation 113
7.5.3 Site-directed mutagenesis using PCR 113

7.6 Agarose gel electrophoresis 114

7.6.1 50 x TAE buffer 114
7.6.2 Ethidium bromide 114

7.7 DNA purification using QIA MiniPrep Kit Protocol 114
7.8 The composition of the buffers was as follows (DNA mini prep buffers): 115
7.9 SDS-Polyacrylamide gel electrophoresis 116

7.9.1 SDS stacking buffer 116
7.9.2 SDS resolving buffer 116
7.9.3 10% (w/v) sodium dodecyl sulfate (SDS) 116
7.9.4 10% (w/v) Ammonium persulfate 117

7.9.5 SDS electrode running buffer (10x) 117
7.9.6 SDS staining solution 117
7.9.7 SDS destaining solution 117
7.9.8 SDS-PAGE protocol 117

7.10 Preparation of Competent Cells 118
7.11 Preparation of Super-Competent Cells 119
7.12 Protein production and purification 120

7.12.1 Transformation into *E. coli* BL21 codon plus (DE3) – RIL competent cells 120
7.12.2 Large-scale expression 120
7.12.3 Base Extraction 120
7.12.4 Ion exchange chromatography 121
7.12.5 Ammonium sulphate precipitation. 122
7.12.6 Hydrophobic interaction chromatography (HIC) 122
7.12.7 Size exclusion chromatography (SEC) 123
7.12.8 Ni2+ affinity chromatography 123

7.13 Concentration of the dialysed protein using Amicon ultrafiltration 123
7.14 Determination of protein concentration 124

7.14.1 Dye Reagent 124
7.14.2 Protein Determination 124

7.15 Enzyme characterization 124

7.15.1 Assay of enzyme activity 124

7.16 GC-MS 125

Reference **142**

CHAPTER 1

Introduction

1.1 General Introduction

Terpenoids constitute the largest family of natural products and to date, the structure and stereochemistry of more than 55,000 different members have been characterized.[1] They represent the most diverse family of natural products; yet they all formally derived from isopentenyl diphosphate (IDP, **1**).[2] In nature, terpenes are biosynthesized by a class of C-C bond forming enzymes called terpene synthases (or cyclases). Most of them are considered to be high fidelity catalysts since they often generate a unique hydrocarbon product with remarkable structural and stereochemical precision. Remarkably however, the sesquiterpene synthases γ-humulene and δ-selinene synthases give rise to more than 30 and 50 sesquiterpenes (C15) respectively.[3]

Isopentenyl diphosphate (IDP, **1**) and dimethylallyl diphosphate (DMADP, **2**) are considered as the universal precursors of isoprenoids in all living organisms (Scheme 1.1).[4] The substrates of terpene synthases, namely geranyl diphosphate (C10, GDP, **4**), farnesyl diphosphate (C15, FDP, **5**) and geranylgeranyl diphosphate (C20, GGDP, **6**) are formed by linear head to tail chain elongation reactions involving the C5 diphosphates **1** and **2**.[5] In contrast, squalene (C30, **7**), and phytoene (C40, **8**) derived from the alternative head-to-head condensation of two molecules of **5** or **6** respectively.[6-8]

The chain elongation reaction mechanism comprises DMADP (**2**) ionization, with formation of an allylic carbocation that further reacts with the double bond of IDP (**1**). This electrophilic addition reaction yields a tertiary carbocation which is quenched by stereospecific proton elimination to geranyldiphosphate (**4**).[9]

A second chain elongation reaction with an additional molecule of IDP (**1**) and geranyl diphosphate (**4**) thus yields farnesyl diphosphate (**5**) (Scheme 1.2).[10] This reaction can be further extended to produce geranylgeranyl diphosphate (**6**) by the addition of one molecule of IDP (**1**) and the loss of diphosphate ion. These elongation products are, the universal precursors of all mono-, sesqui-, and diterpenes.[11] The geometry of the double bonds in all these linear precursors is trans- (e.g respectively GDP, FDP, GGDP). Other

chain elongation terpene synthases could generate *Z*- isomers in longest chain prenyl diphosphates (*e.g*. natural rubber).[12]

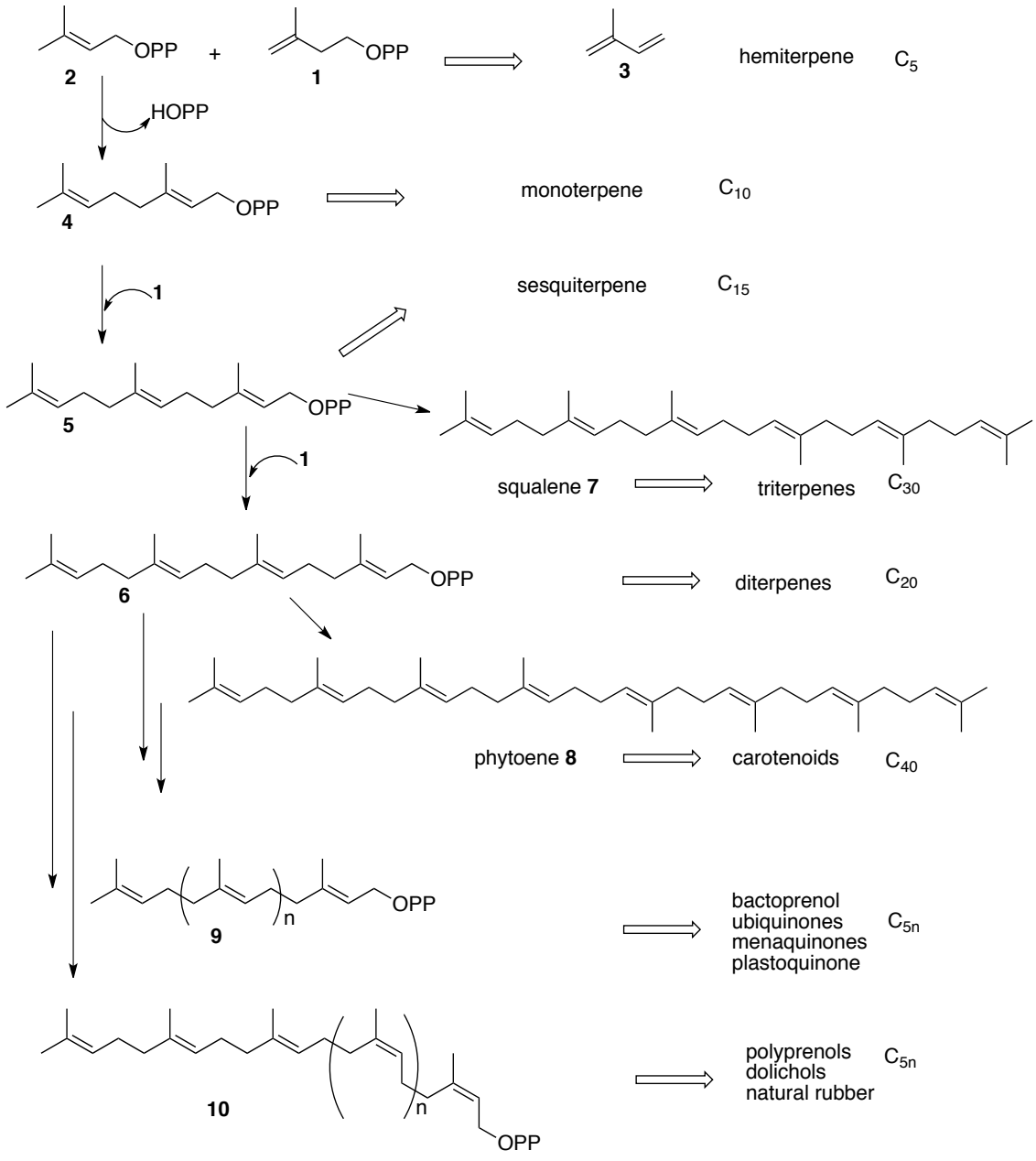

Scheme 1.1: Biogenetic scheme for the formation of the main isoprenoid diphosphates GDP (**4**), FDP (**5**) and GGDP (**6**) series

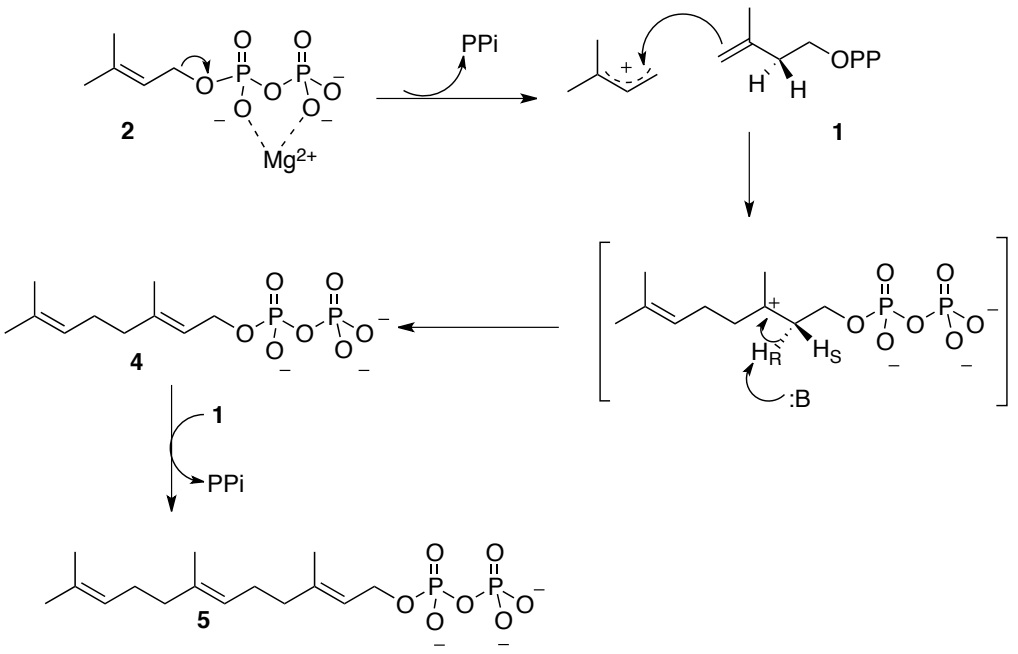

Scheme 1.2: Biosynthesis of geranyl (**4**) and farnesyl (**5**) diphosphates via head to tail chain elongation reaction by IDP (**1**) and DMADP (**2**).

1.2 The biological and ecological functions of terpenes

Terpenoids comprise a vast number of bioactive compounds that play different roles in nature. Primary metabolites are compounds required for reproduction or growth, while those that are not essential for the basic performance of growth and development are defined, as secondary metabolites.[13] In plants, terpenoids act as hormones (gibberellins), photosynthetic pigments (carotenoids), electron carriers (ubiquinone) and structural components of membranes (phytosterols).[14] In addition to these universal functions, many terpenes serve in communication and defense. For example, bark beetle infestation with the associated fungal infections in plants pose a major threat to conifer populations worldwide.[15] Terpenoids are also very useful and available in large number as essential oils, resins, and waxes, providing for commercially useful products such as solvents, flavourings, fragrances, coatings and synthetic intermediates.[16] For artificial purposes some terpenoids are employable as raw materials for pharmaceuticals (*e.g.* artemisinin, taxol) or agrochemicals (pyrethrins, azadirachtin).[14,17-18]

Monoterpenoids are non-nutritive dietary components, usually found in plants and insects as essential oils. However they have a high economic value as flavours and fragrances.[19] Limonene (**11**) is extracted from orange peel oil, and has been shown to prevent several kinds of cancer in rodents.[20] In natural and alternative medicine, (-)-limonene is marketed to relieve gastroesophageal reflux and disease heartburn.[21] Apart from being used as a solvent, limonene is now targeted as a biofuel.[22] (+)-α-Pinene (**12**) has been found to act as a sex pheromone in some insects, attracting female bark beetles.[15] Recent publications have also revealed that verbenone (**13**), an oxidation product of verbenol, plays an important role as dispersal pheromone, and protects high-value pine trees from the destructive mountain pine beetle.[15] Verbenone (**13**) is a bicyclic monoterpenoid ketone, useful as a chiral synthon in syntheses of natural terpenoids, including the total synthesis of the anti-cancer agent taxol.[23] Furthermore, this bioactive enone has been reported as an inhibitor of acetylcholine esterase and hence has potential for the treatment of early stage Alzheimer's disease.[24] In addition, verbenone is utilized in perfumery, aromatherapy, and herbal remedies.[25] Other bioactive monoterpenoids include camphor (**14**), thymol (**15**) and cymene (**16)** (Figure 1.1) which are used as antimicrobial agents.[26]

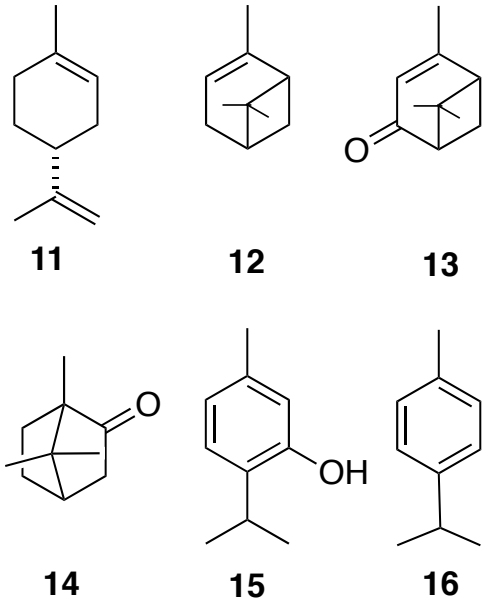

Figure 1.1: Structures of cyclic monoterpenes limonene (**11**), α-pinene (**12**), cymene (**16**) and terpenoids verbenone (**13**), camphor (**14**), thymol (**15**).

Sesquiterpenoids have been used for many years in traditional medicines as therapeutic agents.[27] A good example is the tetracyclic artemisinin (**17**), a sesquiterpenoid endoperoxide lactone obtained from *Artemisia annua*. This natural product has been used in China as an antimalarial and antipyretic drug.[28] Modifications to the parent artemisinin structure, other than the peroxide lactone moiety, retain or even improve the pharmacological properties of artemisinin. The characteristic peroxide moiety is nevertheless essential for anti-malarial activity.[29] For example dihydroartemisinin (**18**) is more potent than the parent compound.[30] Pentalenolactone (**19**) is another sesquiterpenoid formally derived from the hydrocarbon pentalenene and which possesses antibiotic properties (Figure 1.2).[31]

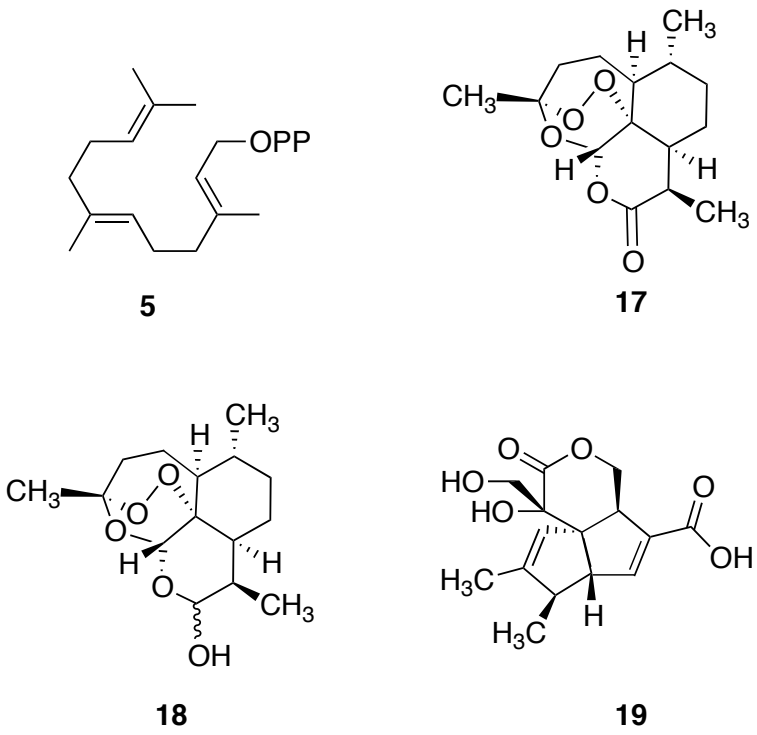

Figure 1.2: Structures of farnesyl diphosphate (**5**), artemisinin (**17**), dihydroartemisinin (**18**) and pentalenolactone (**19**).

Other members of the sesquiterpene family of natural products have been reported to have fungicidal activity against many species of phytopathogenic fungi.[32] For example, d-cadenine (**20**) and 5-*epi*-aristolochene (**21**) are the precursors of the defensive phytoalexins in gossypol (**22**) and capsidiol (**23**) biosynthesis (Figure 1.3), which act against fungal infection in cotton and tobacco plants respectively.[33] Gossypol is a

noncompetitive inhibitior of calcineurin, a calcium dependent serine/threonine phosphatase involved in immune response and neural and muscle development.[34] The dimer **22** has also been investigated as a potential male contraceptive.[35]

As with the other groups of terpenoids, diterpenoids possess 4 units of isoprene, and have quite a few different uses both in nature and in medicine. Paclitaxel (**24**), also known by its original brand name Taxol, is a compound extracted from the Pacific yew (*Taxus brevifolia*) with remarkable antitumour and antileukemic activity. Diterpenoid (**24**) has a unique mechanism of action, because it induces very stable but dysfunctional microtubules thereby hindering the rapid cell division characteristic of malignant cell lines. Paclitaxel has varying antineoplastic activities; it has been successfully used in the treatment of ovarian cancer, metastatic breast cancer, lung cancer, carcinoma of the head and neck, malignant melanoma and other human neoplasms.[36-37]

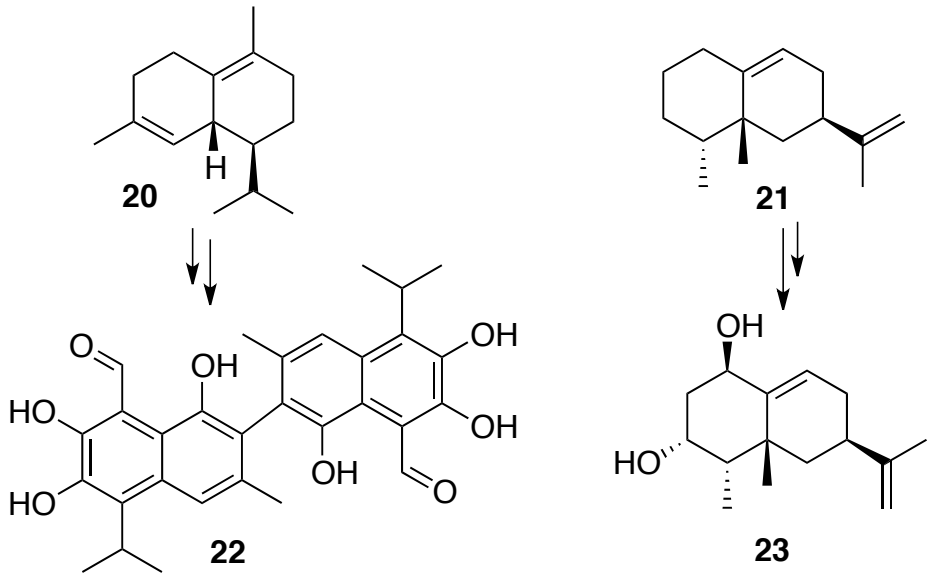

Figure 1.3: Structures of δ-cadinene **(20)**, 5-*epi*-aristolochene (**21**) precursors of gossypol (**22**) and capsidiol (**23**).

The phytoalexin casbene (**25**), a macrocyclic hydrocarbon, produced in high levels when bean plants are under microbial attack, has both antibacterial and antifungal properties (Figure 1.4).[38]

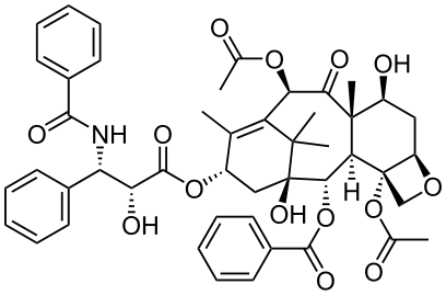

24

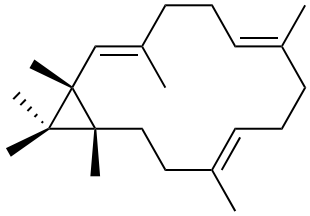

25

Figure 1.4: Structures of paclitaxel (**24**) and casbene (**25**)

Sterols and carotenoids are growth regulators often classified as primary metabolites.[39] Sterols are widely spread among organisms and all of them derived from the C30 linear terpene squalene (**7**), itself derived from two molecules of FDP (**5**) (Scheme 1.1). The squalene analogue, squalene oxide (**26**), undergoes enzyme-catalysed cyclisation to afford lanosterol (**27**).[40-41] The major sterol in animals is cholesterol (**28**), with ergosterol (**29**) dominating in fungi, plant sterols include stigmasterol (**30**) and sitosterol (**31**) (Scheme 1.3). In animals, cholesterol is the source of steroidal metabolites such as sexual hormones, bile acids, and vitamin D. Importantly steroids are implicated in maintaining the membrane fluitidy and permeability.[41] Recent research indicates an important role for cholesterol (**28**) in several diseases such as the development of cardiac and vascular diseases, dementias, diabetes and cancer.[42-43]

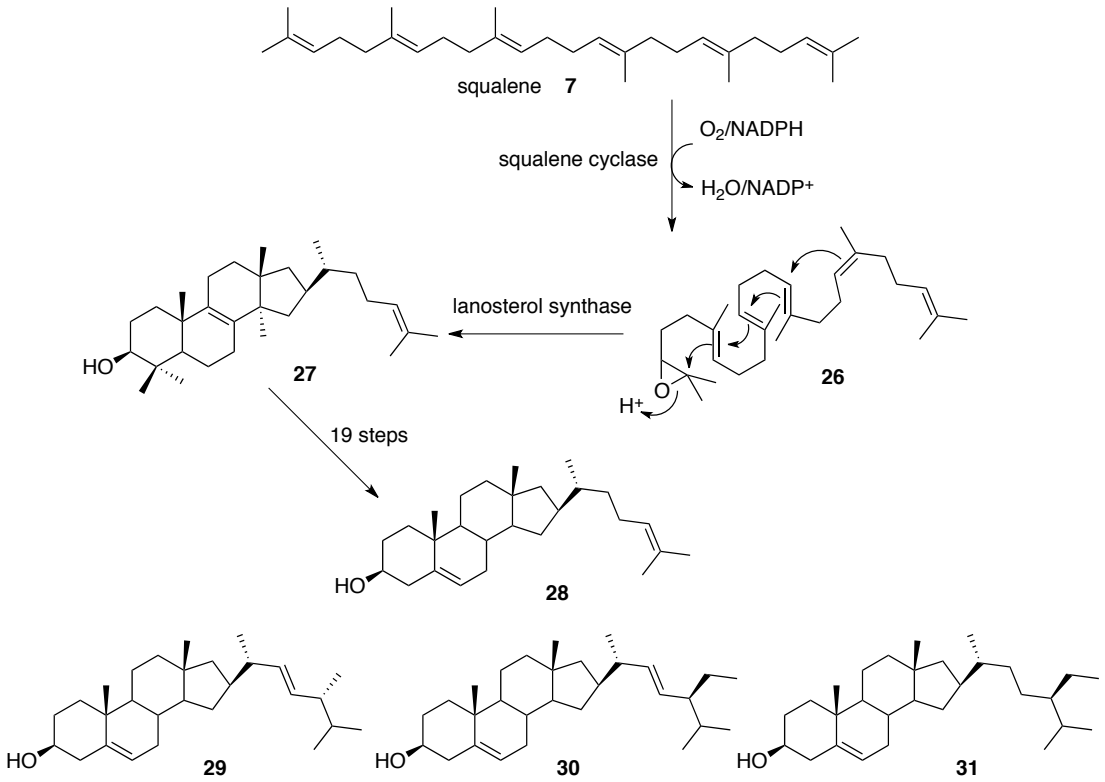

Scheme 1.3: Generation of animal, fungal and plant sterols lanosterol (**27**)**,** cholesterol (**28**), ergosterol (**29**), stigmasterol (**30**) and sitosterol (**31**)

More than 600 different carotenoids have been isolated and characterized from natural sources. Carotenoids are biosynthesized from two GGDP (**6**) units. Phytoene (**8**), the C40 terpene precursor, is the parent molecule of carotenoids.[44] This group of molecules is central for the absorption of light in photosynthetic organisms due to their highly conjugated structures.[45] Phytoene (**8**) can also be converted to vitamin A (**32**, retinol), which has important functions in the vision process and resistance to infectious disease in mammals (Figure 1.5).[46-48]

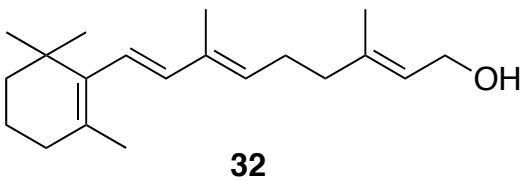

32

Figure 1.5: Structure of vitamin A (**32**)

Quinones are another type of terpenoid natural product essential in biochemical reactions as electron transfer mediators. Oxidative phosphorylation and photosynthesis are a pair of examples.[49-50] The structure contains a polyisoprene chain, the length of which is species-specific.[51] Quinones can undergo facile and reversible electron transfer reactions (Figure 1.6).[52]

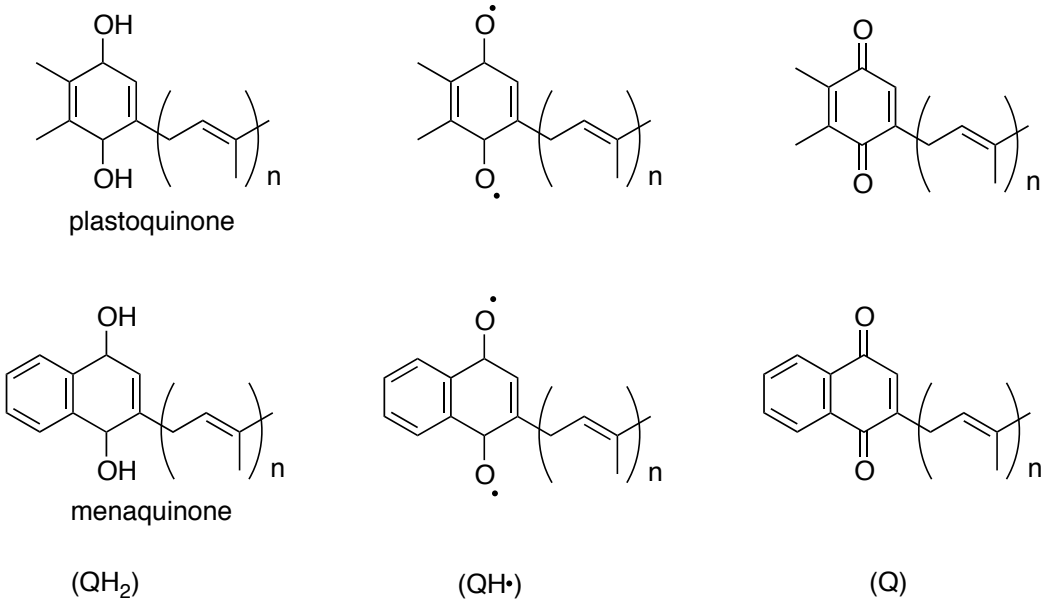

Figure 1.6: Structures of quinones in different redox states.

1.3 Biosynthesis of terpenes

The initial postulate of the "isoprene rule" put forward by Wallach stated that most terpenoids could be hypothetically constructed by a repetitive joining of isoprene (2-methyl-1,3-butadiene, **3**) units and possess the formula C_5H_8 or $(C_5H_8)_x$.[30] The "biogenetic isoprene rule" was later proposed by Leopold Ruzicka, which did not address the precise character of biological precursors and assumes only that they are "isoprenoid" in structure.[55] The carbon skeleton of terpenes is composed of isoprene units linked either in a regular head to tail fashion or in an irregular sequence.[55] Isoprene units joined in irregular sequence are encountered less frequently, and only a few closely related organisms synthesise these compounds. For example, a number of

natural monoterpene structures contain carbon skeletons, which, although obviously derived from isoprene C5 units, do not seem to fit the regular head-to-tail coupling mechanism (Figure 1.7). These structures are named irregular monoterpenes.[56]

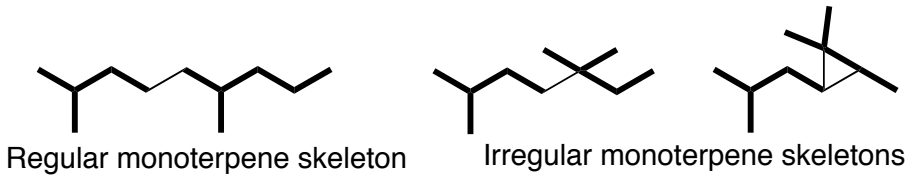

Figure 1.7: Examples of regular and irregular monoterpene skeletons

The isoprene unit can be identified in most terpenoid structures, as a vitally important component but **3** itself is not the biological precursor of terpenoids. Rather, two biosynthetic equivalents of isoprene, isopentenyl diphosphate (IDP) (**1**) and dimethylallyl diphosphate (DMADP) (**2**), are indeed the building blocks of isoprenoids.[57] There are two known pathways used to produce the IDP (**1**) and DMADP (**2**) in nature, the mevalonic acid (MVA) and non-mevalonate (or deoxyxylulose phosphate, DXP) pathway[58] The mevalonic acid pathway (Scheme 1.4) generally takes place in the cytosol and is mainly responsible for the formation of sesquiterpenes and triterpenes. Mammals, higher plants, fungi and some bacteria use this pathway to generate IDP (**1**) and DMADP (**2**). The non-mevalonate pathway (Scheme 1.5) takes place in the plastids and is responsible for the formation of monoterpenes, diterpenes and tetraterpenes.[59]

1.3.1 Mevalonic acid (MVA) pathway

This pathway starts with three units of acetyl-CoA (**33**). The first two units of acetyl-CoA are linked in a Claisen condensation reaction catalysed by acetoacetyl-CoA synthase with the release of coenzyme A to afford the acetoacetyl-CoA (**34**). A third molecule of acetyl-CoA is added in an aldol-like reaction with the help of β-hydroxy-β-methylglutaryl-CoA (HMG-CoA) synthase to afford the product, HMG-CoA (**35**).[59] HMG-CoA reductase is the enzyme that catalyses the reduction of the thioester group of HMG-CoA to the primary alcohol, (3*R*)-mevalonic acid (**37**). The cofactors used in this

reaction are two equivalents of NADPH.[60] The two hydroxy groups of (3*R*)-mevalonic acid (**37**) are phosphorylated (tertiary alcohol) and diphosphorylated (primary alcohol) by three molecules of ATP to yield mevalonic acid triphosphate (**39**). The final product IDP (**1**) comes from the decarboxylation of mevalonic acid triphosphate. IDP (**1**) and DMADP (**2**) are interconvertible by stereospecific isomerisation. It was shown by tritium-labelling experiments that only the pro-*R* proton on C2 of **2** is involved in the isomerisation process (Scheme 1.4).[61]

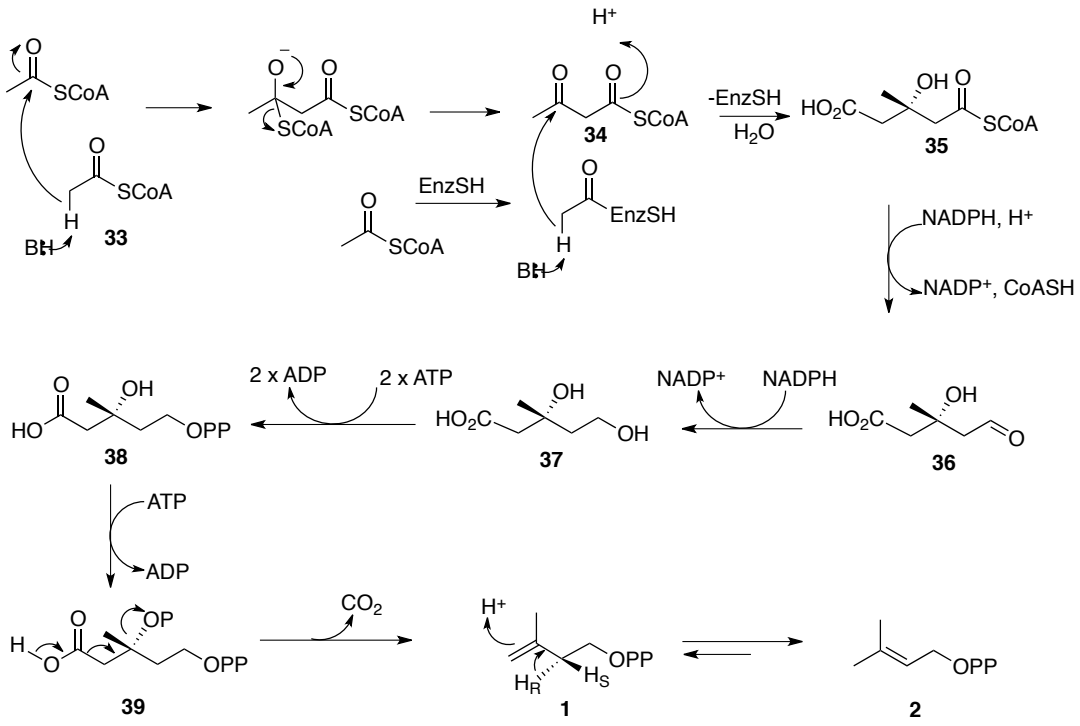

Scheme 1.4: Mevalonic acid pathway to IDP (**1**) and DMADP (**2**).

1.3.2 Non-mevalonate pathway

This pathway was discovered by Rohmer and co-workers at the end of the last century, using ^{13}C NMR labeling experiments.[62,63] A whole series of ^{13}C-labeled glucose isotopomers were used as minimal feedants and converted into a series of hopanoids by the bacterium *Zymomonas mobilis* - the results showed that the carbon skeleton was derived from a C2 subunit formed from pyruvate (**40**) by decarboxylation and a C3

subunit derived from a triose phosphate derivative (Scheme 1.5).[62,63] Incorporation of ^{13}C- labeled pyruvate and ^{13}C- labeled glycerol using *E. coli* mutants, lacking a single enzyme of the triose phosphate metabolic pathway, showed that D-glyceraldehyde phosphate (GAP, **41**) together with pyruvate (**40**) are the precursors of DMAPP and IDP in the alternative pathway.[64] This metabolic route was found to occur in the chloroplasts of algae, cyanobacteria, eubacteria and apicomplexa. This pathway is also named as the pyruvate/glyceraldehyde-3-phosphate pathway or sometimes as the MEP pathway, due to the fact that pyruvate (**40**) and D-glyceraldehyde-3-phosphate (**41**) are the starting compounds of this pathway and that 2-C-methyl-D-erythritol-4-phosphate (MEP) (**44**) is an important intermediate in the pathway.

1-Deoxy-D-xylulose 5-phosphate (DXP) (**42**) is formed from pyruvate and glyceraldehyde 3-phosphate by thiamine diphosphate mediated decarboxylation of pyruvate, yielding an enamine. Nucleophilic attack of glyceraldehyde 3-phosphate by the enamine, followed by the release from thiamine diphosphate generates DXP, which is a key intermediate in the biosynthesis of pyridoxal phosphate and thiamine. After a pinacol-like rearrangement of DXP, and NADPH, a reaction catalyzed by DXP-reductoisomerase giving 2-C-methyl-D-erythritol-4-phosphate (MEP, **44**) as the product. The formation of 2-phospho-4-cytidinediphosphate-2-C-methylerythritol (**45**) takes place by reaction of MEP with cytidine triphosphate (CTP) and is followed by ATP-dependent phosphorylation.[65] The two final dehydration steps are catalysed by the 2-C-methyl-D-erythritol 2,4-cyclodiphosphate reductase and 4-hydroxy-3-methylbut-2-enyl diphosphate reductase respectively, resulting in DMADP (**2**) and IDP (**1**) as the final products.

Since animals, fungi and yeast do not use the non-MVA pathway at all,[66] detailed research on the enzymes involved in the non-MVA pathway are targets for antibacterial, herbicidal or antimalarial drug therapies.[66,67]

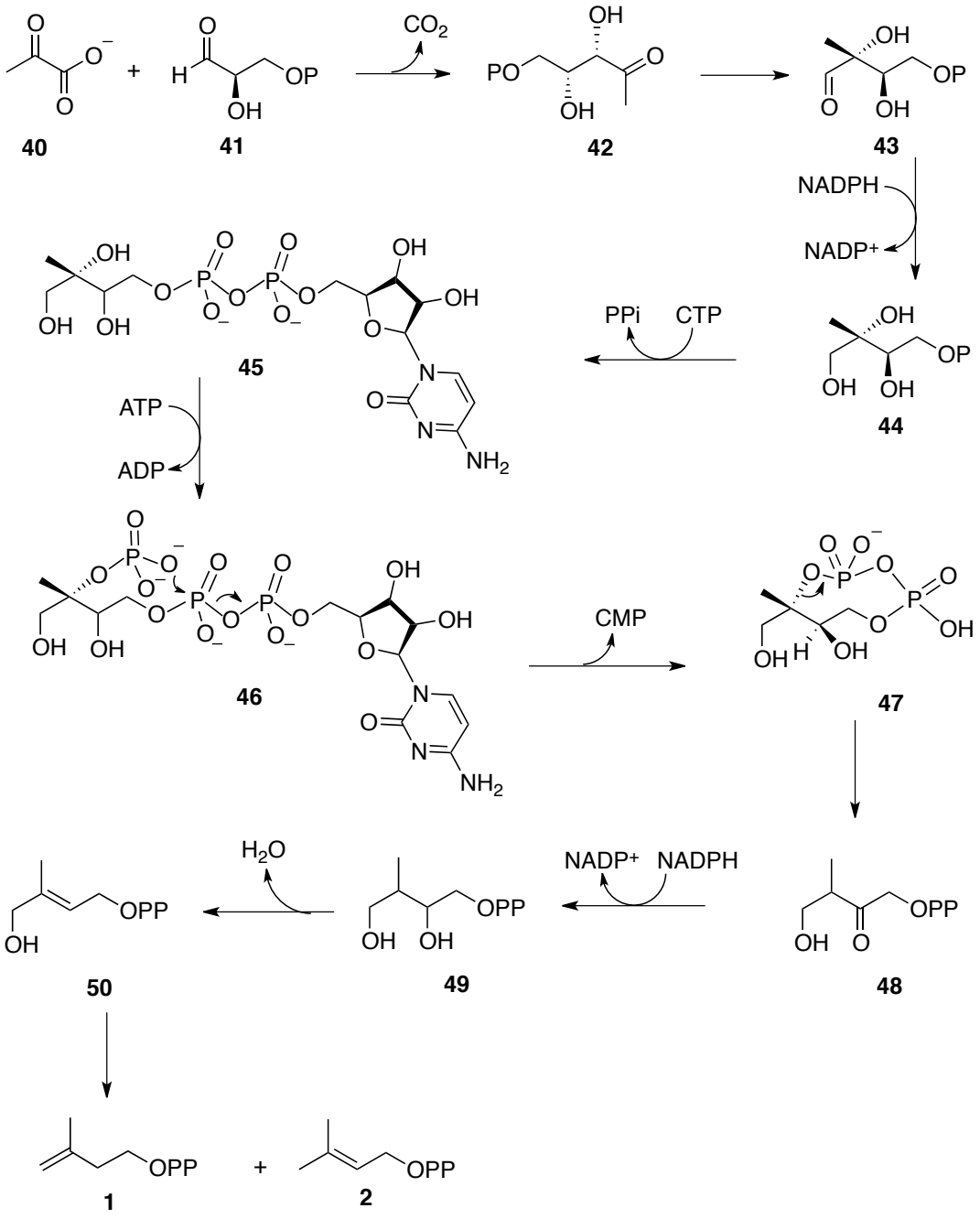

Scheme 1.5: The non-mevalonate pathway to IDP and DMADP

1.4 Terpene synthases

Terpene synthases catalyse some of the most complex reactions found in chemistry and biology. They are divalent metal cation dependent enzymes. The divalent metals are usually Mg^{2+} or Mn^{2+}, with Mg^{2+} being used most often.[68] As an exception, the presence of metal ions are not absolutely required for class II terpenoid synthases (*vide infra*).[69] The essential function of a terpene synthase is to catalyse the formation of terpenoid products from linear polyisoprenoid substrates in a reaction that usually shows distinguished structural and streochemical precision. Terpenoid synthases can be divided into two classes, depending on the first step of the enzymatic reaction.[70] To start catalysis, class I terpene synthases generate a carbocation by the loss of the diphosphate group. Isoprenyl diphosphate synthases, monoterpene and sesquiterpene synthases belong in this grouping. Class II terpenoid synthases generate the initial carbocation by protonation of a carbon-carbon double bond or an epoxide. Enzymes from this class include some diterpene, triterpene and tetraterpene synthases.[70] The carbocationic intermediates are sheltered from the bulk solvent in a hydrophobic pocket that provides, in addition, an environment capable of stabilising specific carbocations, thus it might be expected that the active sites of these proteins typically contain several aromatic amino acids.[71-73]

Despite often insignificant overall sequence similarity (typically below 25-35%) bacterial, fungal and animal terpene synthases all share a common fold, the class-I terpenoid fold, an α-barrel usually containing between 10 and 12 α-helices arranged in anti-parallel fashion.[74,75] Plant terpene synthases however, do have significant sequence similarity amongst themselves (50-90%).[76] For example, δ-selinene synthase and γ-humulene synthase both from the gymnosperm *Abies grandis* have 83% sequence similarity.[77] Substrate specificity varies among terpene synthases. GDP (**4**) and GGDP (**6**) are the exclusive substrates accepted by monoterpene and diterpene synthases respectively. On the other hand, sesquiterpene and triterpene synthases generally do not exhibit this strict substrate selectivity. For example, the sesquiterpene synthase (*E*)-β-farnesene synthase can use the monoterpene linear precursor GDP (**4**) to synthesise monoterpenes such us limonene (**6**), terpinolene (**51**) and myrcene (**52**). Some terpene synthases produce only one major product, for instance, δ-cadinene synthase makes δ-

cadinene (**15**) as the sole product.[78] However, some other terpene synthases produce more than one product, aristolochene synthase from *P. roqueforti* produces in addition to the major product aristolochene (**16**), two side products, valencene (**53**) and germacrene A (**54**).[79] γ-Humulene synthase from Grand Fir produces 52 different products.[77]

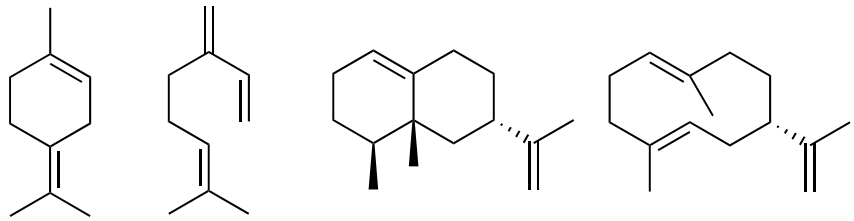

Figure 1.8: Structure of terpinolene (**51**), myrcene (**52**), valencene (**53**) and germacrene A (**54**)

Terpene synthase cDNAs encode proteins of 550-850 amino acids; corresponding to relative molecular masses of 50-100,000 Da. In general monoterpene synthases are 600-650 amino acids in length[80,81] and are 50-70 residues larger than their sesquiterpene synthase counterparts produced in the cytosol.[82-84] The size difference is due to the presence of an N-terminal plastid-targeting peptide in monoterpene synthases. Diterpene synthases are approximately 200 amino acids longer than sesquiterpene synthases due to a conserved N-terminal domain,[76] is often referred to as the conifer diterpene internal sequence (CDIS) domain due to high conservation in diterpene synthases.

Despite the differences in reaction mechanism, the classes I and II enzymes clearly belong to the terpene synthase gene family.[76] Several residues conserved amongst terpene synthases have been identified by sequence alignment, the most prominent of which are the amino acid residues of the metal binding motifs. Class I terpene synthases contain two metal motifs at the entrance of the active sites: the "aspartate-rich" (N, D) DXX (D/E) metal binding motif, and less specific (L,V) (V,L,A)-(**N,D**)D(L,I,V)X(**S,T**)XXX**,** which is usually abbreviated as "**NSE**/**DTE**" motif, in

which the boldface residues are implicated in binding three magnesium ions.[75,85] Class I terpene synthases have a conical active site that is bounded by about five helices.[86] The conical shape of the active site is imposed by the helices and the loops connecting them. The loops are comparatively long at the top and short at the bottom of the active site.[74,75]

Protonation-dependent class II terpene synthases contain only a DXDD metal binding motif, in which the central aspartate residue acts as a proton donor that generates the initial carbocation.[87] The squalene-hopene synthase (triterpene synthase) from *Alicyclobacillus* belongs to this class.[86] The bifunctional abietadiene synthase from the Grand Fir shows distinct cyclisation reactions catalysed by its class I and class II synthase domains, but the triple-domain taxadiene synthase from *Taxus brevifolia* functions as a class I terpenoid synthase as the conserved DXDD motif was absent. Plant synthases such as (+)-bornyl diphosphate synthase and 5-*epi*-aristolochene synthase contain both domains; only the class 1 domain is catalytically active.[88]

1.4.1 Crystal structures of terpene synthases

Several crystal structures of terpene synthases have been solved to date and the number grows each year. Aristolochene synthase from *Penicillium roqueforti*[89] and *Aspergillus terreus*,[90] 5-epi-aristolochene synthase from *Nicotiana tabacum*,[91] farnesyl diphosphate synthase from *Staphylococcus aureus*, pentalenene synthase from *Streptomyces UC5319*,[74] bornyl diphosphate synthase from *Salvia officinalis*,[88] limonene synthase from *Mentha spicata*[92] are representative examples (Figure 1.9)

The crystal structure of aristolochene synthase from *Aspergillus terreus* illustrates the important tertiary structural features from microbial sesquiterpene synthases. The 2.2 Å crystal structure reveals a tetrameric quaternary structure with a characteristic class I terpene synthase fold. There are a total of thirteen α-helices, six of which form the active site cleft.[90] The 2.5 A resolution crystal structure of aristolochene synthase from *Penicillium roqueforti* was the first of the fungal terpenoid synthases solved. This enzyme has eleven α-helices in the structure of which six form the active site cavity. The overall structure of both enzymes is very similar; they share 61% amino acid

sequence identity.

All plant sesquiterpene synthases contain an additional N-terminal domain. The 5-*epi*-aristolochene synthase from *Nicotiana tabacum* catalyses the cyclisation of farnesyl diphosphate to form the bicyclic hydrocarbon 5-*epi*-aristolochene.[91] This was the first example of a plant sesquiterpene crystal structure. The enzyme was complexed with two substrate analogues, farnesyl hydroxyphosphonate and trifluorofarnesyl diphosphate. They revealed the coordination of three Mg^{2+} ions to the metal binding motifs discussed earlier.

Solution of the X-ray crystal structure of pentalenene synthase showed that this enzyme also folds into a typical class I terpenoid synthase structure. Its tertiary structure is defined by 11 α–helices, 5 of which envelop the active site cavity. The lower section of the enzyme active site cleft is hydrophobic and contains a handful of aromatic and aliphatic residues, but the upper part is more hydrophilic and consists of polar side chains. A similar fold to that of pentalenene synthase is also uncovered in farnesyl diphosphate synthase, even though only 15% sequence identity is found between these two enzymes.[74]

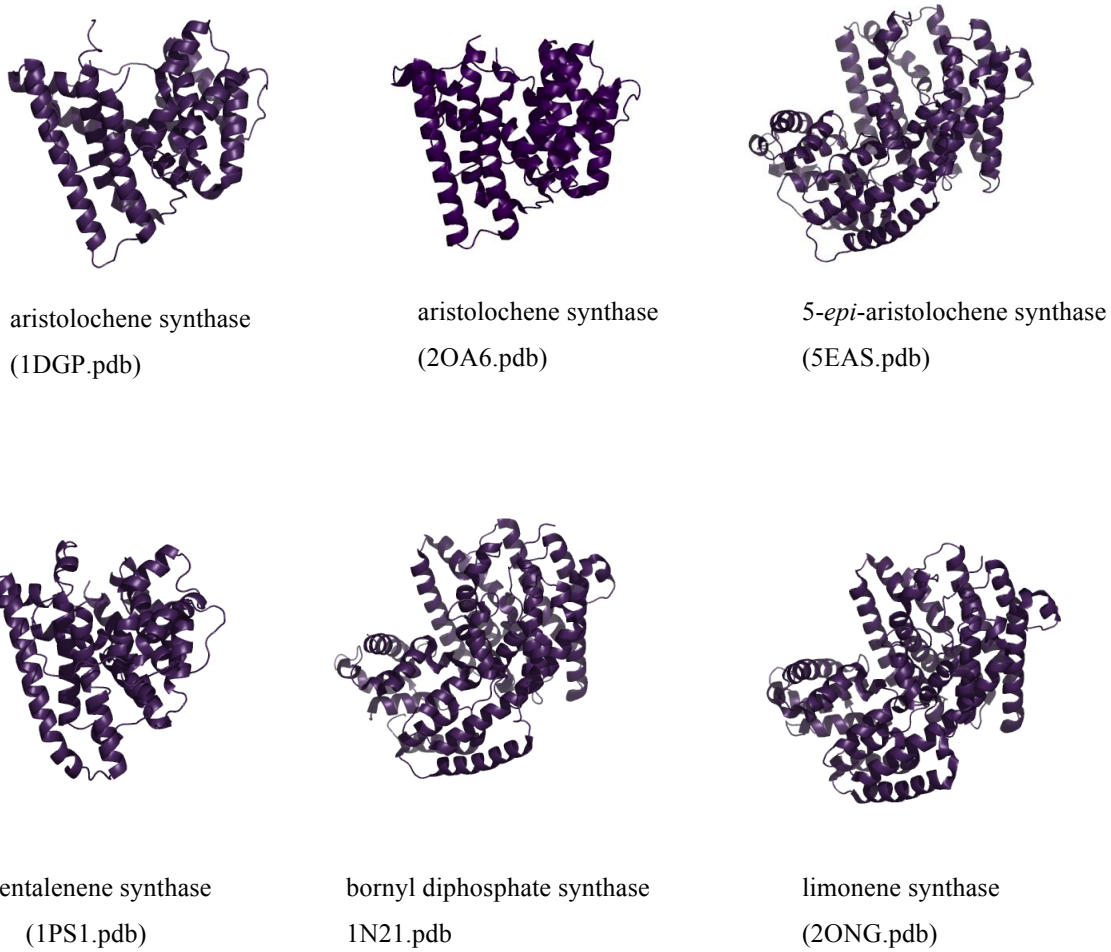

Figure 1.9: Ribbon diagram illustration of the crystal structures of some terpene synthases

Limonene synthase is similar to 5-*epi*-aristolochene synthase in having two helical domains: a C-terminal domain with the active site and an N-terminal domain of unknown function.[92] The N-terminal domain folds back right through the C-terminal domain to form a cap in the active site. This is postulated to shelter reactive carbocationic intermediates from solvent. A study of intron conservation patterns in terpenoid synthase genes has denoted that modern terpenoid synthases evolved from an ancestral enzyme in which both domains were catalytically active.[93] A flexible structure, specifically in the active site, would be expected for an enzyme that binds two structurally different diphosphates such as GDP (**4**) and LDP (**55**) during the reaction. This may due to the tandem arginine residues R58 and R59, positioned in the N-terminal strand. The 2.7 A resolution crystal structure reveals a homodimeric quaternary

structure with two forms of liganded substrate (2-fluorogeranyldiphosphate) and intermediate (2-fluorolinalyldiphosphate) analogues.

Two tandem arginine pairs have been found in many monoterpene synthases.[88] Polypeptide deletion studies on the limonene synthase of *Mentha spicata* revealed that the enzyme activity was not affected by deletion of the N-terminal region preceding this tandem argine pair. Deletion of this motif made the limonene synthase unable to accept GDP (**4**) as a substrate although linalyl diphosphate (LDP, **55**) was still usable by the deletion mutant, suggesting that the arginine motif might participate in the isomerisation of GDP (**4**) to linalyl cation.[92] The N terminal polypeptide domain is involved in many hydrogen bond interactions with the C-terminal domain including R56 with D355.

Bornyl diphosphate synthase

The first crystal structure of a monoterpene synthase was solved for (+)-bornyl diphosphate synthase (BDPS) from *Salvia officinalis*.[88] This enzyme crystallised as a homodimer - each monomer containing two α-helical domains. The C-terminal domain contains the characteristic class I terpene fold. The N-terminal domain forms an α-barrel similar to that of 5-*epi*-aristolochene synthase.[91] This domain has no well defined function; nevertheless, the disordered N-terminal polypeptide segment caps the active site in the C-terminal domain upon ligand binding and becomes ordered.

Figure 1.10: Stereoplot of the native BDPS monomer, including the active site (blue).[88]

The C-terminal domain of BDPS consists of 12 α-helices, six of which (C, D, F, G, H and J) are responsible for the hydrophobic active site cleft. The aspartate-rich D^{351}DIYD motif is positioned at the C-terminal end of helix D (Figure 1.10). Asp351 and Asp355 coordinate to Mg^{2+}_{A} and Mg^{2+}_{C}. Asp 496, Thr500 and Glu504 chelate Mg^{2+}_{B} on the opposite site of the active site cleft as the second metal binding motif (DTE).

Coordination of PP_i- Mg^{2+}_{3} by BDPS activates several conformational changes in the protein, which presumably lead to an active site cavity secluded from bulk solvent. The disorder in the unliganded structure (N-terminus E50-A63 and loop segments D227-D234, T500-D509 and F578-S583) becomes ordered and caps the active site in the enzyme-ligand complex. A single water molecule (water 110) was found to be trapped in the active site cavity after the conformational change.

The structures of BDPS complexed with aza analogues of presumed carbocationic intermediates (3-aza-2,3-dihydro-geranyldiphosphate (**56**), 2-azabornane (**57**), 7-aza-7,8-dihydro-limonene (**58**)) (Figure 1.11) reveal fundamentally identical molecular recognition of the diphosphate moiety.[94,95] Comparisons between BDPS and aza analogues of putative intermediates and also the product, indicate that the hydrophobic active site serves as a template for substrate and intermediates through a complicated cyclisation process, even though the diphosphate group is rigidly bound. Several aliphatic and aromatic residues in the active site, including W323, I344, V452 and F578 along with water molecule number 110 line the hydrophobic active site. This water molecule makes hydrogen bonds to the diphosphate group of **56 a**nd the backbone carbonyl of S451 and the side chain of Tyr-426. This suggests that it cannot easily react with carbocation intermediates to prematurely quench the cyclisation cascade. Perhaps, water number 110 could serve as a diphosphate-assisted general base to account for the generation of cyclic olefin side products such as pinene (**12**), camphene (**14**), and limonene (**11**).[88]

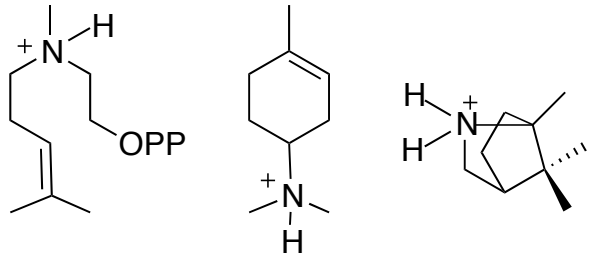

56 **57** **58**

Figure 1.11: Structures of 3-aza-2,3-dihydro-geranyldiphosphate (**56**), 7-aza-7,8-dihydro-limonene (**57**) and 2-azabornane (**58**)

1.5 Monoterpene synthases: Reaction mechanisms

It has been established that monoterpene synthases possess a common carbocationic reaction mechanism initiated by the divalent metal ion-dependent ionization of the substrate.[96] They have K_m values in the low micromolar range and have relatively low turnover numbers (<1 s^{-1}).[97-99] Most monoterpene synthases are multiproduct enzymes with great active site flexibility to generate product diversity, but they are generally specific in using only C10 isoprenyl diphosphate substrates, GDP (**4**), linalyl diphosphate LDP (**55**)), or neryl diphosphate NDP (**59**) (cis-isomer of **4**) (Figure 1.12) with product diversity often including several monoterpene structural types (Figure 1.13). GDP is generally considered the natural C10 substrate of monoterpene synthases.[97,98] However recent characterisation of enzymes from cultivated tomato plants have showed that they use NDP (**59**) as the substrate of monoterpene production.[100] Structural characterisation of monoterpene synthases from their native plant sources has demonstrated that 'lower eukaryote' like liver-worts, ferns, and algae resemble their higher plant counterparts in enzymological characteristics.[101,102] These results suggests a common plant ancestor.

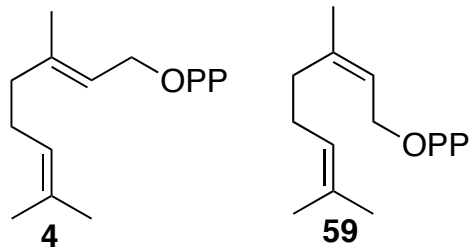

Figure 1.12: The predominant monoterpene precursor, GDP (**4**) and its *cis*-isomer NDP (**59**)

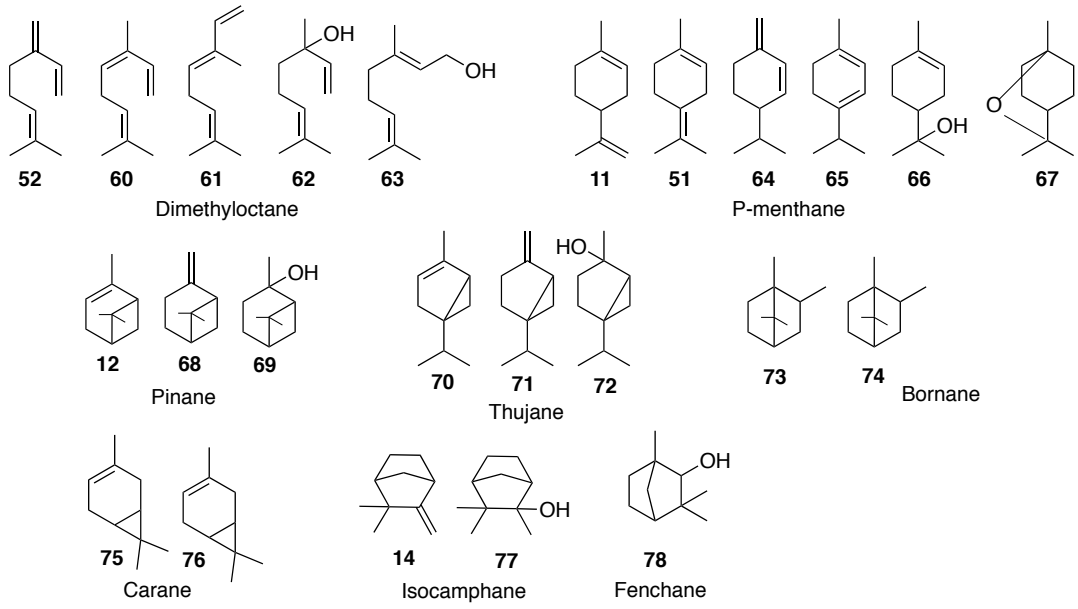

52. Myrcene
60. *Z*-β-Ocimene
61. *E*-β-Ocimene
62. Linalool
63. Geraniol
11. Limonene

51. Terpinolene
64. β-Phellandrene
65. α-Terpinene
66. α-Terpineol
67. 1,8-Cineol
12. α-Pinene

68. β-Pinene
69. Pinan-2-ol
70. α-Thujene
71. Sabinene
72. Sabinene hydrate
73. Bornyl diphosphate

74. Borneol
75. 3-Carene
76. 2-Carene
14. Camphene
77. Camphene hydrate
78. Fenchol

Figure 1.13: Product diversity of monoterpenes

1.5.1 Ionisation and isomerisation of GDP

GDP (**4**), the major precursor of the monoterpenoids, undergoes an ionisation and isomerisation to enzyme-bound linalyl diphosphate (LDP, **55**). For a monoterpene synthase to produce cyclic monoterpene products it must first overcome the topological impediment to direct cyclisation of geranyl diphosphate, imposed by the trans geometry of the C2–C3 double bond, by way of a preliminary isomerisation step to permit subsequent cyclisation (Scheme 1.6). After rotation about the C2–C3 bond to afford the cis conformer, LDP is itself ionized with C6–C1 ring closure to provide the corresponding α-terpinyl carbocation (**79**) from which all cyclic monoterpenes are derived. These early reaction steps appear to be common to all monoterpene cyclisations, with subsequent steps involving termination of the reaction either by deprotonation, nucleophilic capture, further electrophilic cyclisation to the remaining double bond, hydride shift, or Wagner–Meerwein rearrangement before termination. Alternatively, a deprotonation can occur beore cyclisation leading to acyclic monoterpenes such as myrcene. Acyclic monoterpenes are formed from either GDP or LDP via carbocations.[103-106] In order to prove the electrophilic nature (ionisation) of the cyclisation reaction, incubations were carried out using 2-fluoro-GDP (**80**) and 2-fluoro-LDP (**81**).[107,108] The results from these experiments showed 100-fold rate suppression, and displayed evidence of the electrophilic nature of the cyclisation reaction involving either GDP (**4**) or LDP (**55**). Kinetic analysis with these analogues using purified (-)-limonene synthase and (+)-bornyl diphosphate synthase revealed that both fluoro analogues are competitive inhibitors.[109] This provided additional compelling evidence showing that both ionisations occur in the same active site.

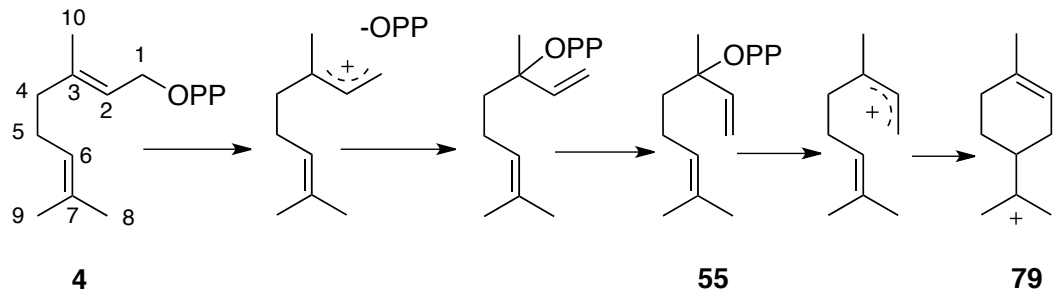

Scheme 1.6: Production of cyclic α-terpinyl cation (**79**) from GDP (**4**)

The mechanism of the acyclic monoterpene reactions proceed by ionisation into geranyl cation followed by proton loss to form (*E*)-β-ocimene (**61**)[110] and myrcene (**52**),[81,110] or addition of water to form geraniol (**63**)[111] or linalool (**62**).[112] These acyclic monoterpenes can be derived also from the linalyl cation (Scheme 1.7).

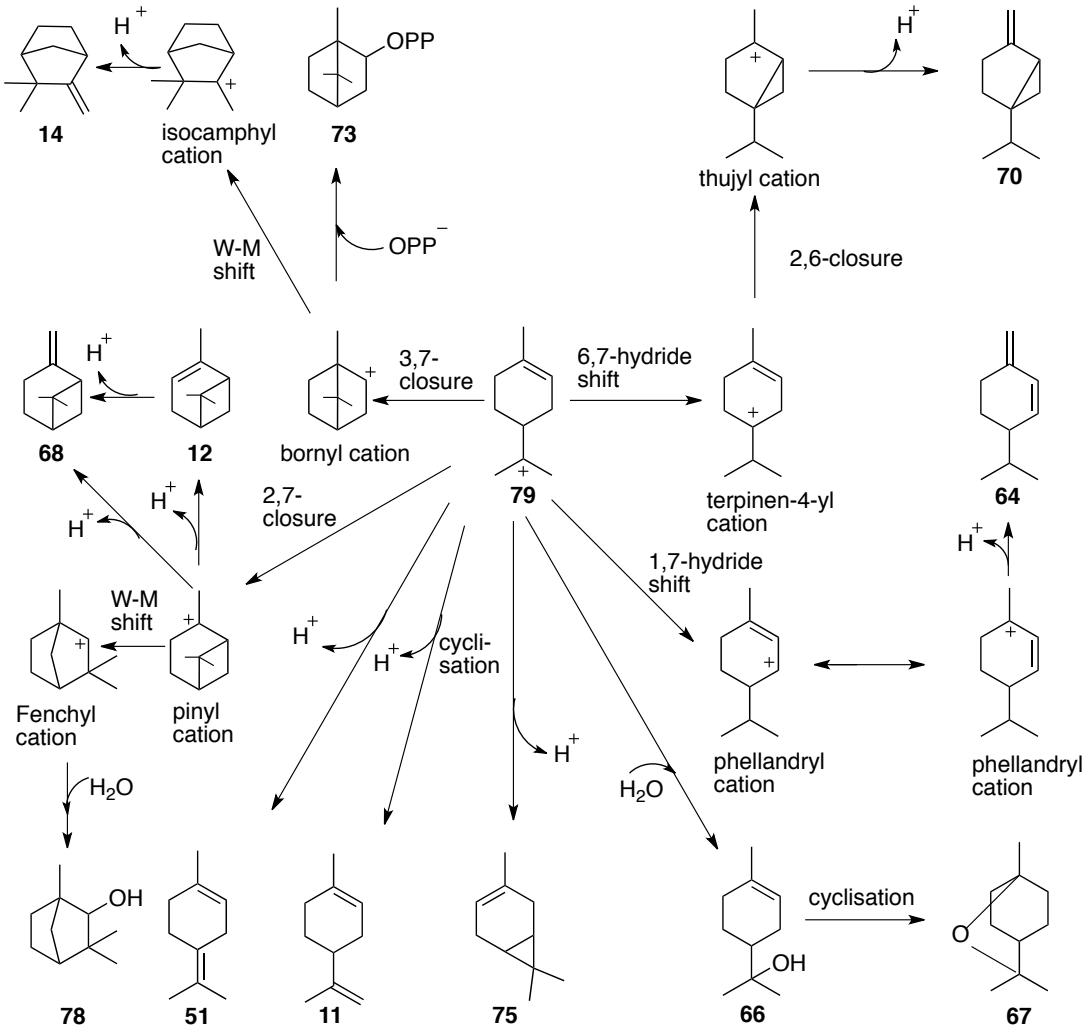

Scheme 1.7: Examples of carbocationic reactions leading to cyclic monoterpenes.[96]

The α-terpinyl cation is an important intermediate involved in the formation of all cyclic monoterpenes. From this intermediate, proton loss leads to limonene (**11**)[112, 113] or

terpinolene (**51**), or if water is involved α- terpineol (**66**).[105, 114] In contrast, internal addition leads to 1,8-cineole (**67**). A [1,2]- or [1,3]-hydride shift of the α-terpinyl cation followed by proton loss yields the terpinene (**9**) and phellandrene (**64**) products.[114,115] The thujane monoterpene produced by a [1,2]-hydride shift followed by cyclopropyl ring closure and tertiary cation quench by deprotonation, yields in the case, α-thujene (**70**) and sabinene (**71**) or if by water capture sabinene hydrate (**72**). The α-terpinyl cation withstands additional cyclisations resulting from electrophilic attack of the carbocationic centre on one of the carbon atoms of the remaining double bond. A Markonikov addition (2,7-cyclisation) to α-terpinyl cation initiates formation of the pinyl cation, which undergoes proton loss to yield α-pinene (**12**) or β-pinene (**13**).[116,117] Anti-Markovnikov addition (3,7-cyclisation) of α-terpinyl cation produces the bornyl cation, and diphosphate capture leads to bornyl diphosphate (**73**).[118] (**74**) and camphene (**14**).[119] Fenchol (**78**) is formed from the pinyl cation, via Wagner-Meerwein rearrangement and water quench.[117] Wagner-Meerwein rearrangement (6,2-rearrangement) of the bornyl cation lead to isocamphyl cation and deprotonation results camphene (**14**). A 5,7-closure of α-terpinyl cation forms a cyclopropyl ring leading to 3-carene (**75**).[120]

1.5.2 (+)-α-Pinene synthase

(+)-α-Pinene synthase catalyses the metal ion-dependent ionisation and isomerisation of GDP (**4**) to (+)-α-pinene (**12**). The proposed enzyme catalysed mechanism involves ionisation and isomerisation of this substrate to enzyme bound linalyl diphosphate **(55**) (Scheme 1.8), rotation about C2-C3, a second ionization, and cyclisation to the α-terpinyl cation, to form the first cyclic intermediate *en route* to both monocyclic and bicyclic products. Electrophilic addition of the α-terpinyl cation to the 2,3-double bond and proton elimination generates (+)-α-pinene.[116,117]

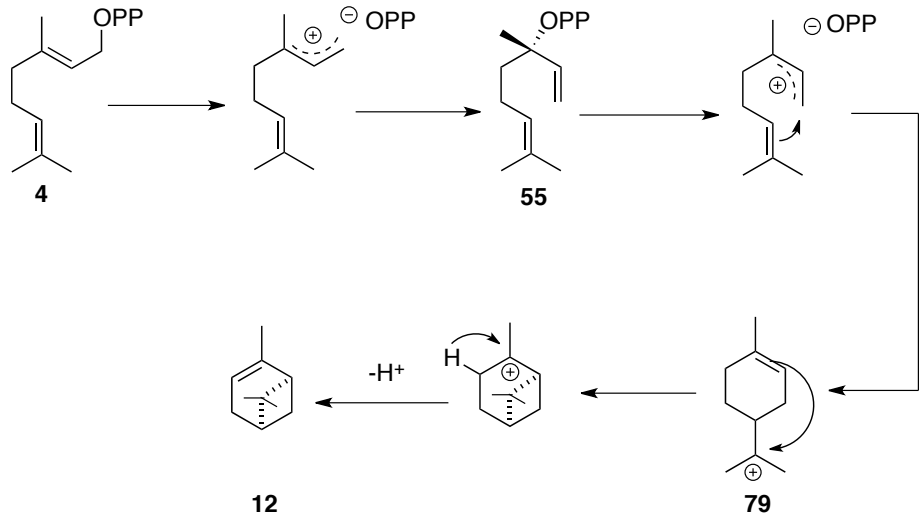

Scheme 1.8: Proposed mechanism for the conversion of GDP (**4**) to α-pinene (**12**)

In order to gain structural information about the (+)-α-pinene synthase from loblolly pine (*Pinus taeda*), computer modeling was needed because a crystal structure of this synthase is not yet available.[121] The structures of tobacco 5-*epi*-aristolochene synthase and bornyl diphosphate synthase were used as templates to construct the (+)-α-pinene synthase homology model. The first 50-60 amino acids are high in serine and threonine content and low in acidic residues.[121] The $R_{65}R_{66}$ tandem arginine pair was judged to play a role in the isomerisation step. The metal binding motif $D_{379}D_{380}IYD_{383}$ and the highly conserved tandem tryptophan pair $W_{329}W_{330}$ are all structural repeats present commonly in monoterpene synthases.

(+)-α-Pinene synthase, both native and recombinant, requires K^+ for optimum activity. The predicted active site is distinguished by the conserved aspartate residues (379, 383, 524) and conserved arginines in close vicinity to the diphosphate moiety. Several aromatic residues provide a deep pocket underneath these charged residues.[121] This above mentioned computer model provides a tool to investigate structure-function relationships in α-pinene synthase the precursor of both verbenol and verbenone

Bark beetle infestations pose a major threat to conifer populations worldwide[122] with millions of acres of pine trees having been lost due to attacks by mountain pine beetles such as *Dendroctonus ponderosae.*[123] Several factors have contributed to recent outbreaks of these insects.[123,124] Many years of drought caused a decline in the defenses

of pine tree and warmer than average winters allowed a greater number of beetle larvae to survive.[124] These beetles produce aggregation and anti-aggregation pheromones that modulate the beetle population density on the trees, many of these are monoterpenoids or monoterpenoid derivatives.[124] These monoterpenoid pheromones are messenger chemicals (semiochemicals). The male beetle uses (+)-α-pinene (**12**) produced by the tree for host selection and then converts it to verbenol, which acts as an attractant for female beetles. The beetles then produce the oxidation product (+)-verbenone (**13**), which acts as a dispersal pheromone to modulate the density of the attack.[15,124] In a program to limit tree damage from beetle infestation, foresters have hung small bags of synthetic verbenone on trees as a beetle repellant.[123] When the beetle populations are low, trees systematically attack by drowning the beetles in sap. If that fails the trees produce defensive resins that kill maturing beetle larvae.[125,126]

Verbenone (**13**) is a bicyclic ketone terpene, is also a useful chiral synthon and has been used in the total synthesis of taxol.[127] Furthermore this bioactive enone has been reported as an inhibitor of acetylcholine esterase and hence has potential for the treatment of early stage Alzheimer's disease.[128] Also this fine chemical is utilised in perfumery, aromatherapy and herbal remedies.[129]

1.6 Aim of the project

In view of the importance of (+)-α-pinene and verbenone, the aim of this project was to use (+)-α-pinene synthase as a pilot synthetic platform to produce verbenone. The project was divided into two parts. The first part is dedicated to heterologous expression, purification and characterization of recombinant (+)-α-pinene synthase. Several expression conditions and many purification methods were tried in order to get optimum results. Furthering the understanding of the protein, i.e. examination of the potential catalytic role of several aromatic amino acids in stabilizing the carbocationic intermediates generated in the active site of (+)-α-pinene synthase during the natural conversion of GDP (**4**) through site directed mutagenesis was planned.

Once (+)-α-pinene synthase was fully optimized, a chemoenzymatic synthesis of (+)-verbenone (**13**) from GDP (**4**) using the enzyme as the essential biocatalyst was described. In addition to this, synthesis of some chemically modified GDP analogues to obtain (+)-α-pinene analogues using (+)-α-pinene synthase was also intended. These (+)-α-pinene analogues were postulated to display, for practical purposes, enhanced biological activities due to potential improvements in their physical properties (e.g. potency and stability).

CHAPTER 2

Heterologous expression, purification and characterization of recombinant (+)-α-pinene synthase

2.1 Introduction

The purification of plant mono- and diterpene synthases from their native hosts has been shown to be complicated due to difficulties arising from solubility and activity issues.[130,131] Synthase activity in crude extracts are significantly reduced due to the low abundance of these proteins in plant tissue and the presence of large amounts of interfering oils, resins and high levels of competing activities.[130,131] Plants utilize specialized tissues (e.g. glandular trichomes) to synthesise mono- and diterpenes,[132] and restrict production to certain developmental stages,[133] or short periods of transient defense reactions,[134] which makes the expression highly up-regulated. To overcome these complications, many plant terpene synthases are currently identified, cloned and heterologously overexpressed in microbes.[76]

Even though, operationally soluble enzymes localized in plastids such as mono- and diterpene plant synthases are notorious for the difficulties associated with their purification in the lab. Monoterpene synthases are difficult to solubilize and activate because they have, as opposed to cytosolic sesquiterpene synthases, an N-terminal plastid targeting polypeptide that, in vivo, is precisely cut upon maturation. *In vitro*, this "cut" is done by empirical truncation of the N-terminal domain; several cuts (truncation) are often necessary to produce pseudomature soluble mono- or diterpene synthases. This lack of precision greatly affects the heterologous expression and purification of plant monoterpene proteins (e.g. APS). The N-terminal transit peptides of plant synthases are believed to target the plastids for proteolytic processing to the mature forms. Because of this self-association and tight binding to host chaperones many mono and diterpene synthases are translated as preproteins.[135] Expecting that purification issues were likely to arise with APS, the plant gene was first codon optimised for expression in *E. coli*. Codon optimization can alter both naturally occurring and recombinant gene sequences to achieve the highest possible levels of productivity in any given expression system by increasing the translational efficiency.

However, after gene design and expression, APS was obtained as inactive inclusion bodies and several protein purification techniques were needed in order to get soluble, catalytically active APS. Previous successfully used purification protocols for monoterpenes synthases include, ion exchange chromatography, ammonium sulphate precipitation, hydrophobic interaction chromatography, size exclusion chromatography and affinity chromatography.[88,136-138] Although His-tagged terpene synthases are catalytically active when expressed, such fusions are, in some cases, inappropriate for detailed crystallographic studies.[88,137-139] Therefore before introducing a His-tag into APS, several different purification protocols were attempted with this particular synthase.

2.2 Transformation and purification of the cDNA of α-pinene synthase (APS)

A synthetic gene (EpochBioLabs) codon optimised for expression in *E. coli* encoding the monoterpene α-pinene synthase from *Pinus taeda* (loblolly pine*:* EMBL/GeneBank accession No. AF543530),[15] was cloned into the expression vector pET 21d between the *Nco*I and *Bam*HI restriction sites by PCR amplification and ligation as described in previous work by the Allemann group.[71,72] After expression in *E. coli* XL1-Blue cells and DNA purification, the correct insertion (direction of translation) of the transit DNA fragment was verified by sequencing. The purity and molecular weight of this cDNA was estimated by agarose gel electrophoresis (Figure 2.1). To confirm the size of cDNA more accurately (Figure 2.2), the cDNA synthesized by *E. coli* (above) was digested with the restriction enzyme *Bam*HI to afford a linear DNA (≈ 7.1 kb) that was also analysed by electrophoresis in agarose using a different marker. The purified cDNA was then sent for sequencing with positive results.

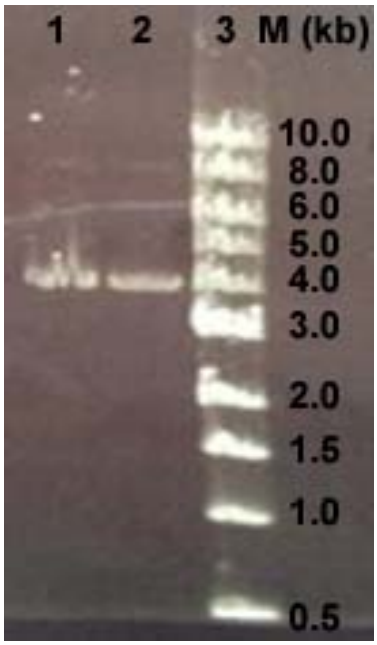

Figure 2.1: An image of the agarose gel of the cDNA used for expression of the APS gene. Lane 1-2: APS cDNA samples. Lane 3: DNA Ladder.

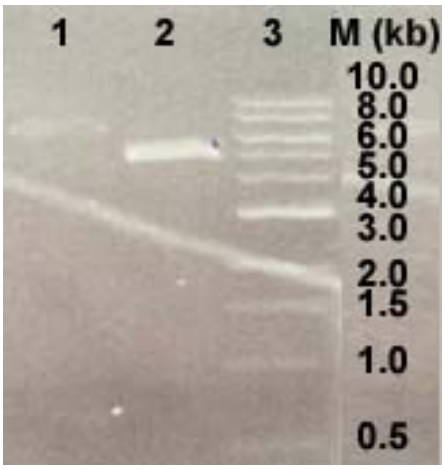

Figure 2.2: Agarose gel analysis of cDNA and linear DNA containing the APS gene. Lane 1: DNA digested with BamHI (≈ 7.1 kb). Lane 2: cDNA (≈ 5.6 kb). Lane 3: DNA ladder.

2.3 Heterologous (large) expression of APS in *E. coli*

For protein expression in the present case, the *E. coli* BL21 (DE3) strain was used with bacterial fermentation at 37 °C. A single colony was selected and used to inoculate 100 mL of LB medium containing ampicillin (LB-amp) at a final concentration of 0.1

mg/mL. The culture was incubated overnight at 37 °C, with shaking at 150 rpm. Each of 6 x 500 mL of sterile LB-amp medium was inoculated with a portion (5 mL) of the overnight culture. Cells were incubated at 37 °C with shaking at 150 rpm until the optical density (measured at 600 nm, reached 0.5-0.8 units). Each culture was independently induced for protein expression by the addition of IPTG (0.5 mM) at 37 °C. Fermentation was maintained for an additional 3.5 h (37 °C). Cells were harvested by centrifugation in a Sorvall RC5C Plus centrifuge (Thermo Fisher scientific, USA) (6000 x g RCF, 15 min) using SLA-3000 rotor. The supernatant solution was discarded and the pellets of *E. coli* containing the over expressed enzyme were resuspended in cell lysis buffer. The resuspended cells were lysed by sonication on an ice bath and the cell lysate was clarified by centrifugation at 5 °C (17000 x g RCF, 30 min). Unfortunately, this exploratory protocol yielded only small amounts of the desired soluble protein, and most of the APS required extraction from inclusion bodies (Figure 2.3).

Therefore a variety of cell strains and expression conditions were tested to achieve efficient production of APS. Culture incubation was carried out at 37 °C for 3.5 h or at 16 °C for 18 h. The following *E. coli* strains were used - BL21(DE3), BL21(DE3) pLysS, BL21-Codon Plus-(DE3)-RIL and BL21-Codon Plus-(DE3)-RP.

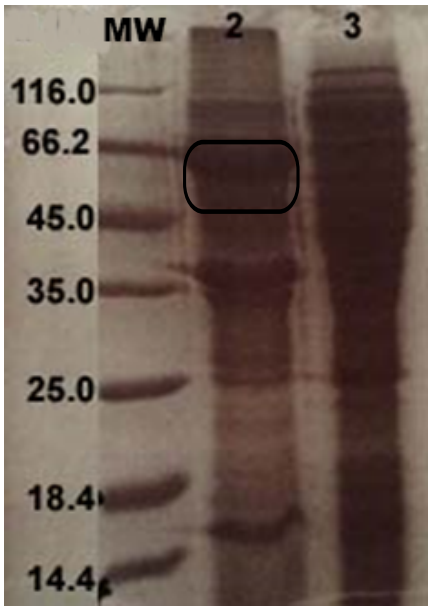

Figure 2.3: SDS-polyacrylamide gel analysis of the initial attempt at production of APS from *E. coli* BL21 (DE3) cells. Lane 1: Protein Marker. Lane 2: pellet after base extraction. Lane 3: supernatant solution after base extraction.

Codon Plus cells contain extra copies of tRNA genes (AGA and AGG for R, AUA for I, CUA for L and CCC for P) that are not usually expressed in *E. coli* but are used in other organisms such as plants. Indeed, the best results were obtained using *E. coli* BL21-Codon Plus-(DE3)-RIL cells with expression at 16 °C for 18 h. This strain rescues expression of proteins originating from plants with AT rich genomes.[140]

2.4 Isolation of Recombinant APS

After a large-scale APS expression using *E. coli* BL21-Codon Plus-(DE3)-RIL cells with protein induction (IPTG (0.5 mM)) at 16 °C for 18 h as described above, the cells were harvested by centrifugation (6000 g, 15 min, 4 °C) and lysed by sonication at 0 °C. Protein analysis by SDS PAGE indicated that APS readily aggregated and was found, for the most part, as inclusion bodies. In order to solubilise APS, a previously developed methodology for microbial sesquiterpene synthases was employed. Briefly, the pellet was re-suspended in cell lysis buffer (Tris-base (50 mM), EDTA (5 mM), β-mercaptoethanol (5 mM) and 100 mL glycerol (10% v/v), pH 8.0.) and the pH of the resulting milky suspension was then increased to 12.0 by drop-wise addition of NaOH (5 M) at 4 °C. After protein denaturation (i.e. clarification), the basic solution was stirred for 30 min at 4 °C. Refolding was then achieved by neutralization (pH = 8) with slow addition of HCl (1 M) and stirring (30 min) at 4 °C. The suspension containing the solubilised protein was centrifuged (17000 g, 30 min, 4 °C). This efficient and standard protocol has been used to extract microbial sesquiterpene synthases from similar inclusion bodies extensively. As shown by the SDS-polyacrylamide gel in Figure 2.4 almost all of the required protein was found in the supernatant solution after centrifugation.

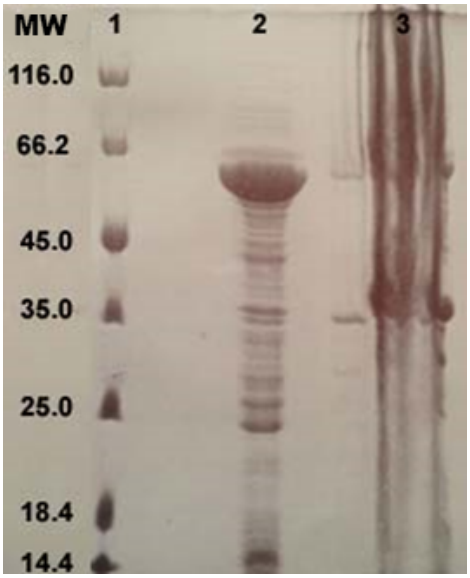

Figure 2.4: SDS-polyacrylamide gel of APS from *E. coli* BL21-Codon Plus-(DE3)-RIL cells using the optimum growth conditions. Lane 1: Protein Marker. Lane 2: supernatant solution after base extraction. Lane 3: pellet after base extraction.

2.5 Enzyme Purification

After the successful production of soluble APS, it was then necessary to purify APS to carry out its biochemical characterization and further explore to possibly of getting α-pinene synthase crystals for x-ray crystallographic studies. Unless otherwise stated, Fast Protein Liquid Chromatography (FPLC) was used to purify APS.

2.5.1 Ion exchange chromatography

Initially several attempts to purify α-pinene synthase (APS) were carried out by variation of solution pH using ion exchange resins as the stationary phases. Ion exchange chromatography (IEC) is based on the difference in the strength of the interaction between a sample and the oppositely charged solid support. Elution is often accomplished by increasing salt concentration in the eluent over time. Both positively charged and negatively charged resins are commercially available. Resource Q and Q-Sepharose are positively charged and are therefore strong anion exchangers due to the presence of quaternary ammonium group on the solid support. Diethylaminoethyl

(DEAE)-sepharose is also positively charged but relatively weaker as an anion exchanger; it contains an ionisable tertiary amine group on the solid support. Resource S and SP-Sepharose are negatively charged, and hence are used as cation exchangers. The charged groups of SP-Sepharose and Resource S are sulfonate ions on the solid support.

For purification of APS, a DEAE-sepharose column was used in the first trial. Since the theoretical pI of the protein is 5.86 (ExPASy-SIB Bioinformatics Resource Portal; compute pI/Mw tool), it should be negatively charged at pH 8.3 and hence should bind to a positively charge resin such us DEAE-sepharose. However only a small portion of the protein bound to the resin. The majority, as indicated by SDS-polyacrylamide gel (Figure 2.5), was found in the unbound flow-through solution.

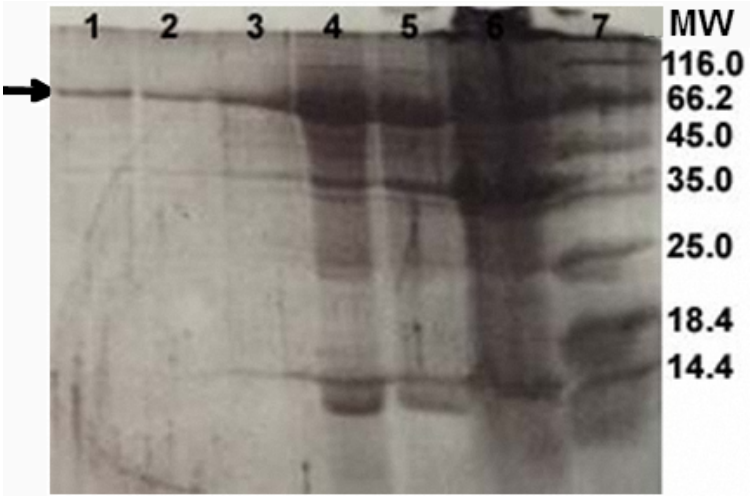

Figure 2.5: SDS-polyacrylamide gel of APS from *E. coli* BL21- Codon Plus-(DE3)–RIL cells using the optimum growth conditions. Lane 1,2: DEAE-sepharose eluate. Lane 3,4: DEAE-sepharose flow-through. Lane 5: Supernatant solution after base extraction. Lane 6: pellet after base extraction. Lane 7: Protein Markers.

From the predicted pI of APS the positively charged Q sepharose resin (*vide supra*) should be better suited. This resin was explored in small-scale purification experiments, along with the negatively charged SP sepharose as a control.

In addition, since the initial DEAE sepharose purification attempt was partially successful, this resin was tried again on a small scale. On the expectation that better results might be obtained by allowing protein sample and resin to equilibrate slowly for a longer period of time, the following procedure was followed. Briefly, a few grams of each resin, previously equilibrated with cell lysis buffer was placed in separate Eppendorf™ tubes followed by addition of cell lysis buffer solution (500 µL) containing the crude solubilized APS from inclusion bodies. Gentle mixing by simply inverting the Eppendorf™ tube was maintained for 10 min. The mixture was then centrifuged for 1 min at 17,000 g and the flow through solution decanted. Cell lysis buffer containing 1 M NaCl was added to the resulting pellet and both phases were mixed gently to extract any possible bound protein. After centrifugation in a benchtop cerntrifuge (1 min at 17,000 g), the flow through solution again was decanted. After freeze-drying both supernatant solutions were re-dissolved in 20 mL of cell lysis buffer and analysed by SDS-PAGE (Figure 2.6).

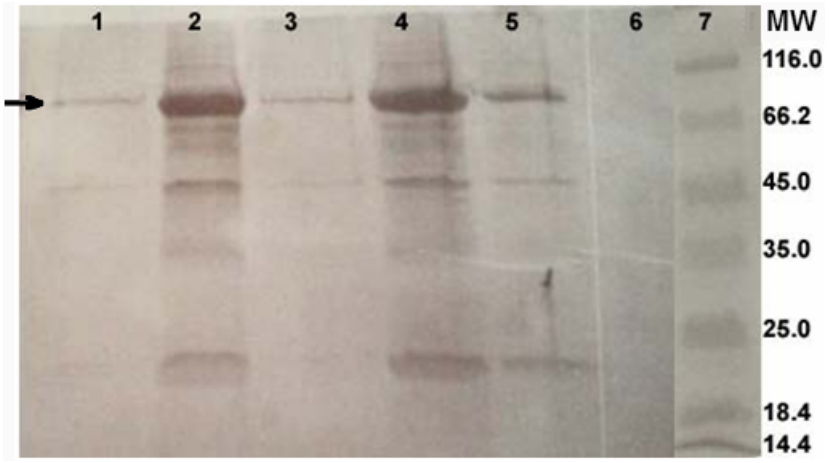

Figure 2.6: SDS-polyacrylamide gel of the flow through solution (supernatant 2) and eluate from the DEAE-sepharose, Q-sepharose, and SP-sepharose ion exchange columns. Lane 1: Q-sepharose eluate. Lane 2: Q-sepharose flow-through. Lane 3: DEAE eluate. Lane 4: DEAE flow-through. Lane 5: SP-sepharose flow-through. Lane 6: SP-sepharose eluate.

Unfortunately in both the DEAE and Q-sepharose experiments nearly 97% of the protein was found in supernatant, thus only 3% of the APS interacted with these resins. For SP sepharose, no visible band corresponding to APS was found in the SDS-PAGE analysis (Figure 2.6) of supernatant 2 indicating that in this case the protein did not bind at all. Percentages were estimated from relative band intensities using SDS-PAGE.

Finally, a DEAE resin drip column left for rotation at cold room temperature for 3 h and then the usual drip column purification was carried out as stated below, hoping that these conditions will secure a better protein-resin binding and hence better separation. The drip column (1.5 × 1.5 cm) was eluted using a stepwise NaCl gradient (0.2-1.0 M)). About four column volumes (CV) in 2 mL fractions at each NaCl concentration step were collected. All fractions were analysed by measuring their absorbance at 280 nm (Figure 2.7).

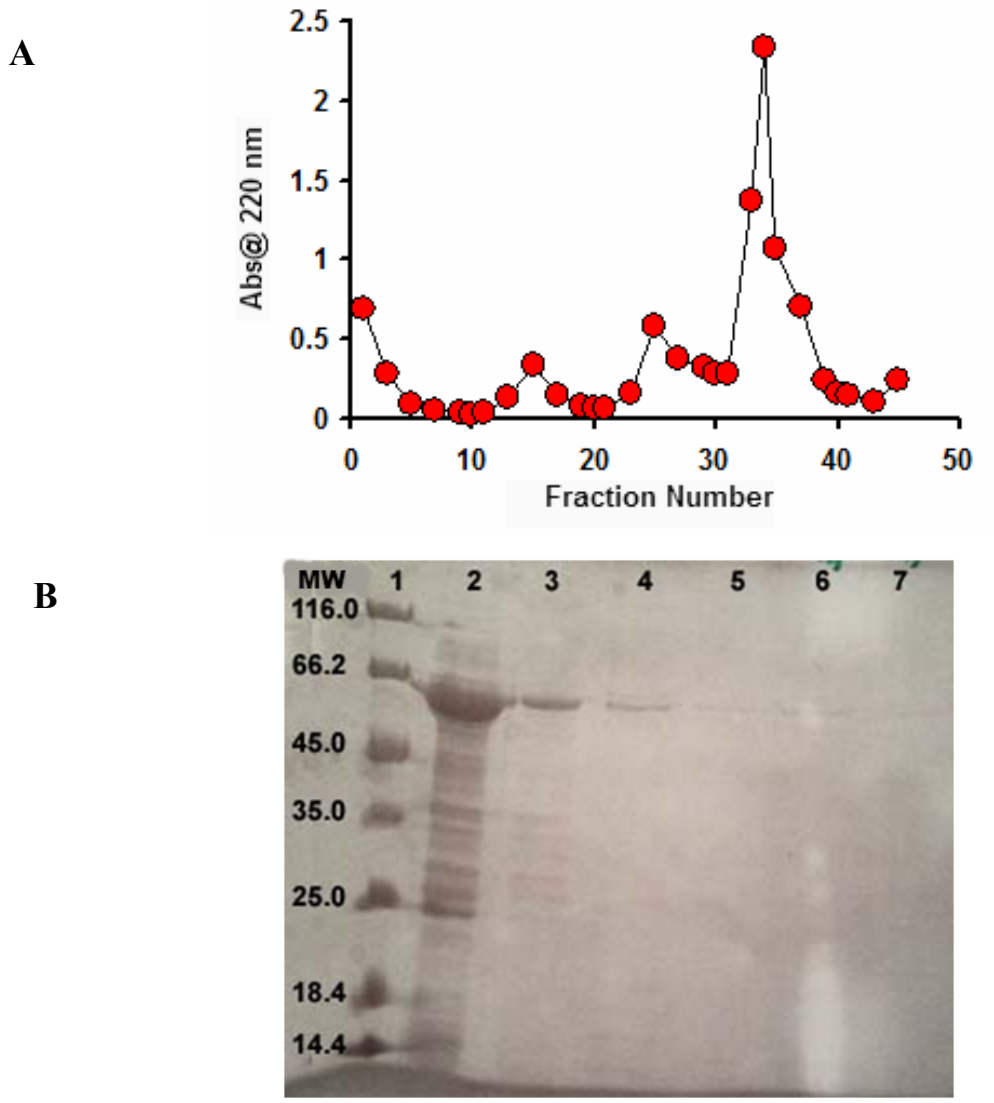

Figure 2.7: A) Absorbance profile from the DEAE sepharose elution. B) SDS-polyacrylamide gel of the eluate from the same DEAE sepharose column. Lane 1: Protein marker. Lane 2: supernatant solution after base extraction. Lane 3: Flow-through solution. Lane 4: fraction 25. Lane 5: fraction 15. Lane 6: fraction 34. Lane 7: fraction 35

Two additional ion exchange drip columns charged with either Resource S (6 mL) or Resource Q (8 mL) were also tested as means of APS purification. These columns were, after equilibration, loaded with Tris buffer (20 mM Tris base, 5 mM EDTA, 5 mM βME, pH 7.0) solutions of APS, and eluted with the same loading buffer supplemented with 1 M NaCl. Again, no positive results were obtained. All protein eluted with the initial loading, unsalted buffer (i.e. in the flow-through solution, Figure 2.8).

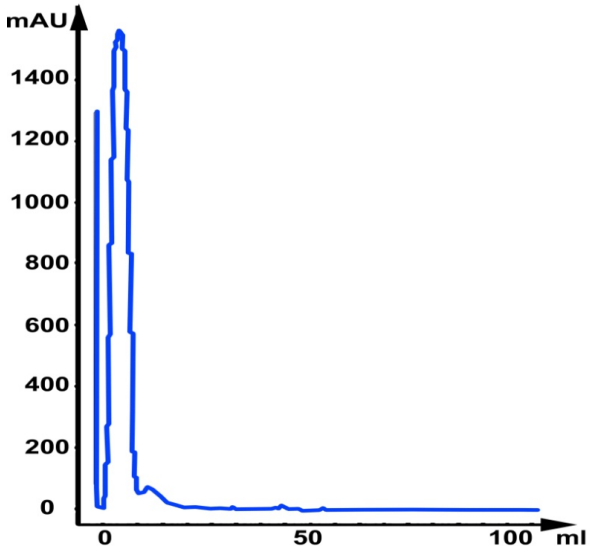

Figure 2.8: Elution profile from a Resource S column for the supernatant solution after base extraction.

2.5.2 Ammonium sulphate precipitation

Ammonium sulphate precipitation is an alternative method used to purify proteins.[141] This methodology is based on previous observations showing that protein aggregation might be overcome at high salt concentrations due to neutralization of charges at their solvent exposed surfaces Thus, this protocol might constitute, in some cases, a simple means of fractionating proteins. Charge neutralization means that proteins will tend to bind together, form large complexes and precipitate out of the solution, allowing collection by centrifugation. Since each protein will start to aggregate at a characteristic salt concentration, this approach provides a simple way of enriching a particular soluble protein from a mixture. Furthermore the tendency of different proteins in the lysate to

aggregate differs as a function of ammonium sulfate concentration, proteins are separated in distinct fractions.

In the present case, the percentage of ammonium sulfate saturation was increased stepwise from 10% to 90% adding powdered ammonium sulphate to the crude enzyme solution, and stirring for 1 h after each addition.[142] Unfortunately, after adding 60% ammonium sulphate, APS precipitated along with nearly all the other *E. coli* proteins present, obtained after sonication. This method did not improve the purity of APS as shown in Figure 2.9.

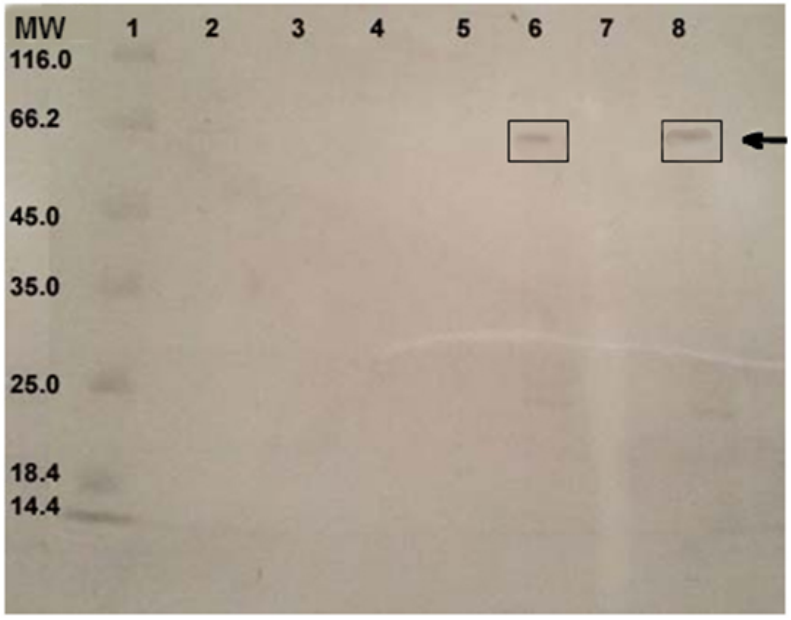

Figure 2.9: SDS-PAGE analysis of various ammonium sulphate precipitates from the base extracted crude cell lysate. Lane 1: protein marker. Lane 2: 20% saturated. Lane 3: 30% saturated. Lane 4: 40% saturated. Lane 5: 50% saturated. Lane 6: 60% saturated. Lane 7: 70% saturated. Lane 8: 80% saturated.

2.5.3 Hydrophobic interaction chromatography (HIC)

Hydrophobic Interaction Chromatography[135] (HIC) is a separation technique that uses the physical property of hydrophobicity to separate proteins from one another. In this type of separation/purification, hydrophobic hydrocarbon groups (e.g. phenyl, octyl, or butyl) form the contact surface of the stationary column to allow interactions with the exposed surface of a well-folded protein. As a result, proteins passing through the column that have hydrophobic residues on their surfaces elute more slowly, and

separate from those that do not. To secure this protein-resin non-covalent interaction, a buffer with a high ionic strength is initially applied to the column. The high salt content of the buffer reduces the solvation of the protein sample, thus as solvation decreases, the exposed hydrophobic regions of the protein are adsorbed, resulting in retention of the enzyme. Then, as the salt concentration is gradually decreased elution occurs in order of increasing hydrophobicity.

Various 1 mL HIC columns of different media were tested to purify APS (materials and methods). Briefly, after equilibration with start buffer (50 mM sodium phosphate buffer, 1 M NaCl, pH 7.0), the HIC column was loaded with a solution of the protein in starting buffer. Proteins were eluted with a decreasing NaCl gradient (1 M to 0 M) in 15 column volumes using a flow rate of 1 mL/min. 1 mL fractions were collected. Unfortunately, as exemplified in Figure 2.10 for the Hi Trap phenyl HP column, protein did not bind to any of the employed HIC columns, and eluted only 2 minutes after loading.

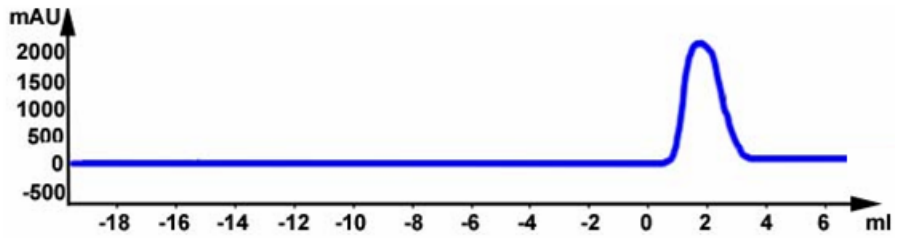

Figure 2.10: Elution profile of APS using a Hi Trap phenyl HP column. All protein eluted 2 minutes after loading to the column.

2.5.4 Size exclusion chromatography

To separate molecules of different molecular weights, **s**ize exclusion chromatography[94,143] (SEC) uses stationary materials (resins) harbouring porous particles/materials. Thus, molecules that are smaller than the pore size of the resin will enter the particles and remain in the column. The average residence time of the particles depends mostly on size, but the shape of the analyte is also important. In contrast, larger molecules, will elute as part of the flow-through, or void volume. Different molecules therefore have different total transit times through the column. Molecules that are smaller than the pore size can enter all pores, and have the longest residence time on the

column and elute together as the last peak in the chromatogram. This last peak in the chromatogram determines the total permeation limit.

For the present APS protein, size exclusion chromatography (SEC) was performed on a Superdex-200 (330 mL) column. This column was selected over Superdex-75 (330 mL) because the MW of APS[13] (65000) is close to the upper limit of the latter (i.e. Superdex-75 work best for proteins with MW of 3000-70000 and Superdex-200 best for proteins with MW of 10000-600000) range. Although most of APS (95%) eluted at the void volume and as an aggregate, it was possible to get 90% pure protein as aggregate (Figure 2.11). when Tris buffer (20 mM Tris, 5 mM EDTA, 5 mM βME and 0.15 M NaCl at pH 8.0) was used at a constant flow rate of 2 mL/min.

A

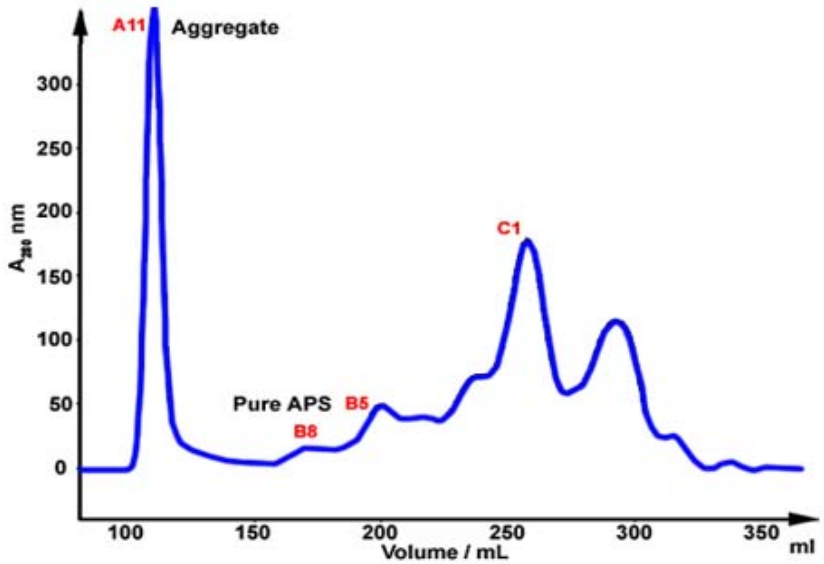

B

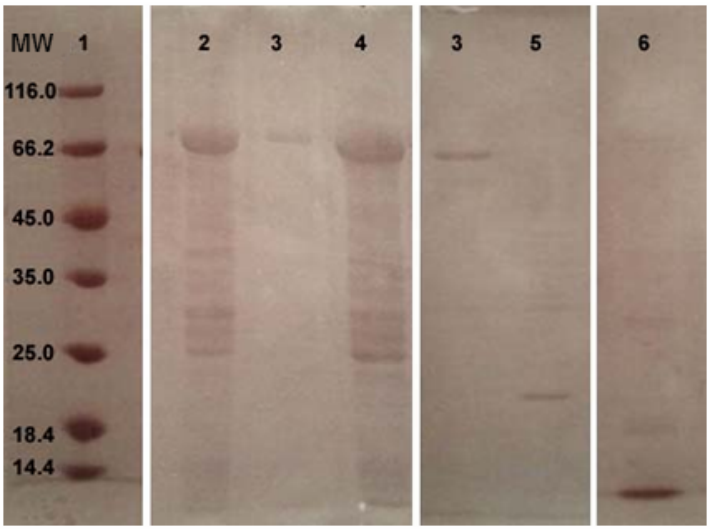

Figure 2.11: A: Elution profile of the base extracted APS solution from a Superdex 200 SEC column. B: SDS-polyacrylamide gel of the flow through solution and eluate from the Superdex 200 column. Lane 1: Protein marker. Lane 2: fraction A11 (aggregate peak). Lane 3: fraction B8. Lane 4: crude protein. Lane 5: fraction B5. Lane 6: fraction C1.

Following this preliminary result, different concentrations of crude protein were used to reduce aggregation prior elution from the SEC column. Unfortunately, dilution of the protein up to x 5 or the use of detergents such us 0.1% (v/v Tween 20 detergent did not substantially improve the amount of purified protein isolated (Figure 2.12).

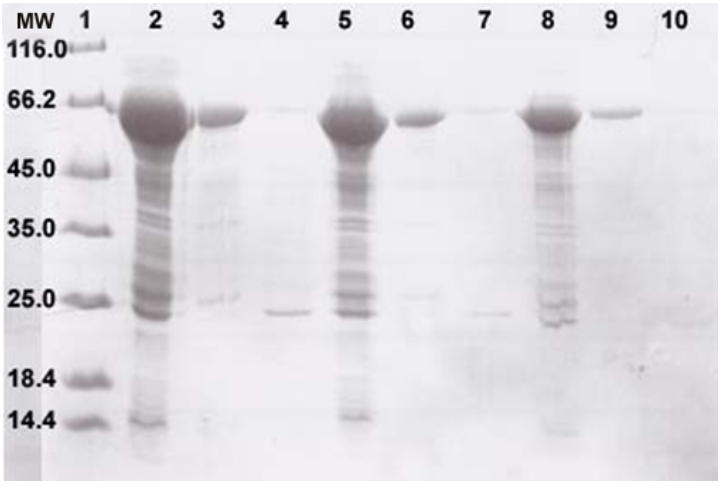

Figure 2.12: SDS-polyacrylamide gel of the flow through solution and eluate from the Superdex 200 column. Lane 1: protein marker. Lane 2: crude protein (no dilution). Lane 3: Fraction A11 (no dilution). Lane 4: Fraction B8 (no dilution). Lane 5: crude protein (2x dilution). Lane 6: fraction A11 (2x dilution). Lane 7: fraction B8 (2x dilution). Lane 8: crude protein (5x dilution). Lane 9: fraction A11 (5x dilution). Lane 10: fraction B10 (5x dilution).

2.5.5 Affinity Column Chromatography

Insertion of a histidine tag into APS

A widely used method for protein purification is by inserting six histidine residues at the N or C terminus of a protein.[9,10] This is achieved by DNA engineering. This 'his-tag' will then bind Ni^{2+} ions specifically and so can be used to separate the his-tagged protein from all other proteins. A concern however, is that the presence of the his-tag may affect the enzyme activity and so, in addition, it was decided to insert a TEV (Tobacco Etch Virus) cleavage site between the APS gene and the N-terminal his-tag. Since the expression vector pET 21d, harbouring the APS gene was initially designed to possess two stop codons, followed by 18 base pairs, a sequence coding for six histidine residues follow by a stop codon, it was straightforward to insert the TEV cleavage site by replacing the two stop codons. This DNA manipulation results in the desirable, removable tag of 6x histidines at the N-terminus of the protein.

PCR was performed in order to remove the two stop codons and to insert the codons for a TEV cleavage site (ENLYFQG) before the his-tag coding region. In the forward direction (5' to 3') a primer was designed to contain the existing hexa-histidine tag codons. In the reverse direction, a primer was designed to match the first 18 base pairs of the APS gene (N terminus) followed by a TEV cleavage site over-hang. The target plasmid was amplified by PCR and re-circularised using T4 DNA ligase. The expected expression vector was confirmed by DNA sequencing (Figure 2.13).

atttgccgcgtgtttcattacggctacaaataccgtgacggctttagtgtggcc

I C R V F H Y G Y K Y R D G F S V A

agtattgaaattaagaacctggtgacccgcaccgtcgtcgaaaccgtcccactg

S I E I K N L V T R T V V E T V P L

gaaaacctgtattttcagggccaccaccaccaccaccactgagat

E N L Y F Q G H H H H H H - D

Figure 2.13: Partial DNA sequence of the his-tagged APS (HAPS) gene. Part of the HAPS coding region is shown in blue, the TEV cleavage site coding region is shown in red, his-tag in green and stop codon in brown. The amino acid sequence that the gene encodes for is shown below the DNA sequence as a one-letter code.

For the final production of His tagged α-pinene synthase protein (HAPS), *E. coli* BL21 Codon Plus (DE3) RIL cells were used to express the gene described above. Thus, cultures were grown at 37 °C followed by induction using IPTG (0.5 mM) at 37 °C for 4 hours as previously described (section 2.3) for APS. The protein was found again as inclusion bodies and then solubilised as described in section 2.4 by acid/base treatment. Purification of the resulting solution HAPS supernatant 2 using Ni affinity chromatography was then attempted. The supernatant 2 obtained after base extraction as described in section 2.4 was dialysed against binding buffer (100 mM Tris, 500 mM NaCl, 1mM imidazole, and 5 mM βME) and loaded onto a Ni^{2+} affinity column (*HisTrap FF Crude*, 1 mL column) pre-equilibrated with binding buffer using an *AKTA FPLC* system. Binding buffer (20 column volumes) was then passed through at a flow rate of 1 mL/min, and fractions (10 mL) were collected. Protein was eluted at 1 mL/min/fraction using a 20 to 500 mM gradient of imidazole in binding buffer over 10 column volumes. Fractions containing HAPS were collected and protein purity was assessed using SDS-PAGE (Figure 2.14).

Similarly, the nickel affinity purification of APS was also accomplished using a Ni^{2+}-Sepharose™ 6 Fast Flow drip column (GE Healthcare, 5 mL) following a procedure similar to that described above. In short, after equilibration, and loading, the column was washed with binding buffer (10 column volumes) prior to elution of HAPS

(approximately at 2-3 mL/min) using a 50 to 500 mM imidazole gradient in binding buffer. HAPS eluted at approximately 50-200 mM imidazole as indicated by SDS gel (Figure 2.15).

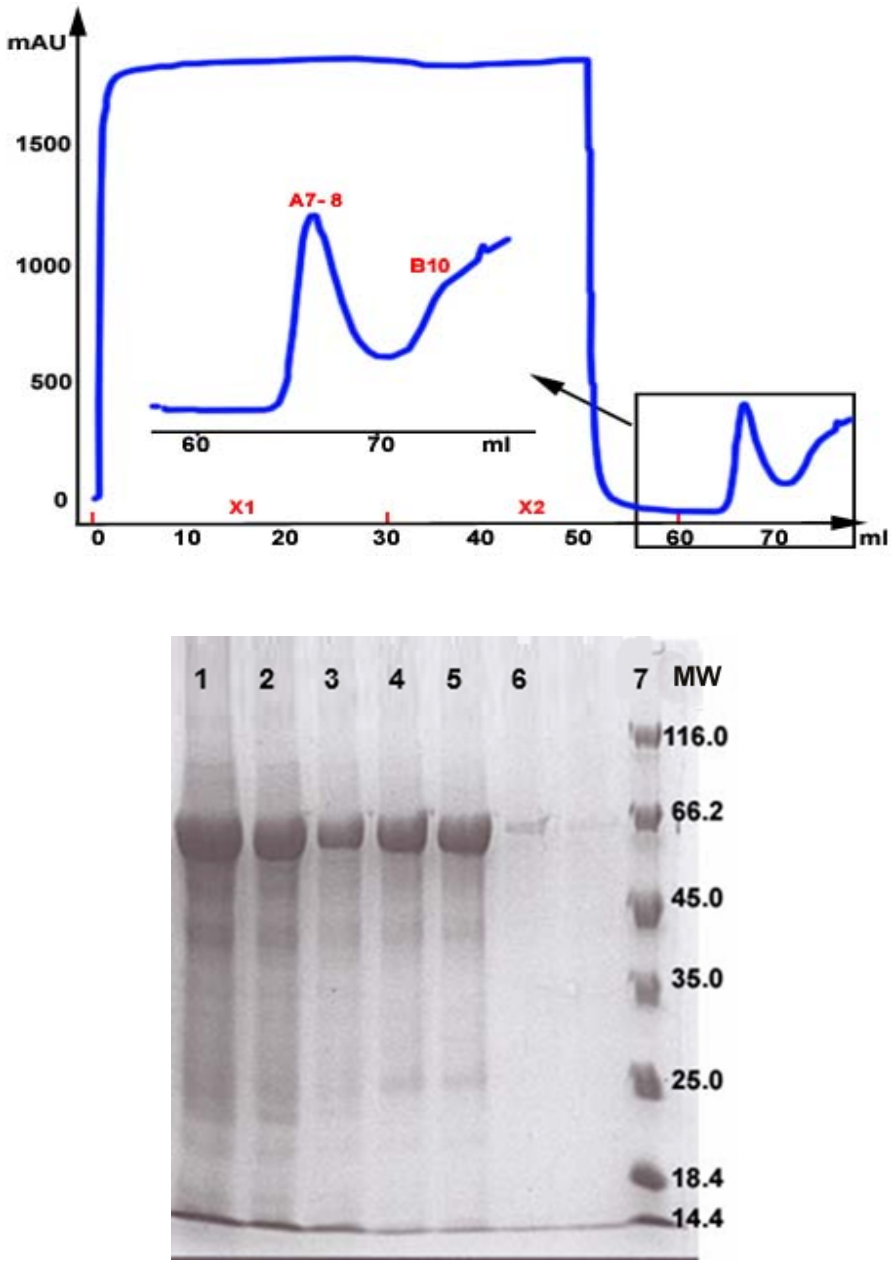

Figure 2.14: A) Elution profile of the base-extracted HAPS solution from a HisTrap FF column. B) SDS-polyacrylamide gel of the flow through solution and eluate from the Ni2+ affinity chromatography. Lane 1: crude protein solution. Lane 2: fraction X1. Lane 3: fraction X2. Lane 4: fraction A7. Lane 5: fraction A8. Lane 6: fraction B10. Lane 7: protein marker.

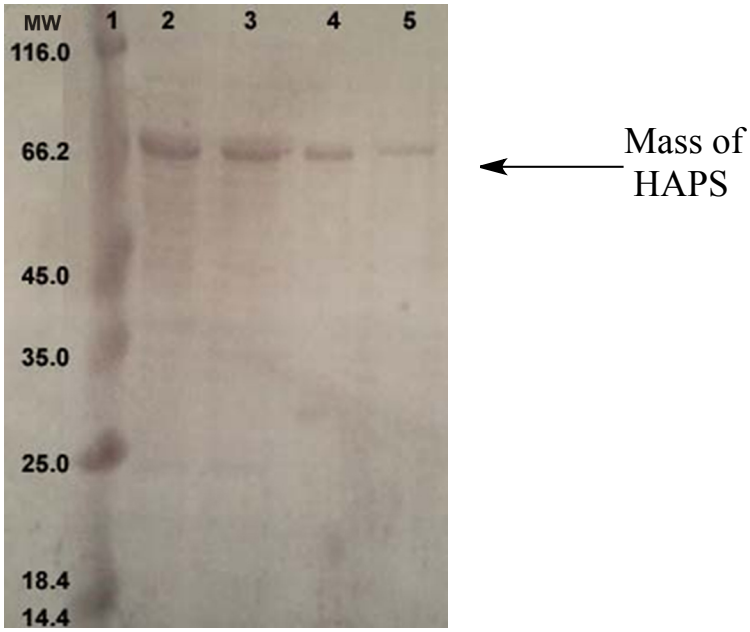

Figure 2.15: SDS-polyacrylamide gel of the flow through solution and eluate from the Ni^{2+} sepharose drip column. Lane 1: protein marker. Lane 2: crude protein after base extraction. Lane 3: flow-through. Lane 4: eluate with 150 mM imidazole. Lane 5: eluate with 200 mM imidazole.

Fractions containing protein of the correct molecular weight were pooled and dialyzed overnight against storing buffer (10 mM Tris, 5 mM βME, pH 7.5.) HAPS was concentrated to a final volume of ~10 mL (AMICON system, YM 30). This YM 30 ultrafiltration disc is made out of regenerated cellulose and has 30 *kDa* nominal molecular weight limit (*NMWL*). Typically this membrane is used for desalting or alternatively concentrating of proteins. Glycerol (10% total volume) was added and the resulting dialysed solution was aliquoted (1 mL) and stored at -20°C. The concentration of protein was measured using the Bradford method[144] and found to be 40 μM.

2.6 Product profile of purified (+)-HAPS.

The ability of HAPS to produce (+)-α-pinene was assessed on an analytical scale. HAPS (20 μM) were incubated with GDP (2.0 mM, 25 μL) in reaction buffer (0.5 mL, 100 mM Bis-Tris propane, 50 mM KCl and 20 mM $MgCl_2$, pH 7.5). The aqueous layer was overlaid with 0.5 mL pentane and sealed to trap enzymatic volatiles produced by HAPS. After gentle shaking overnight at room temperature, the organic layer was removed and the aqueous layer was extracted with additional pentane (0.5 mL x 2). The

pooled pentane extracts were passed through a short silica gel column (≈ 3 g silica) in a Pasteur pipette prior to analysis of products by GC-MS. Injections (10 µL) were performed in split mode (split ratio 5:1) at 50 °C. The GC program was as follows: initial oven temperature of 49 °C, held for 1 min followed by a ramp of 4 °C min^{-1} for 25.25 min to final temp of 150 °C.

The total ion chromatogram (TIC) showed a single major product (*m/z* 136) (Figure 2.16), identified as α-pinene by co-elution with an authentic standard from Sigma-Aldrich. This experiment clearly indicated that the HAPS obtained was catalytically active and gave the expected product. Incubations were repeated without enzyme (background), and the analysis of volatiles was also done without the silica gel filtration step. These experiments revealed the mandatory presence of HAPS for the production of α-pinene, and the absence of any enzyme generated C10 alcohol.

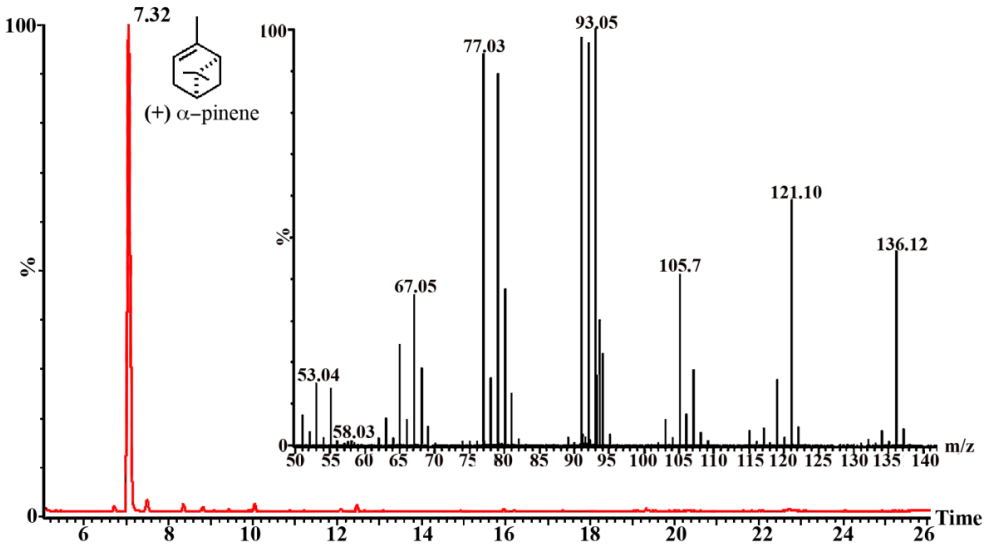

Figure 2.16: Total ion chromatogram of the pentane extractable products from incubation of GDP with HAPS. The product was identified as (+)-α -pinene by coinjection with an authentic standard (Sigma-Aldrich). Inset: EI^+-mass spectrum of (+)-α -pinene.

As had been reported previously,[5] in addition to (+)-α-pinene (**2**) (91%) the recombinant enzyme also generated small amounts of camphene, β-pinene , β-myrcene, 3-carene, limonene and terpinolene and an unidentified monoterpene (98% conversion from GDP (Figure 2.17)). The figure was calculated from calibration curves using racemic α-pinene (see section 3.3.1 for details).

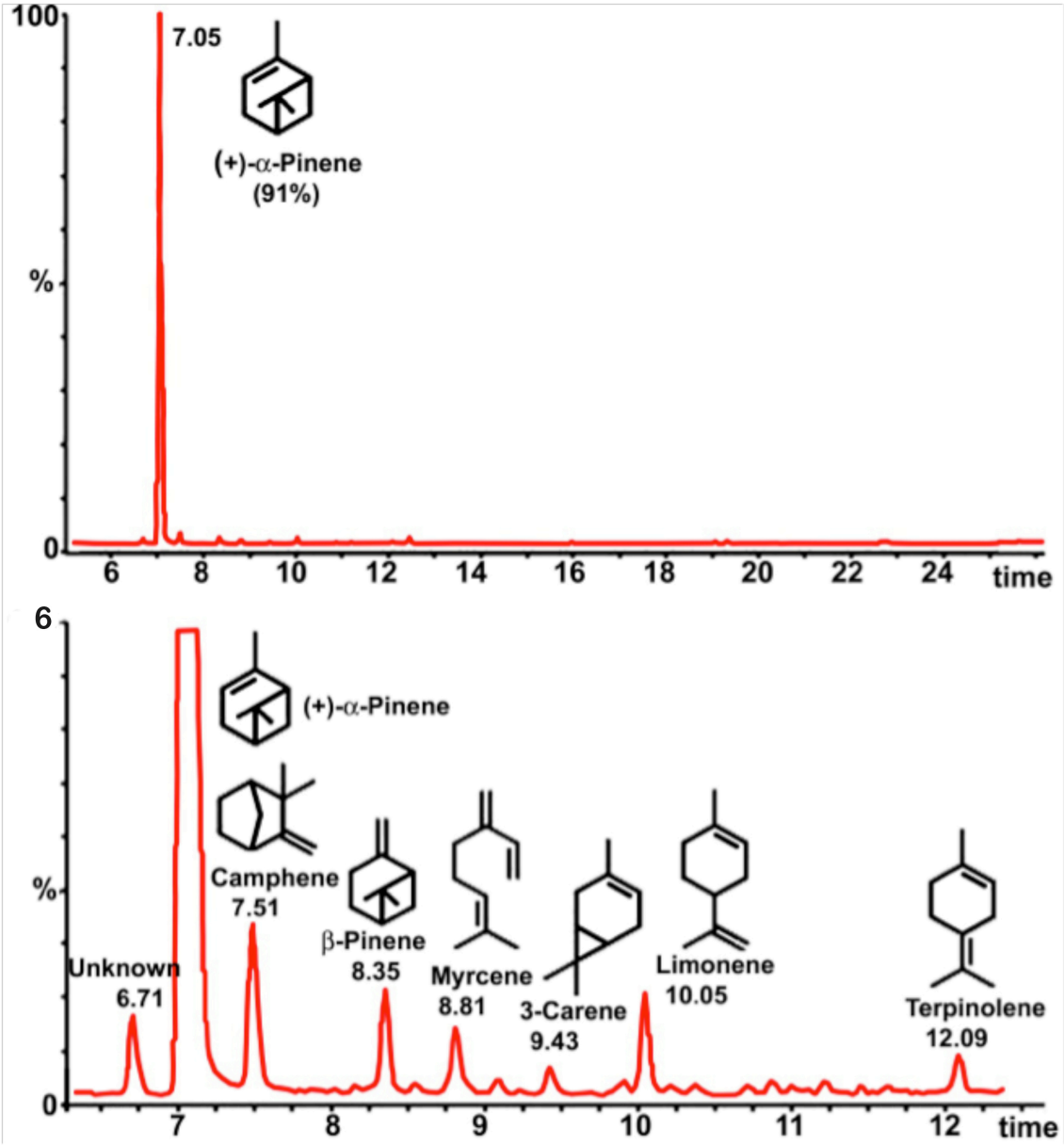

Figure 2.17: Top: Total ion chromatogram of the pentane extractable products derived from incubation of GDP with HAPS at two levels of sensitivity. Bottom: Expanded TIC highlighting 6-12 min time span.

All products except the peak at 6.71 min were identified by co-elution with authentic material and comparison with their mass spectra with those available in the NIST (National Institute of Standards and Technology) library. The compound eluting at 6.71 min was tentatively identified as tricyclene (1,7,7-trimethyltricyclo-[2.2.1.$0^{2.6}$]-heptane, based on MS comparisons (Figure 2.18 and 2.19).

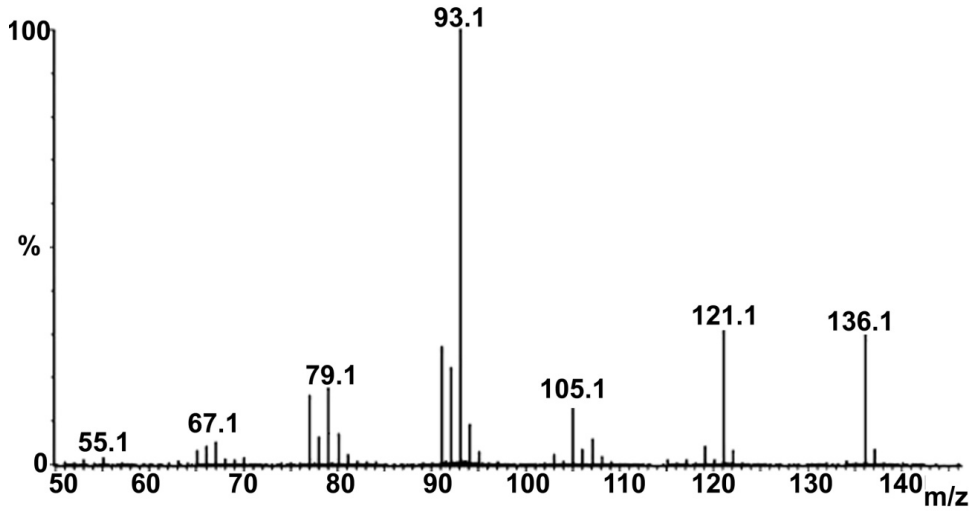

Figure 2.18: Mass spectrum of the compound eluting at 6.71 min in Fig. 2.17.

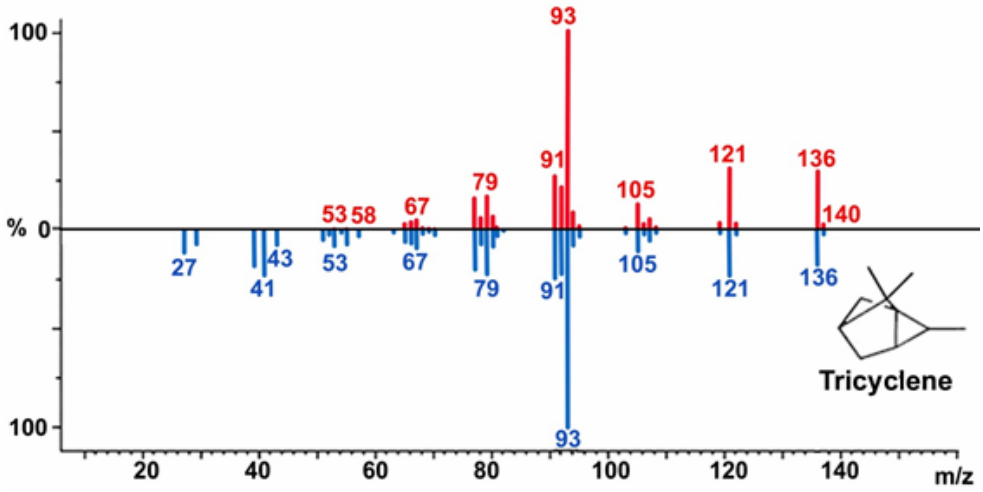

Figure 2.19: Head to tail comparison of the mass spectrum of the compound eluting at 6.71 min in Fig. 2.17 (red) with the mass spectrum of tricyclene from the NIST library (blue).

2.6.1 Chiral GC analysis of (+)-α-pinene

Gas Chromatography with flame ionisation detector (GC-FID) (Perkin Elmer 8700) analysis of the extracts from incubations of GDP and HAPS using a chiral stationary phase (Supelco DM beta-Dex L20 column (30 m x 0.25 mm internal diameter) and comparisons with an authentic sample of (±)-α -pinene (Fig. 2.22) indicated that the enzymatic (+)-α-pinene was enantiomerically pure ((>98%). Chiral GC analyses was performed isothermally at 80 °C (Figure 2.20).

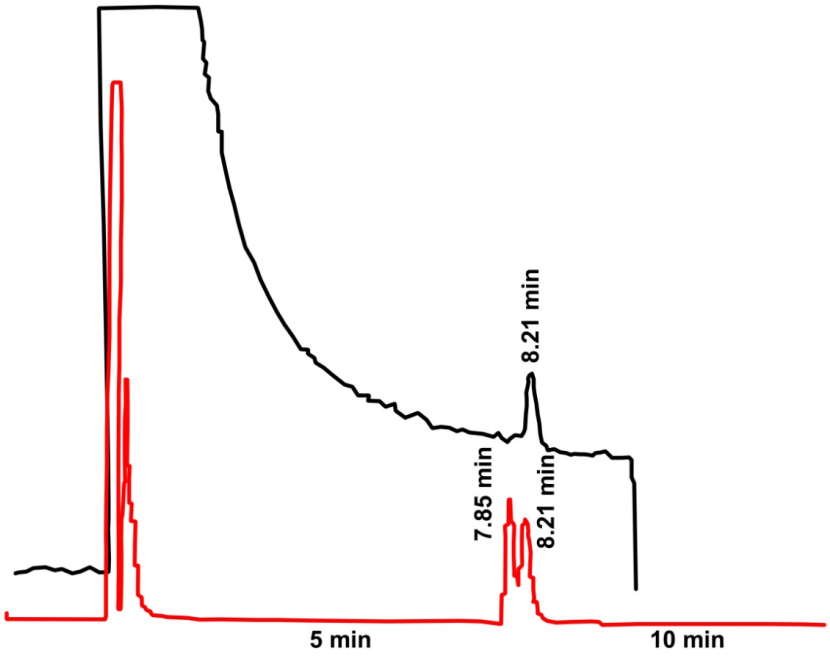

Figure 2.20: Red: FID gas chromatogram of commercial (±)-α-pinene passed over a β-cyclodextrin stationary phase. Black: (+)-α-pinene generated from incubation of GDP with HAPS.

2.7 Optimisation of (+)-APS catalysed production of α-pinene

To evaluate the optimum conditions for large-scale production of (+)-a-pinene by HAPS, a fixed concentration of enzyme (10 μM, 25 μL) was first incubated with fixed concentration of GDP on an analytical scale at different pH, temperatures, concentrations of substrate, cofactors (metals). To determine the optimal enzyme concentration, incubations were performed at varying enzyme and fixed GDP concentrations.

2.7.1 Optimum Mg^{2+} concentration

For analysis of the optimum Mg^{2+} concentration, 2mM GDP was used in a 0.5 mL final volume. The buffer consisted of Bis-Tris propane (100 mM), KCl (50 mM), $MgCl_2$ and DTT (1 mM), pH 7.5). The concentration of Mg^{2+} ion in the assay buffer was varied from 5 mM to 500 mM. Each mixture was overlaid with pentane (0.5 mL) and initiated by addition of enzyme (10 μM, 25 μL). After incubation for 16 h the pentane layer was removed (as described above, section 2.6), and then analysed by GC-MS. The total ion count of the integrated α-pinene peak was used to estimate the quantity of α-pinene produced. The optimal Mg^{2+} ion concentration of α-pinene synthase was found to be 100 mM (Figure 2.21).

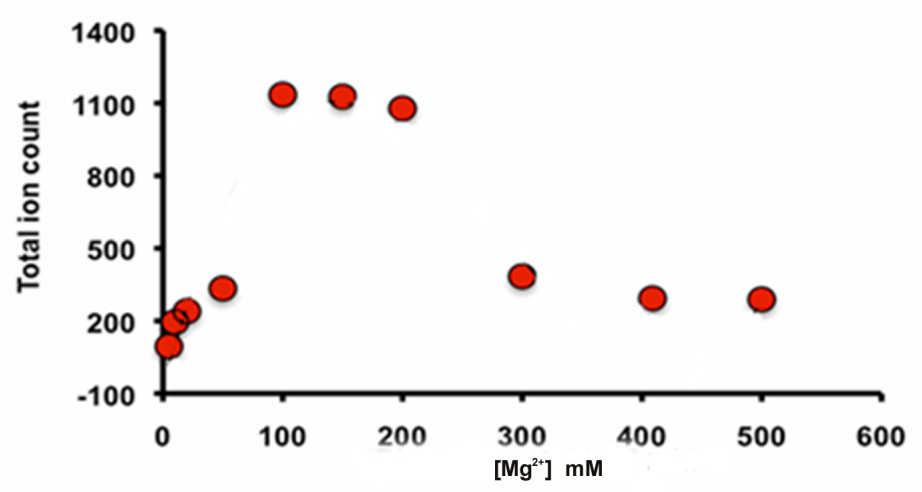

Figure 2.21: Effect of $[Mg^{2+}]$ on the total ion count for HAPS catalysed production of α-pinene

2.7.2 Optimum pH

To find the optimum pH for production of α-pinene, the enzyme was incubated with GDP under analytical conditions as stated above (section 2.6.1), varying the pH of the buffer from pH 6.0 to 9.5. The optimum Mg^{2+} (100 mM) concentration was used and the enzyme concentration was held constant (10 μM, 25 μL) as before. The optimal pH for the production of α-pinene was found to be 7.5 (Figure 2.22).

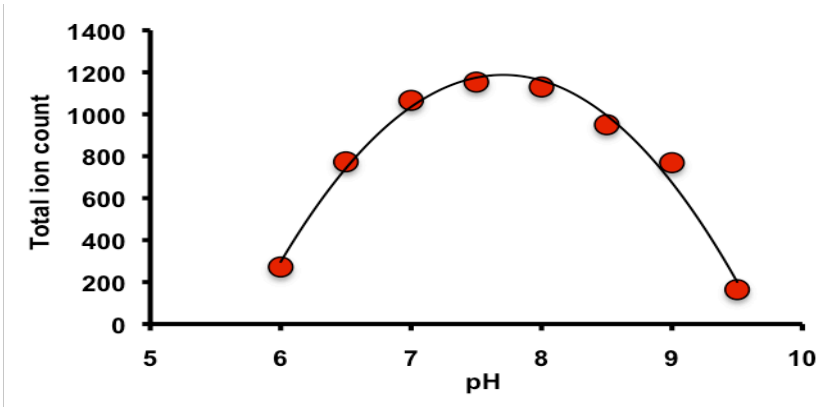

Figure 2.22: Effect of pH on the total ion count for HAPS catalysed production of α-pinene

2.7.3 Optimum temperature

To find out the optimum temperature for HAPS catalysis several runs were carried out under identical conditions. The optimum temperature for the enzyme activity was found to be 20 °C (Figure 2.23).

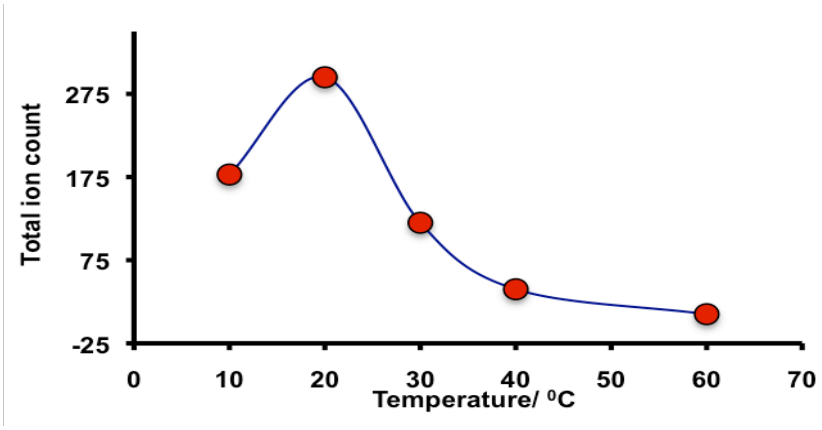

Figure 2.23: Effect of temperature for HAPS catalysed production of α-pinene.

Thus the best buffer solution and incubation conditions for the production of α-pinene were found to be Bis-Tris propane (100 mM), KCl (50 mM), $MgCl_2$ (100 mM) and DTT (1 mM), pH 7.5 at 20 °C.

2.8 Kinetic studies

The kinetic evaluation (K_M and k_{cat}) of HAPS was carried out using radiolabelled [1-^{3}H (specific activity 20 Ci/mmol)]-GDP under optimised reaction conditions (*vide supra*). As a start, the incubations were performed using 1 μM HAPS with 10 μM of [1-^{3}H] GDP in a buffer containing 100 mM Bis-Tris propane, pH 7.5, 50 mM KCl and 10 mM $MgCl_2$ and 1 mM DTT.

2.8.1 Time optimisation

Incubations were performed using different times (5 to 30 min) (for details see section 3.3.2). A reaction time of 20 min was chosen based on the linearity of the plot shown below (Figure 3.24).

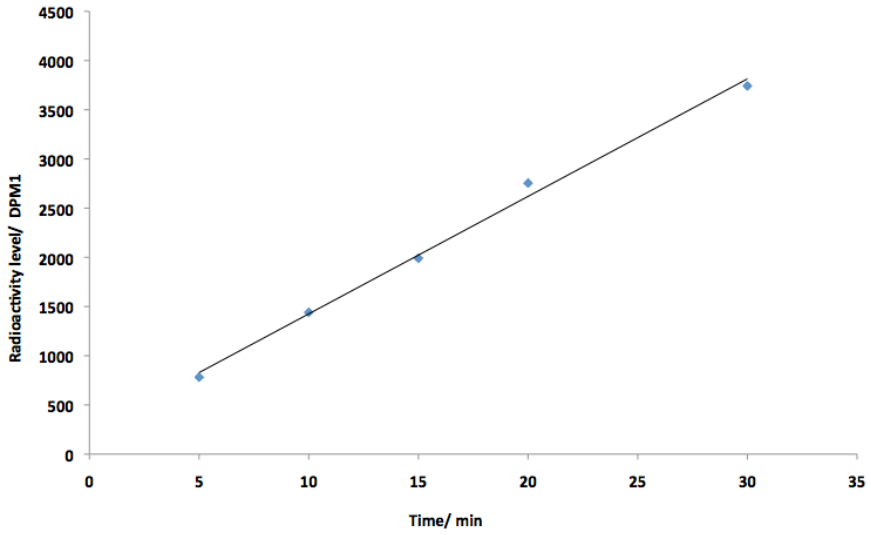

Figure 2.24: Time course for the production of pentane extractable products from incubation of [1-^{3}H]-GDP with HAPS.

2.8.2 Enzyme concentration optimisation

In this case, reactions (20 min) were performed at variable enzyme concentration (0 - 5 µM) using the aforementioned buffer solution (Figure 2.25).

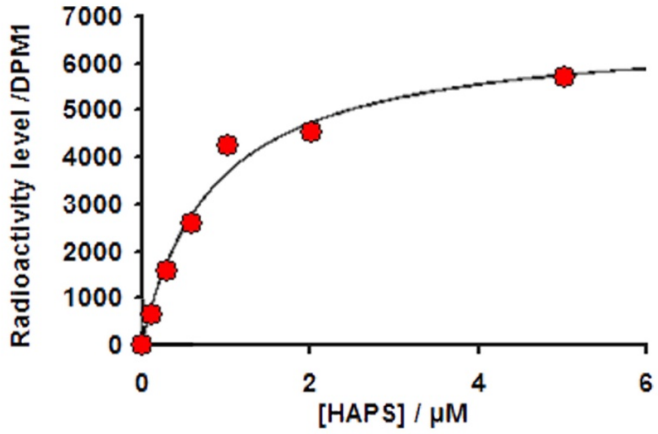

Figure 2.25: Plot of [HAPS] versus radioactivity (in DPM) for the formation of radiolabelled pentane extractable products after 20 min incubations of [1-^{3}H]-GDP with HAPS.

A concentration of 0.4 µM HAPS was defined as the optimal one from the initial linear range. Some terpene synthases have a tendency to aggregate at high concentrations leading to lower activity of the enzyme. This low concentration (0.4 µM HAPS) of HAPS (Figure 2.25) was selected to guarantee that no aggregation of the enzyme would occur, ensuring the necessary Michaelis-Menten conditions (rate proportional to [E]) needed for kinetic measurements.

2.8.3 Magnesium concentration optimisation

Using 0.4 µM of enzyme in buffer (100 mM Bis-Tris propane, pH 7.5, 50 mM KCl and 1mM DTT for 20 min (Figure 2.26) at different Mg^{2+} concentrations (5 µM to 50 µM), a concentration of 20 µM for Mg^{2+} was determined as optimal.

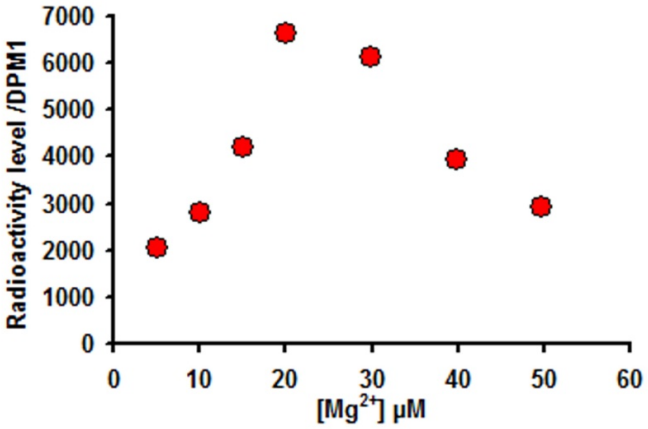

Figure 2.26: Plot of [Mg^{2+}] versus reaction velocity for the formation of radiolabelled pentane extractable products after 20 min incubations of [1-^{3}H]-GDP with HAPS

2.8.4 Temperature optimisation

To assess the optimal incubation temperature needed, reactions were performed at variable temperatures (10 to 45 °C) in a buffer containing 0.4 µM of enzyme, 20 mM Mg^{2+}, 100 mM Bis-Tris propane, pH 7.5, 50 mM KCl and 1mM DTT for 20 min (Figure 2.27).

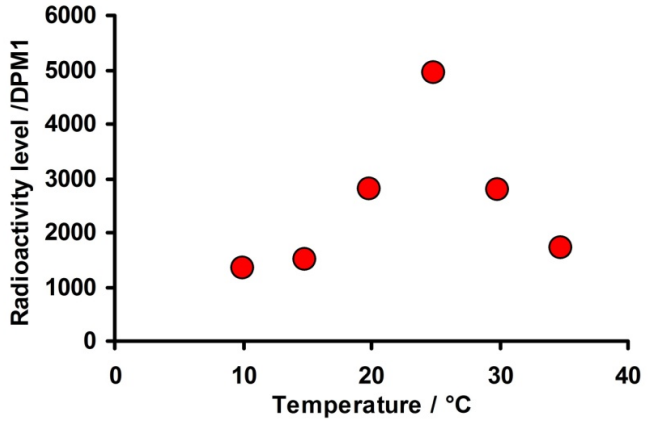

Figure 2.27: Plot of temperature versus reaction velocity for the formation of radiolabelled pentane extractable products after 20 min incubations of [1-^{3}H]-GDP with HAPS

A temperature of 25 °C was defined as the optimal temperature as it gives the best activity within a reasonable amount of time.

2.8.5 Determination of kinetic parameters for HAPS

The steady state kinetic parameters K_M and k_{cat} were determined using the optimised conditions described above (0.4 μM of enzyme, 20 mM Mg^{2+}, 25 °C and 20 min). Kinetic assays were performed using a variable concentration of [1-^{3}H] GDP from 10 to 120 μM (Figure 2.28).

The reaction mixtures containing GDP, protein and buffer were prepared on ice using eppendorf vials in a total volume of 250 mL and overlaid with 1 mL of HPLC-grade hexane prior incubation at 20 °C with shaking for 20 min. The reactions were then immediately ice-cooled and quenched by addition of 200 μL of a 100 mM EDTA solution (pH 8.5) and briefly vortexing. The hexane overlay and two additional 1 mL hexane extracts were passed through a short pipette column containing silica gel. The column was washed with an additional 1 mL of hexane, and the combined filtrates were analysed by liquid scintillation counting using 15 mL of scintillation cocktail. Steady-state kinetic parameters for wild-type HAPS were obtained by Michaelis-Menten equation ($V = (V_{max}[S]) / (K_M + [S])$) using the graphical procedures developed by Lineweaver-Burk[145,146] using the commercial SigmaPlot package (Systat Software).

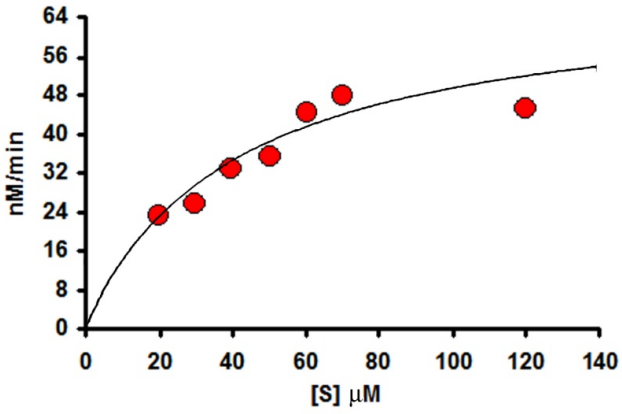

Figure 2.28: Michaelis-Menten profile for HAPS, incubating 0.4 μM HAPS with different concentrations of [1-^{3}H] GDP.

Based on three individual kinetic runs, the K_M value was found to be 40 ± 8 μM, and the k_{cat} value 0.001 ± 0.0004 s^{-1}. The K_M value is in good agreement with those previously reported.[15] The N-terminal hexa-histidine tag did not appear to affect the activity of the enzyme and all further experiments were performed with HAPS.

CHAPTER 3

Chemoenzymatic synthesis of the alarm pheromone (+)-verbenone from geranyl diphosphate (GDP)

3.1 Introduction

Semiochemicals can be defined as chemicals emitted by living organisms that provoke a behavioral or physiological reaction in other individuals. They can be classified as pheromones or allelochemicals based on how they are used and who gains advantage from them.[147] Semiochemicals such as phenolics, terpenoids and alkaloids have been exploited for their antimicrobial and insect–behaviour–modifying properties.[148] Volatile terpenoids are known to be involved in direct or indirect defense to attract or repel predators.[149,150] They are available in relatively large amounts as resins, waxes and essential oils, and are important renewable resources, providing a range of commercially useful products such as solvents, flavorings and fragrances, coatings, adhesives and synthetic intermediates.[158] The use of semiochemicals are environmentally friendly and reduce the utilisation of harmful and expensive insecticides and pesticides.[151,152] They also reduce negative effects on public health and environmental outcomes.[153]

Outbreaks of bark beetles and their associated fungal infections are major risks for conifer populations worldwide, destroying hundreds of acres of valuable trees every year.[159] In response to threats, conifers secrete various admixtures of defensive compounds. However bark beetles overcome the trees' defenses by mass attack, which is ultimately directed by aggregation pheromones emitted by the beetles, and the ability to vector phytopathogenic fungi.[154] Norway spruce (*Picea abies*) when attacked by *Ips typographus* beetles uses the monoterpene α-pinene (**12**) as a cue for host selection. Male beetles convert this C10 hydrocarbon into verbenone (**13**), which then serves as a dispersal alarm pheromone to modulate attack density.

A  B 

Figure 3.1: A. Image of a mountain pine beetle (*Dentroctonus ponderosae)*, B. Dead pine trees in a forest as a result of the beetles.

The prospect of generating enzymatically, relatively large quantities of enantiomerically pure (+)-α-pinene (**12**) (98%) from readily available geranyl diphosphate (**4**) (Chapter 2), opens the possibility of an alternative and attractive synthesis of (+)-verbenone (**13**) in enantiopure form. This chapter describes the efforts toward the development of an enzyme-guided asymmetric synthesis of (+)-verbenone (**13**) from GDP (**4**) in a simple two-step, one pot transformation. It should be mentioned that though (1*R*)-(+)-α-pinene (**12**) is commercially available in high enantiomeric excess (97%), the necessity of producing α-pinene enzymatically might not appear obvious. However, this pilot project was intended mostly as a proof of concept using a relatively simple target, and hence accumulate valuable evidence to assess in-depth the suitability of the approach to target more complex terpenoids such as artemisinin (**17**) or gossypol (**22**). Indeed, a chemoenzymatic synthesis of the antimalarial artemisinin (**17**) is a current endeavour within the Allemann group. In the ideal scenario, an *in situ* and high-yielding regiospecific allylic oxidation of the HAPS-generated α-pinene (**12**) will generate verbenone (**13**) in one step, without the need for purifying reaction intermediates (verbenol, **82**) (Figure 3.2), or the use of enzymes to further tailor α-pinene.

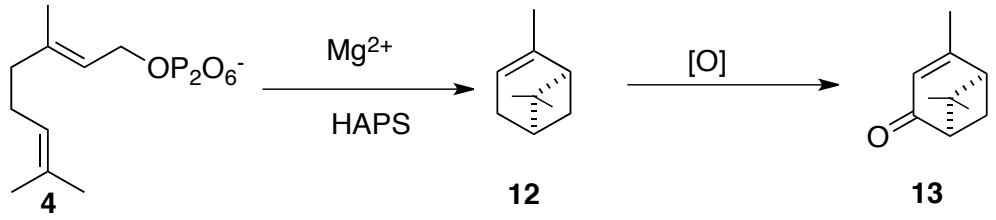

Figure 3.2: Proposed two-step synthesis of (+)-verbenone (**13**) from GDP (**4**).

3.2 Existing methods for the conversion of α-pinene to verbenone

Several methods have been previously reported for the conversion of α-pinene (**12**) to verbenone (**13**). What follows is a summary of previous syntheses.

Air oxidation is able to convert α-pinene (**12**) into verbenone (**13)**, however because this oxidation is very unselective, verbenone (**13**) is produced only in low to moderate yield, after cumbersome purification protocols.[155,156] For example, when molecular oxygen is used in combination with a Co(II) catalyst such as [Co(4-methylpyridine)$_2$Br$_2$], verbenone (**13**) was obtained in only 37% yield after heating for 6.5 h at 100 °C. The most abundant side products were verbenol (**82**) and α-pinene oxide (**83**). Other minor products, derived from further rearrangement of the α-pinene oxide byproduct, included α-campholene aldehyde (**84**), trans-pinocarveol (**85**), trans-carveol (**86**), trans-sobrerol (**87**) and trans-3-pinen-2-ol (**88**) (Figure 3.3).

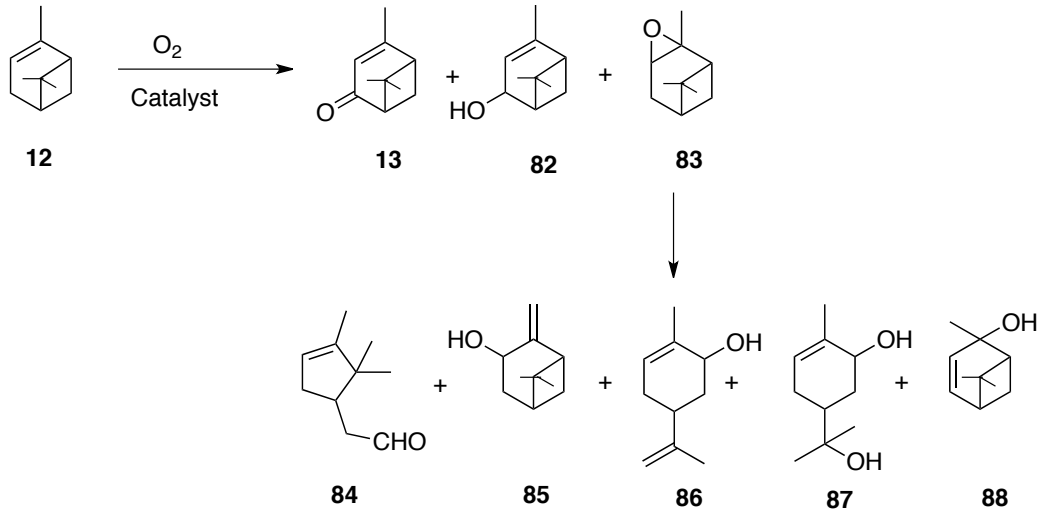

Figure 3.3: Side products from the α-pinene oxidation with molecular oxygen.[156]

Various homogeneous and heterogeneous catalysts have also been used to effect this conversion[157,158] including a three step process that uses $Pb(OAc)_4$ followed by base-catalysed hydrolysis of the product and oxidation of the epimeric verbenol with $Na_2Cr_2O_7$.[159]

Conversion of **12** to **13** using cell suspension cultures from *Psychotria brachyceras* and *Rauvolfia sellowii* has been reported,[160] thus showing the potential of native plant cell suspension cultures in organic synthesis. These protocols give rise initially to the precursor of verbenone, the allylic alcohol trans-verbenol, which is futher, but slowly, oxidized to verbenone. This microbial-based technology is therefore better suited for the preparation of the aggregation pheromone verbenol (Figure. 3.4) in moderate yield (56.9-68.5 % after incubation for 10 days). Nevertheless, other oxidized products such as *trans*-pinocarveol, *cis*-verbenol and myrtenol were inevitably produced as minor products.

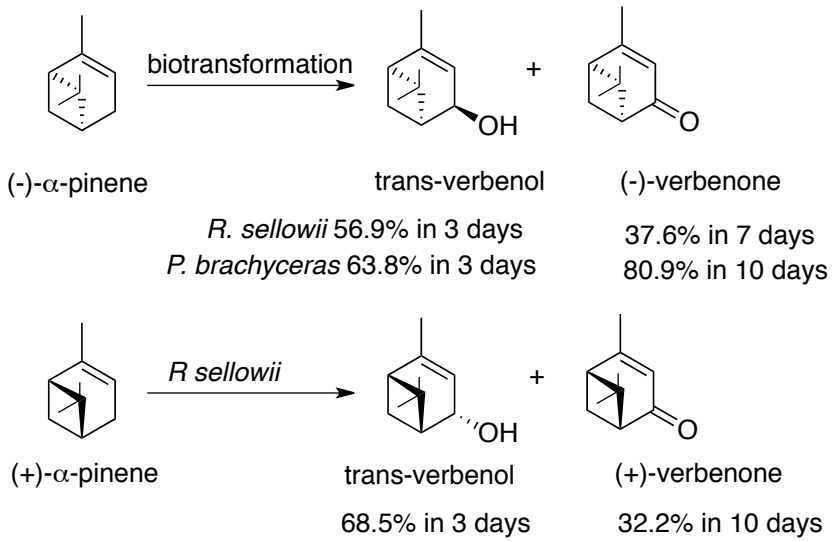

Figure 3.4: Biotransformation of α-pinene carried out by *Psychotria brachyceras* and *Rauvolfia sellowii*.[160]

It has been shown previously that α-pinene (**12**) can be converted to verbenone (**13**) without the need for isolating the precursor verbenol (**82**).[161] This relatively high yielding (65%) approach involves the chromium-catalysed t-butyl hydroperoxide oxidation of the hydrocarbon (α-pinene, **12**) to the enone (verbenone, **13**), and hence seemed ideal to attempt a total synthesis of **13** starting from GDP (**4**) with our in-house generated HAPS.[161] It was speculated that the simplicity and high yield of this methodology combined with the compatibility of the reagents with those utilize in terpene synthase catalysed reactions (buffer, pH, co-factors…etc) might allow the use of an advantageous two-phase system to carry out the enzymatic (**4** to **12**) and oxidation (**12** to **13**) reactions in the same flask (Figure 3.5).

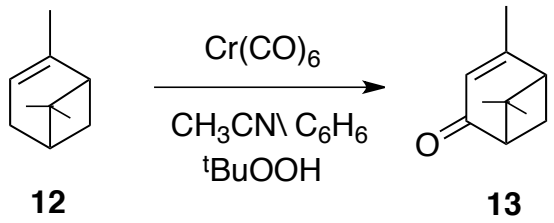

Figure 3.5: Synthesis of (±)-verbenone (**13**) from (±)-α-pinene (**12**)

3.3 (+)-α-Pinene synthase (HAPS)

By comparison, a chemical total synthesis of **α**-pinene (**12**) and then verbenone (**13**) would necessarily require the construction of a complex [3.1.1]-bicyclo ring system with control of the stereochemistry at the two bridged centers and the regiospecific introduction of a trisubstituted double bond. It is worth mentioning that to date no total synthesis of α-pinene exists. In contrast, the Mg^{2+}-dependent enzymatic cyclisation of GDP (**4**) catalysed by HAPS achieves all these complex synthetic tasks in one single step.[159,162] Thus the combination of this enzymatic reaction with an oxidation catalyst such us ($Cr(CO)_6$) might allow a novel chemoenzymatic synthesis of verbenone.

A codon optimised synthetic gene for HAPS from *Pinus taeda* was inserted into the vector pET21d for production of the enzyme in *E. coli*. To facilitate purification, a hexa-histidine tag (His_6) and a TEV cleavage site were inserted at the 3' end of the APS coding region. *E. coli* BL21 (DE3) RIL cells were transformed with the resulting plasmid. APS-His_6, and enzyme production was induced with IPTG. The resulting recombinant α-pinene synthase (HAPS) was purified by Ni^{2+}-affinity chromatography (see section 2.5.5 for details).

3.3.1 Calibration of α-pinene concentration

In order to estimate the chemical yield (or conversion) of the enzymatic reaction, pentane solutions of racemic α-pinene (**12**) of known concentration (0.1-0.9 mM) were prepared as standards, and analysed by GC-MS (conditions as above). The total ion counts under the peak corresponding to α-pinene (**12**) in the TIC were then plotted against the concentration of α-pinene (**12**) to obtain the required calibration curve of α-pinene (**12**) (Figure 3.6).

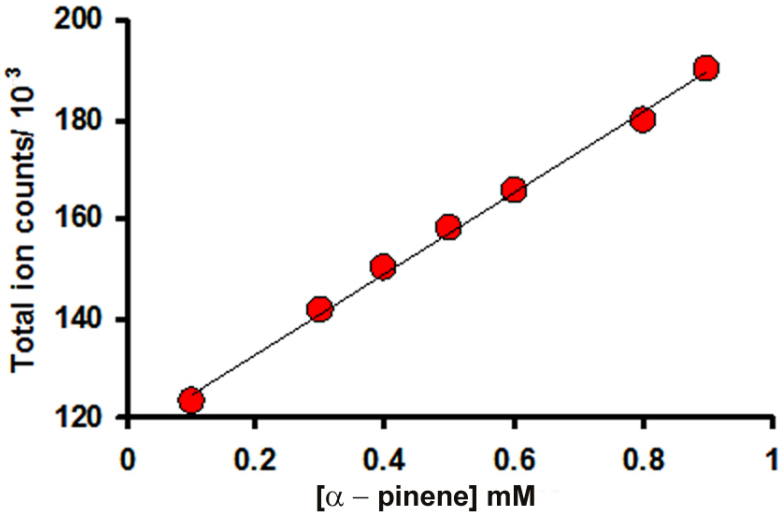

Figure 3.6: Calibration curve for determination of GDP concentration by GC-MS. Graph shows total ion counts (average after 2 repeats) for the integrated α-pinene peak versus known concentrations of racemic α-pinene (Sigma-Aldrich).

3.3.2 Analytical incubation of HAPS with GDP (4)

The ability of HAPS to produce α-pinene (**12**) was tested using analytical scale incubations. In brief, HAPS (20 μM) was incubated with GDP (**4**) (2.0 mM, 25 μL) in incubation buffer (100 mM Bis-Tris propane, pH 7.5, 50 mM KCl and 20 mM $MgCl_2$) in a final volume of 0.5 mL. The reaction solution was overlaid with 0.5 mL pentane to capture volatiles. After gentle shaking overnight at room temperature, the organic layer was removed and the aqueous layer was extracted with additional pentane (0.5 mL). The pooled pentane extracts were filtered through silica (≈3 g) and the eluent was analyzed by GC-MS. The total ion chromatogram (TIC) showed a single major product (*m/z* 136) (Figure 2.16), which was positively identified as α-pinene (**12**) by co-elution with an authentic standard. Incubations were repeated without enzyme, or without filtration to check for possible enzyme derived alcohol products (see section 2.6 for details).

These experiments clearly indicate that the enzymatic preparartion of HAPS was catalytically functional producing 91% of the expected monoterpene when incubated with GDP (**4**).

3.4 Synthesis of verbenone from (±)-α-pinene

To develop the planned 2-step, 1 pot synthesis of verbenone from GDP (**4**), the oxidation reaction was extensively optimized through use of different temperatures, solvents and equivalents of Bu^tOOH and chromium catalyst relative to the substrate racemic α-pinene (**12**).

As background, the oxidation of racemic α-pinene was carried out first, exactly as described by Pearson *et al*.[161] This reaction was conducted on a 2 mmol scale. Thus, to a suspension of α-pinene (**12**) (277 mg, 2.03 mmol) and $Cr(CO)_6$ (224 mg,1.02 mmol) in a mixture of CH_3CN/benzene (5:1; 6 mL) was added dropwise 70% wt. aqueous solution of *t*BuOOH (0.61 ml, 6.1 mmol). The resulting mixture was heated under reflux for 17 h and then cooled in an ice bath. The solids were filtered and washed with additional benzene and ether. The resulting organic layer was extracted with 5% NaOH

(40 mL), and this basic layer was then back extracted with ether (3 x 20 mL). The combined organic extracts were dried ($MgSO_4$), filtered, and the solvent removed under reduced pressure. The residue was purified by flash column chromatography on silica gel to give racemic verbenone in 68% yield.

Hence, in the presence of chromium hexacarbonyl, t-butyl hydroperoxide causes the catalytic oxidation of α-pinene (**12**) to give verbenone (**13**). The authors of the above described reaction state that when benzene is used as the solvent, small amount of epoxides are formed as side products. By changing the solvent to acetonitrile this problem was overcome. α-Pinene (**12**) was not completely soluble in acetonitrile therefore a small amount of benzene was used as co-solvent (10:1 ratio).[161] Under these conditions, the reaction gave 68% yield when α-pinene (**12**) is refluxed for 18-20 hours. The remainder (32%) was starting material. Fortunately, this reaction was also successful when carried out on a small scale (2 mM of enzymatically produced (+)-α-pinene (**12**) in 1 mL of acetonitrile).

3.5 Development of a protocol towards production of verbenone (13) from enzymatically produced α-pinene (12)

The synthesis of verbenone from α-pinene (**12**) as stated in the section 3.4 required 10:1 mixture of benzene and acetonitrile as solvent. However, under the standard enzymatic incubation conditions (Section 2.6) α-pinene (**12**) is extracted from water into pentane, thus the ability of different solvents to trap the enzymatic volatiles produced was tested on small analytical incubations. Solvent screening through use of GC-MS indicated that benzene or CH_3CN alone could not be used due to enzymatic inactivation or precipitation of GDP (**4**), HAPS or both, possibly as a consequence of partial mixing with the aqueous solution. Similarly toluene and xylene also prevented the enzymatic reaction from taking place.

Conveniently, however, the $Cr(CO)_6$ catalysed oxidation of racemic pinene took place when pentane was used as the solvent (Table 1). Nevertheless, the limited solubility of $Cr(CO)_6$ in pentane required use of 20 molar equivalents of this reagent. It is known that in $Cr(CO)_6$ catalysed oxidation reactions;[165] CH_3CN acts both as a solvent and as a

ligand. Indeed, the addition of small amounts of CH_3CN (10% v/v) to pentane led to the efficient oxidation of **12** by ^{t}BuOOH in the presence of only 2 molar equivalents of $Cr(CO)_6$ with a yield of 56%. The slightly lower yield relative to the reaction carried out in CH_3CN could be attributed to use of pentane as a solvent, which likely reduces the stability (and solubility) of the Cr(0) catalyst. Although less efficient than CH_3CN in the single step reaction, pentane was essential for effective enzyme catalysed conversion of **4** to **13**. In addition, four molar equivalents of ^{t}BuOOH relative to the chromium reagent were necessary, but otherwise the results were consistent with previous studies employing this reaction.[161]

Surprisingly, after optimization with racemic α-pinene, when this reaction was attempted with the HAPS-produced (+)-α-pinene (**12**), no oxidation reaction was observed. It is well known that sulfur can poison metal-based catalysts.[164] Thus, it seemed possible that the amounts of β-mercaptoethanol (βME) present in the incubation buffer might be sufficient to inhibit the subsequent oxidation of pinene (**12**) to verbenol (**82**)/verbenone (**13**). This hypothesis was confirmed by carrying out the oxidation reaction of racemic α-pinene (**12**) in the presence of 1 mM βME. When a large excess of ^{t}BuOOH (15–30 molar equivalents) relative to α-pinene (**12**) was used, the reaction smoothly proceeds to verbenone. Thus the deleterious presence of βME could be successfully overcome simply by using an excess of the oxidant. Alternatively, the initial pentane solution containing the HAPS-produced α-pinene could be passed through a short column of silica gel to remove βME prior to $Cr(CO)_6$/^{t}BuOOH oxidation in a different reaction vessel.

Attempts to overcome the 2-phase reaction design were also made using non-aqueous incubations. To this end, aliquots (1 mL) of the stock HAPS solution (4 mM), Mg^{2+} concentration (20 mM) and pH (to 7.5) were adjusted and placed in Eppendorf tubes. Tubes were flash frozen by liq. N_2 and lyophilized.[163] Pentane (1 mL) and GDP (**4**) (2 mM) were added to the resulting residue, and the tube was tightly capped and kept at 25 °C for 12 h with moderate shaking. As a control, 500 μL of the usual aqueous buffer containing the same concentration of GDP (**4**) was added (overlaid with pentane (0.5 mL) and incubated under the same conditions. After incubation, the pentane layers of both experiments were analysed by GC-MS with negative results as (-)-α-pinene was

not detected in either case. This control experiment indicated that the enzyme was deactivated upon lyophilisation.

Table 1: Results of attempts at optimisation of the solvent system and reagent requirements for the chemoenzymatic synthesis of verbenone (**13**) from GDP (**4**)

[βME] in aq. buffer (mM)	$Cr(CO)_6$[a]	^tBuOOH[a]	Organic solvent	Yield (%)
5	—	—	CH_3CN	< 1[b]
5	—	—	C_6H_6	< 1[b]
5	—	—	$C_6H_5CH_3$	< 1[b]
5	—	—	p-xylene	< 1
5	10	15	n-C_5H_{12}	< 3
5	20	30	n-C_5H_{12}	< 3
0	20	30	n-C_5H_{12}	40[c]
0	2	8	10% CH_3CN in n-C_5H_{12}	50[c]

[a] Molar equivalents relative to GDP. [b] Yield is for α-pinene only, insufficient quantities were isolated for the oxidative step to be carried out. [c] Overall isolated yield of (+)-verbenone (**3**). As with the oxidation of commercial racemic α-pinene the remaining material was mostly unreacted α-pinene, in addition to small amounts of unidentified by-products. All the above reactions were carried out at reflux.

3.6 Preparative scale synthesis of (+)-verbenone from GDP

After assessing the scope and limitations of the aforementioned 2-step reaction sequence to convert GDP (**4**) into (+)-verbenone (**13**) using analytical-scale experiments, a preparative scale production of the semiochemical was targeted next. Thus, a dialyzed solution (4 mL) of HAPS (4 mM) was added to a 1.6 mM solution of GDP (**4**, 16 mg, 40 mmol) in incubation buffer (23 mL). The resulting reaction mixture was overlaid with pentane (10 mL), and the reaction vessel was sealed and gently shaken for 24 h at room temp. (+)-α-Pinene (**12**) was obtained in 89% yield from GDP (**4**) as judged by GC-MS comparisons with authentic standards of known concentration (Fig 3.6). To the combined pentane extracts (40 mL), containing the enzymatically produce pinene (ca. 4.9 mg, 36 μmol) was added CH_3CN (4 mL), tBuOOH (70% wt. aqueous solution, 39.8 μL, 0.29 mmol) and $Cr(CO)_6$ (15.8 mg, 72 μmol) followed by heating under reflux for 18 h. After purification by normal phase HPLC (Agilent 1100 series system using a Waters Nova-PAK silica HR (3.9 mm x 300 mm column), using 1% isopropanol in hexane at 1 mL/min, (+)-verbenone (**13**) (t_R = 8.84 min) was isolated

in 50% overall yield and excellent enantiopurity (>98%, $[\alpha]_D^{20}$ =+233.3 dm^{-1} cm^3 g^{-1}, c = 0.06 in $CHCl_3$) as judged by GC-MS (Figure 3.7). The slightly lower relative yield when compared to the reaction carried out in CH_3CN is most likely attributed to the reduced stability and solubility of the Cr(0) catalyst in the pentane. Although less efficient than CH_3CN in the oxidation step, pentane is essential for the effective conversion of GDP to α-pinene. Using this methodology a production capacity of 150 mg L^{-1} of (+)-verbenone was achieved.

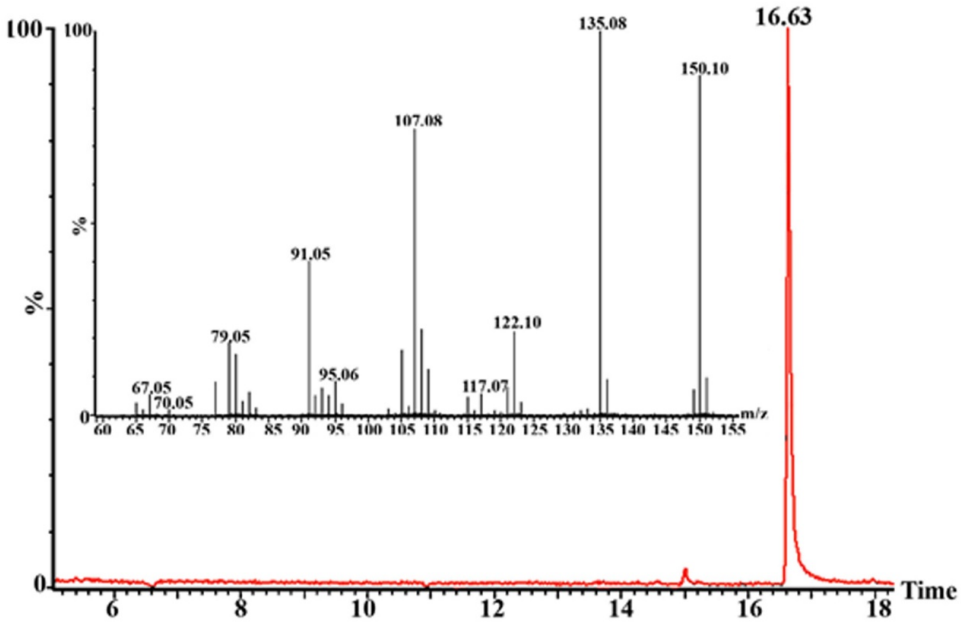

Figure 3.7: Total ion chromatogram of chemoenzymatically synthesized (+)-verbenone. Inset: EI^+ mass spectrum of verbenone.

3.7 Chiral GC analysis of (+)-verbenone

(+)-Verbenone was produced in >98% ee as judged by chiral GC comparison with racemic and commercial (-)-verbenone (Figure 3.8). Chiral GC analyses were performed on a Perkin Elmer 8700 Gas Chromatograph using a Supelco 23404 beta-Dex L20 column (30 m x 0.25 mm internal diameter) with an FID detector.

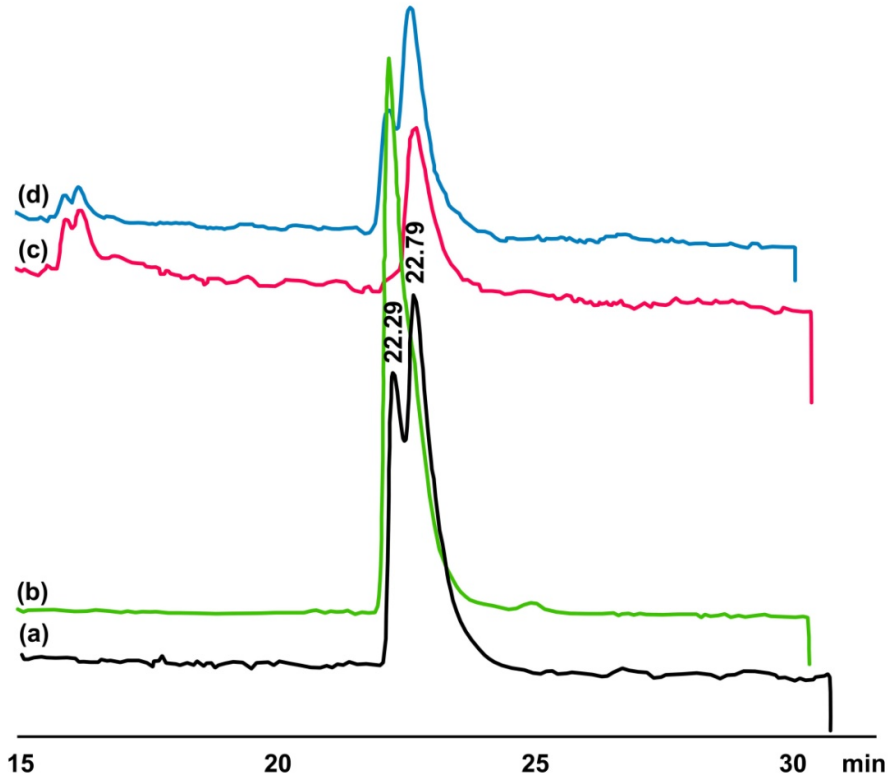

Figure 3.8: Chiral GC-analysis of chemoenzymatically generated verbenone. (a) racemic verbenone generated from racemic pinene using tBuOOH and $Cr(CO)_6$; (b) (-)-verbenone obtained from Sigma-Aldrich; (c) chemoenzymatically generated (+)-verbenone; (d) racemic verbenone spiked with chemoenzymatically generated (+)-verbenone (the peak at t_R = 22.79 min is enhanced).

3.8 Conclusion

A chemoenzymatic synthesis of (+)-verbenone (**13**) in 50% yield and >98% optical purity was achieved in two steps starting from GDP (**4**). This method favourably compares to previous syntheses as it avoids the isolation of intermediates (α-pinene/verbenol) and is, for the most part, devoid of undesirable by-products. Although verbenone (**13**) is a cheap commercially available natural product, this method constitutes a synthetic platform reference for the chemoenzymatic preparation of other valuable fine terpenoids such as artemisinin (**17**) and artemisinin derivates.

CHAPTER 4

Site-directed mutagenesis study of four aromatic residues potentially involved during catalysis by HAPS

4.1 Introduction

Using wild type cDNA as the templates, site-directed mutagenesis (SDM) experiments allow the generation of altered DNAs encoding proteins modified at one particular position. This method is extremely useful for examining the importance of specific residues in protein structure and function. SDM is indeed one of the rational methods used in protein engineering to alter the enzyme's selectivity for its natural substrate as well as its function.[166,167] More in particular, SDM has become a fundamental chemical biology tool to examine the intricate electrophilic pathways mediated by terpene synthases, the enzyme's contributions to catalysis, and to produce enzymes with altered specificities. Over time, fundamental mechanistic insights have been inferred simply by comparing the kinetic parameters and product profile of a given site-directed mutated enzyme with the parent terpene synthase[168,169] This powerful approach has also allowed, just to name one example relevant to this investigation, engineering of a (-)-camphene synthase using the cDNA template of a highly specific (89%) plant (-)-pinene synthase. Nevertheless, despite both wild type synthases having highly homologous amino acid sequence and hence very similar three-dimensional structures, several amino acid substitutions were necessary to alter the catalysis from (-)-pinene synthase to (-)-camphene synthase.[170]

In the present case, SDM was applied to α-pinene synthase (HAPS) to examine the potential catalytic role of several aromatic amino acids, in stabilizing the carbocationic intermediates generated in the active site of HAPS during the natural conversion of GDP (**4**) to the monoterpene α-pinene (**12**) (Figure: 4.1), All mutants generated for this study were expressed, purified and incubated with GDP as described for wild type HAPS. The enzymatic products generated by the HAPS variants were analyzed by GC-MS, and kinetics parameters with radiolabelled GDP (**4**) were determined as described previously for the parent monoterpene synthase.

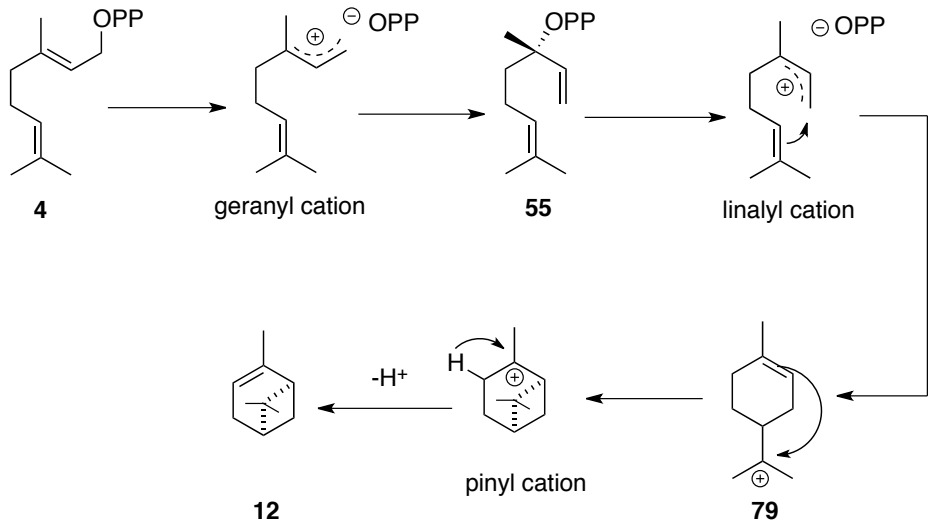

Figure 4.1: Proposed mechanism for the HAPS catalysed conversion of GDP (**4**) to α-pinene (**12**)

4.2 Homology model of HAPS

Several X-ray crystal structures of class I terpene synthases have been solved to date, including three plant monoterpene synthases.[88,92,171] These structural studies have shown that, in general, the active sites of terpene synthase are lined with aromatic amino acid residues.[172,173] Indeed, the presence of these large hydrocarbon residues appears ideal to provide the hydrophobic and desolvated environment needed to secure the stabilization, (e.g. by cation π-interaction) of the carbocation generated after diphosphate ionization and propagation of the cationic reaction cascade.[72,73,174,175,176]

Although no X-ray crystallographic data is available for HAPS, it was possible to construct a structural homology model of HAPS based on the crystallographic coordinates of limonene synthase from *Mentha spicata* as it gave the best fit for the model of HAPS.[92] The crystal structure of limonene synthase co-crystalized with the substrate analogue 2-fluorogeranyl diphosphate (2ONG.pdb) was used to model the structure of HAPS and the fluorinated ligand was preserved. The structural model was constructed through the automated comparative protein modeling server I-Tasser[177] and visualized with the program VMD[178] (Figure 4.2).

A

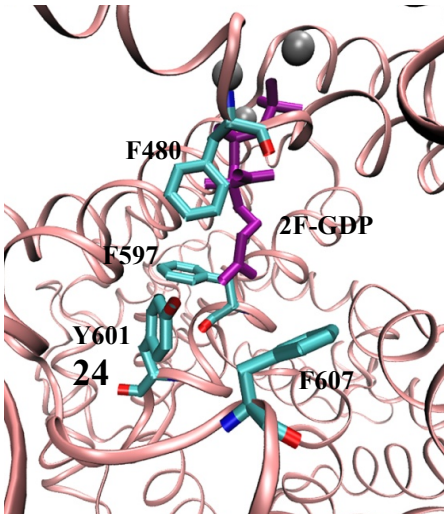

B

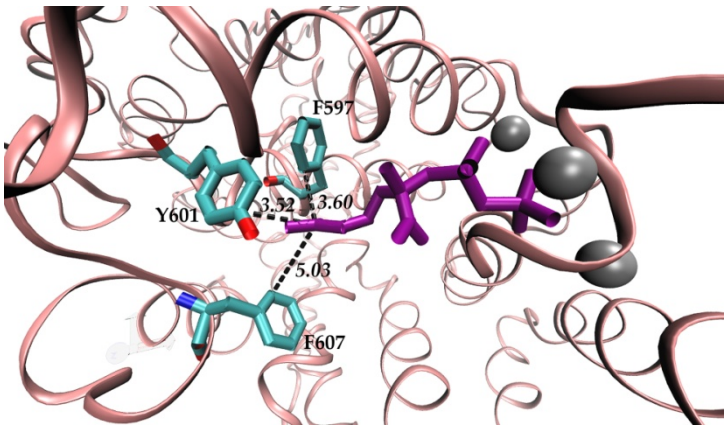

Figure 4.2: Homology model of HAPS with 2-fluorogeranyldiphosphate (2F-GDP - purple) docked at the active site. (A) Active site residues F480, F597, Y601 and F607 targeted for site directed mutagenesis. (B) Another stereo view of active site residues with F597, Y601 and F607.

4.3 Selection of potential carbocation stabilising amino residues

Based on the homology model of HAPS tyrosine (Tyr) 601 and phenylalanines (Phe) 607, 597 and 480 are residues in the proximity of the ligand, 2F-GPP, and hence they could be involved in stabilising nearby carbocationic intermediates via cation- π interactions[72,73,174,175,176] (Figure 4.1). According to the above model, F597, Y601 and F607 could be involved in stabilisation of the 4S-α-terpinyl cation (**79**) since they are

poised close to the distal double bond of the ligand 2F-GDP. Also since F480 is predicted to be located towards the head of the substrate, it could stabilize the initial geranyl and linalyl carbocations formed after loss of pyrophosphate ion (Fig. 4.1).

In this chapter the catalytic roles of these aromatic residues were evaluated by SDM using residues of different size (Ala), electrostatic properties (Ala, and Leu) and hydrogen bonding capabilities (Tyr). Substitutions of aromatic residues by alanine often result in drastic catalytic changes due to the lost of both the aromaticity and steric bulk. Replacement by Leu will preserve (approximately) the size of the residue but the electrostatic effects (π-stabilisation) of an aromatic ring will be lost. Finally Tyr, an aromatic residue that could be involved in hydrogen bonding networks with other residues, or with bulk solvent, and hence substantially change the original active environment of HAPS, upon replacing the natural Phe residues. To this end a series of primers were designed to alter the selected codons in the gene encoding in polymerase chain reactions (PCR) using *Pfu* polymerase (Materials and methods). The native and mutated codons for each of the selected residues are listed below (Table 4.1).

Table 4.1: Comparison of native codons from HAPS with mutated codons.

	Y601A	**Y601F**	**Y601L**	**F607A**	**F607Y**	**F607L**
Native codon	TAC	TAC	TAC	TTT	TTT	TTT
Substituted codon	GCG	TTT	CTG	GCG	TAT	CTG

F480A	**F480Y**	**F480L**	**F597A**	**F597Y**	**F597L**
TTT	TTT	TTT	TTT	TTT	TTT
GCG	TAT	CTG	GCG	TAT	CTG

A total of 12 cDNAs were produced and over-expressed in *E.coli*. Briefly, the methylated parent DNA was digested by Dpn1 restriction enzyme after PCR amplification to remove all parental DNA. XL1-Blue super competent cells were then transformed with the Dpn1 treated mutated plasmid solution. After transformation, the

mutated plasmids were purified by miniprep and gene sequences were confirmed by DNA sequence analysis. Preparative-scale and active preparations of these HAPS mutants were performed exactly as described for the parent enzyme. The functional analysis of the resulting HAPS variants was carried out through GC/MS analysis of pentane extractable products from incubations with GDS as previously indicated for the parent enzymes, the results are shown in Table 4.2. The kinetic parameters were measured using the radioactive assay[146] (See section 2.7.5 for details) and the results are shown in Table 4.3. However, the kinetic parameters of HAPS-F597L and HAPS-F480L were extremely difficult to measure with confidence.

Table 4.2: GC results of mutant HAPS incubation with GDP

Mutant	**Products (GC-MS)**
Y601A/L/F	(Inactive)
F607A	(Inactive)
F607L/Y	α-pinene
F480A	(Inactive)
F480L/Y	α-pinene
F597A	(Inactive)
F597L/Y	α-pinene

Table 4.3: Kinetics parameters of HAPS mutants.

Protein	K_M (μM)	k_{cat} (s^{-1})	k_{cat}/K_M ($M^{-1}s^{-1}$)
WT	40.0 ± 8.0	0.00100 ± 0.00040	25 ± 11
F607L	86.5 ± 32.8	0.00020 ± 0.00004	2.4 ± 1.0
F607Y	133.2 ± 31.9	0.00018 ± 0.00001	1.4 ± 0.3
F597Y	138.8 ± 33.7	0.00082 ± 0.00001	5.7 ± 0.6
F480Y	80.3 ± 26.1	0.00016 ± 0.00002	2.0 ± 0.7

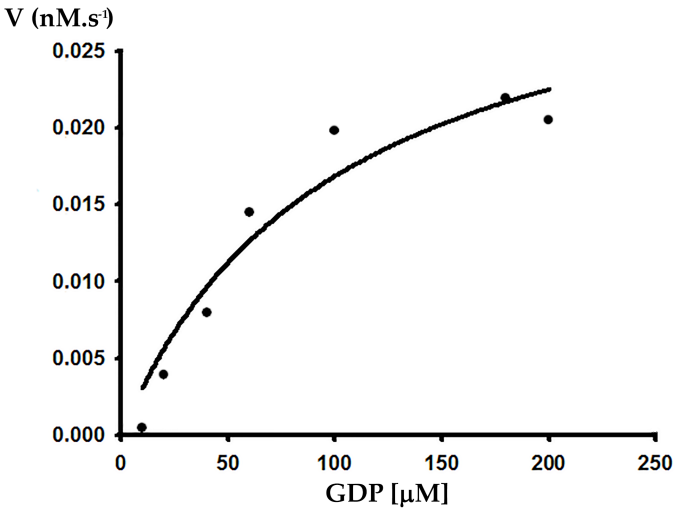

Figure 4.3: Michaelis-Menten profile for HAPS-F607L

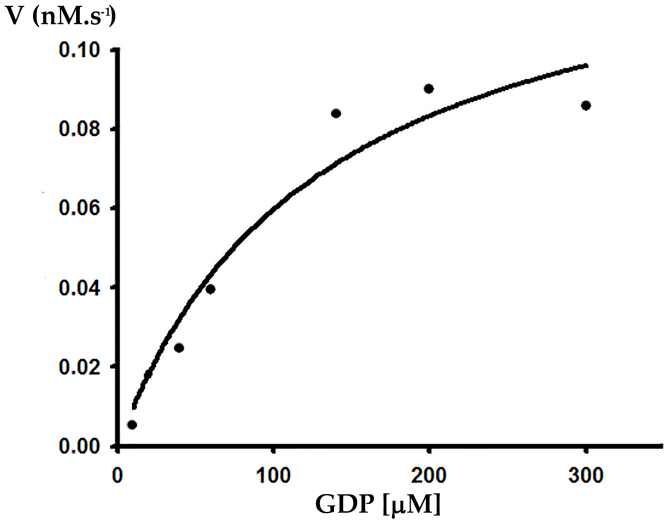

Figure 4.4: Michaelis-Menten profile for HAPS-F607Y

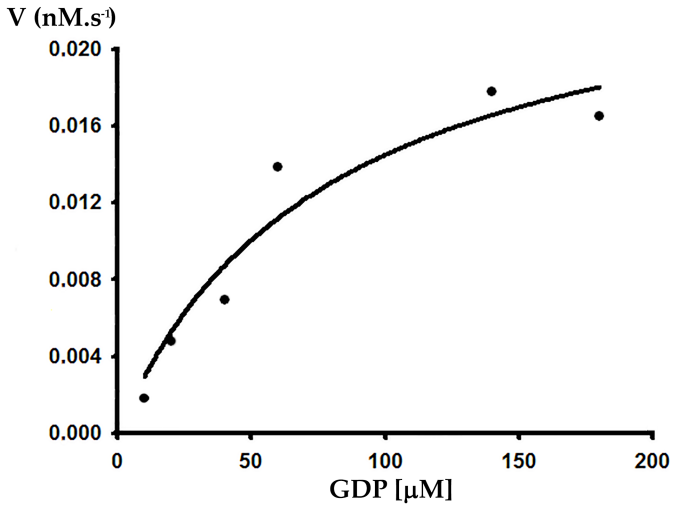

Figure 4.5: Michaelis-Menten profile for HAPS-F480Y

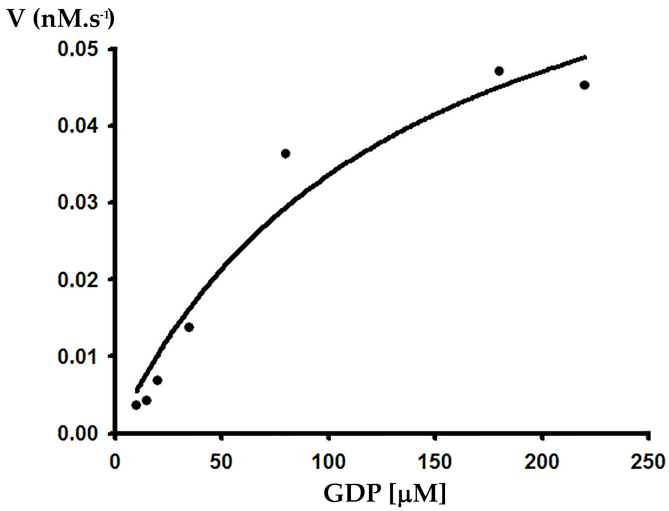

Figure 4.6: Michaelis-Menten profile for HAPS-F597Y

Only 6 variants out of 12 (Table 4.2) were active, and interestingly they all produce α-pinene as the exclusive enzymatic product. Indeed, taking into account the chemical complexity of the reaction catalyzed by HAPS (at least 4 carbocations are involved), it is remarkable that the specificity of the WT enzyme is preserved in the mutants. From the results shown in Table 4.2, it is evident that the replacement of these aromatic amino acids by alanine precludes binding the substrate, or reactions the initial diphosphate ionisation. With the exception of Y601, substitutions by the bulkier leucine

led to active HAPS. Nevertheless, the kinetics parameters of HAPS-F607L clearly indicate that this mutation is catalytically deleterious causing a 5-fold decrease in the reaction rate constant (k_{cat}).

4.4 Conclusion

In conclusion, these 4 aromatic residues are important for the enzyme's function as replacement to each residue making the enzyme less reactive respect to WT enzyme. The replacement by a residue of different electrostatic and hydrogen bonding properties drastically change either the HAPS structure (folding) leading to inactivity or lead to proteins in which the catalytic properties are severely impaired. In addition, the exclusive formation of α-pinene by the active HAPS precludes further and more detailed mechanistic insights. From a chemical ecology point of view, the robust product specificity of HAPS uncovered by SDM may be beneficial for the Loblolly pine.

CHAPTER 5

Synthesis and incubation of some chemically modified GDP analogues

5.1 Introduction

The chemoenzymatic synthesis of (+)-verbenone (**13**) from GDP (**4**) described in chapter 3 demonstrates that terpene synthases (TS) are useful catalysts to construct synthetically challenging natural products in only a few chemical steps. More importantly, due to the often-observed substrate promiscuity of TPS, this synthetic approach appears ideal to prepare modified analogues of natural terpenes (Figure 5.1) with potentially novel biological properties. In this chapter, our efforts toward the synthesis of alkyl modified GDP's as diphosphate surrogates of HAPS and their further enzymatic conversion are described.

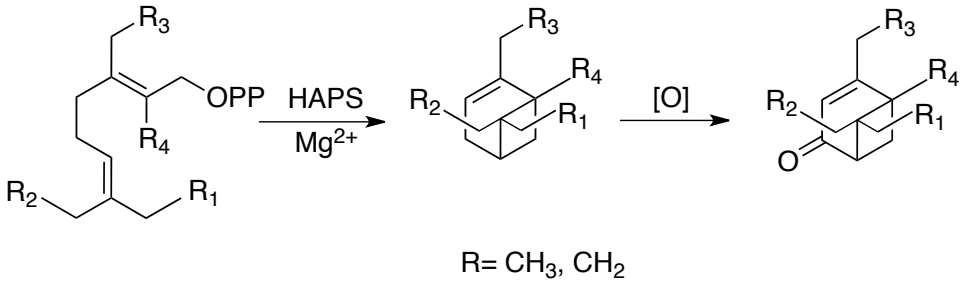

Figure 5.1: Synthetic sequence to chemically modify (+)-α-pinene (**12**) and (+)-verbenone (**13**) analogues using alternative GDP's.

5.2 Preparation of pyrophosphate salts

Few methods have been published to prepare prenyl pyrophosphates. The first protocol ever published involved treatment of an allylic alcohol with inorganic phosphate and trichloroacetonitrile.[181] However, by this methodology, the final diphosphate required extensive purification, and hence the overall yield was often low. A better procedure to prepare primary allylic diphosphates was later introduced by Poulter *et al*.[182] This route involves the conversion of an allylic alcohol into the corresponding halide (Cl or Br), and further nucleophilic displacement of the latter with pyrophosphate. In the present study, GDP (**4**) and all GDP analogues were prepared following this method as recently modified by Coates *et al*. (Scheme 5.1),[183] which is essentially a modification of Poulter's approach.

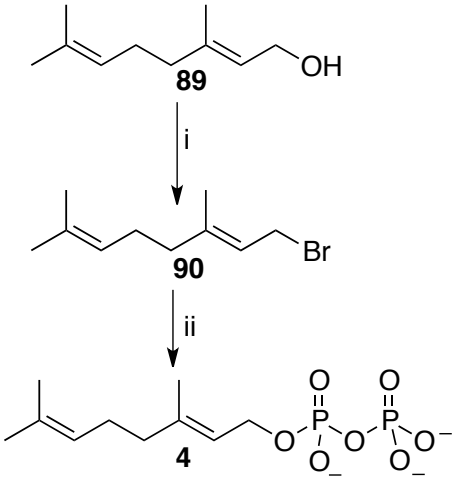

Scheme 5.1: Synthesis of geranyl diphosphate (**4**) from geraniol (**89**).

Reagents and conditions: i) MsCl, Et_3N, THF, LiBr, -45 C to 0 °C, 2 h; ii) $(Bu_4N)_3HP_2O_7$, MeCN, RT, 6 h, 76% over the last two steps.

To illustrate the two-step methodology of Coates, the synthesis of GDP (**4**) is given: geraniol (**89**) was first converted into the corresponding mesylate by treatment with methanesulfonyl chloride (MsCl) in the presence of a hindered base (eg. triethyl amine (Et_3N)) at low temperature (0 °C). Then, addition of a solution of lithium bromide (LiBr) effects the nucleophilic substitution of the mesylate by Br^- anion at room temp. Further exposure of the bromide (**90**) to the tris-tetrabutylammonium salt of pyrophosphoric acid in anhydrous acetonitrile (MeCN), subsequent ion exchange, and purification by reverse phase HPLC gives GDP (**4)** as the tris-ammonium salt in good yield.[184]

5.2.1 Synthesis of neryl diphosphate (NDP)

For the synthesis of neryl diphosphate (NDP, **59**) i.e. the *Z*-isomer of geranyl diphosphate (GDP, **4**) the protocol of Barrero *et al*[185] was followed to prepared the bromide. Thus, reaction of nerol with triphenylphosphine (Ph_3P) and carbon tetrabromide (CBr_4) resulted in the formation of neryl bromide (**92**).[186] Allylic bromide **92** was converted to the corresponding diphosphate **59** essentially as described for GDP[182] following Poulter's approach (Scheme 5.2).

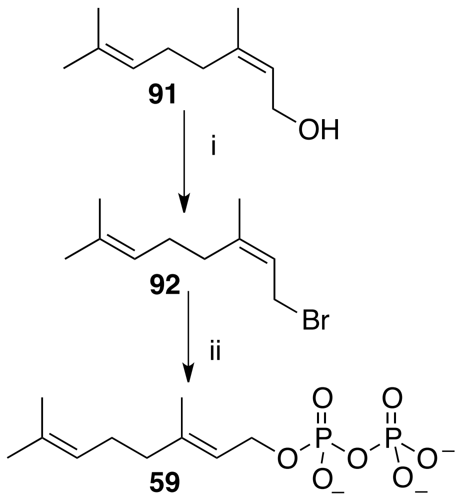

Scheme 5.2: Synthesis of neryl diphosphate (**59**) from nerol (**91**).

Reagents and conditions: i) CBr_4, Ph_3P, C_6H_6, 0°C, 2.5 hr, used directly in the next step; ii) $(Bu_4N)_3HP_2O_7$, MeCN, RT, 6 hr, 65% over two steps.

5.3 Synthesis of 8-methyl GDP

The first step in this synthetic sequence was to oxidise the allylic acetate **93** at C8. Selenium dioxide (SeO_2) was used for this step giving 90% yield (mixture of **94** and **95**). Secondly Swern oxidation was performed in order to produce only **94.** Following this reaction with methyl triphenyl phosphonium bromide formed the alkene **96**. Hydrogenation of **96** by Wilkinson's catalyst produced the alcohol **98** after saponification of the resulting acetate **97**. Activation of the alcohol as the allylic

bromide **99**, followed by reaction with tris tetrabutyl ammonium hydrogen pyrophosphate gave 8-methyl GDP pyrophosphate tetra-n-butylammonium salt **100**. Cation-exchange chromatography followed by reverse phase HPLC purification finally gave the 8-methyl GDP **100** as a white solid, in over-all yield of 55.5% (**98** to **100**).

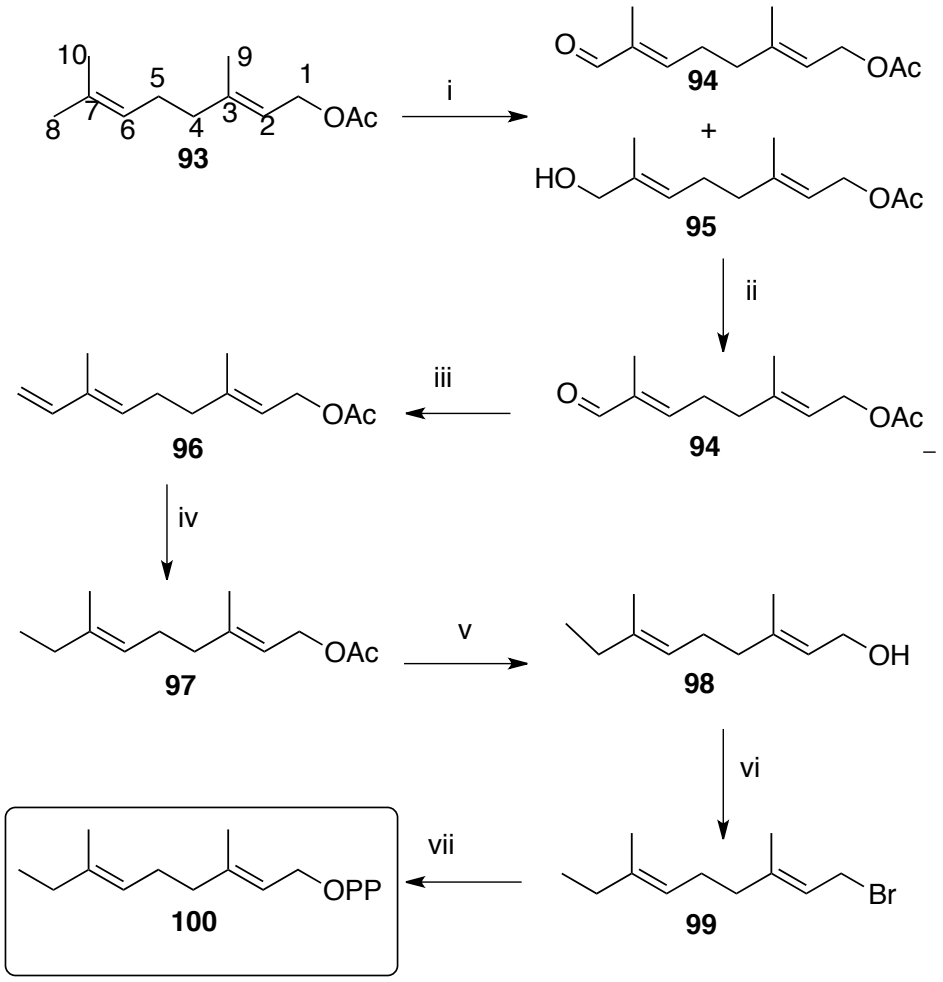

Scheme 5.3: Synthesis of 8-methyl GDP (**100**) from geranyl acetate (**93**).

Reagents and conditions: ^{t}BuOOH, SeO_2, DCM, CH_2Cl_2, $C_6H_6(OH)COOH$, 0 °C to RT, 30 hr, 90%; ii) $(COCl)_2$, Et_3N, DMSO, DCM, -78 °C to RT, O/N, 98%; iii) Ph_3PCH_3Br, n-BuLi, THF, -5 °C , 1hr, 52%; iv) $(Ph_3P)_3RhCl$, H_2, $C_6H_6CH_3$, RT, 24 hr; v) K_2CO_3, MeOH, RT, 85% vi) MsCl, Et_3N, THF, LiBr, -45 °C to 0 °C, 2 hr; vii) $(Bu_4N)_3HP_2O_7$, MeCN, RT, 55%.

5.3.1 Allylic oxidation of geranyl acetate (84) with selenium dioxide and tert-butyl hydroperoxide

The first step of the synthetic sequence outlined in Scheme 5.3 is the allylic oxidation of acetate **93** at C8. Selenium dioxide is often the reagent of choice as it allows regioselective oxidations at the less hinder position in aliphatic chains such as **94.**[187] In the presence of tert-butyl hydroperoxide, the selenium oxidation of **84** is catalytic; the byproduct SeO is reoxidized back to SeO_2, thus preventing/minimizing formation of the more harmful reduced forms of selenium.[187]

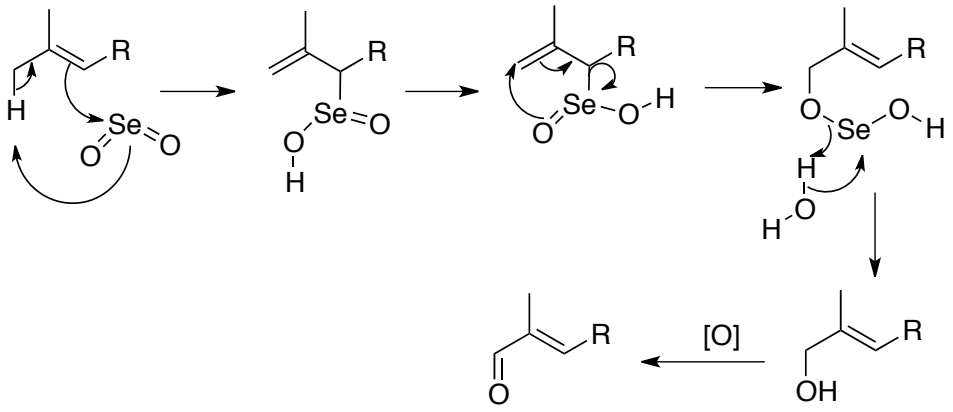

Scheme 5.4: Mechanism for selenium dioxide oxidation.

The mechanism of this reaction is believed to begin with deprotonation (Scheme 5.4) at C8, and concomitant electrophilic addition of SeO_2 onto the C7,C8 double bond of **94**. The resulting adduct undergoes allylic rearrangement and further solvolysis to generate alcohol **95.** In the absence of an acid, or in stoichiometric amounts, the alcohol is oxidized further to the corresponding aldehyde **94**. To prevent this inconvenient side reaction, oxidation of **86** was more effectively accomplished by Swern oxidation.

5.3.2 Wittig olefination of 85 to form 87

The Wittig reaction is an important method for the formation of alkenes. The double bond forms at the location of the original aldehyde or ketone. Here to convert aldehyde **94** into **96**, methyl triphenyl phosphonium bromide (Ph_3PCH_3Br) was used. The reactive ylide, prepared in situ by reaction with a strong base such us butyllithium (n-BuLi), undergoes a 2+2 cycloaddition with aldehyde **94** to form an unstable intermediate that breaks down upon warming releasing the desired alkene product **96** and triphenylphosphine oxide (Scheme 5.5) as the byproduct.

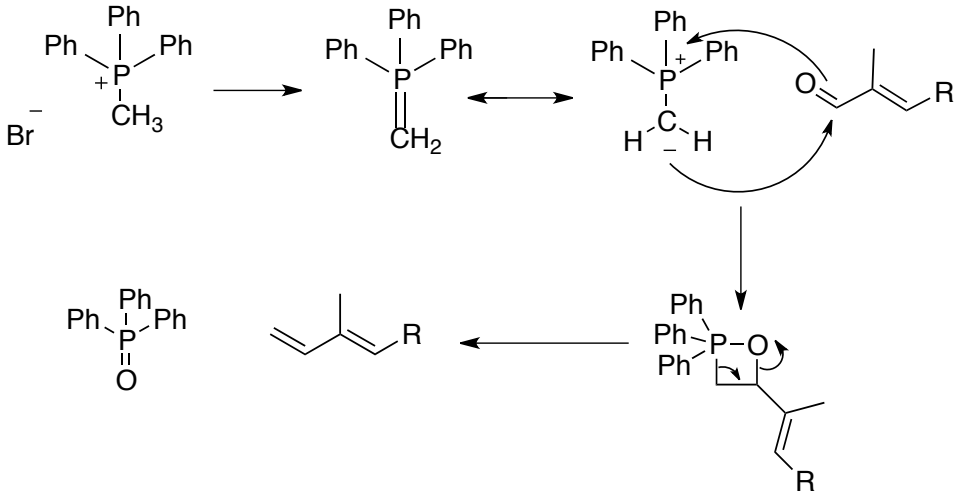

Scheme 5.5: Mechanism for Wittig olefination

5.3.3 Hydrogenation of 96 using Wilkinson's catalyst to give 97

The complex $RhCl(PPh_3)_3$ (also known as Wilkinson's catalyst) became the first highly active homogeneous hydrogenation catalyst that compared in rates with heterogeneous counterparts.[190, 191]

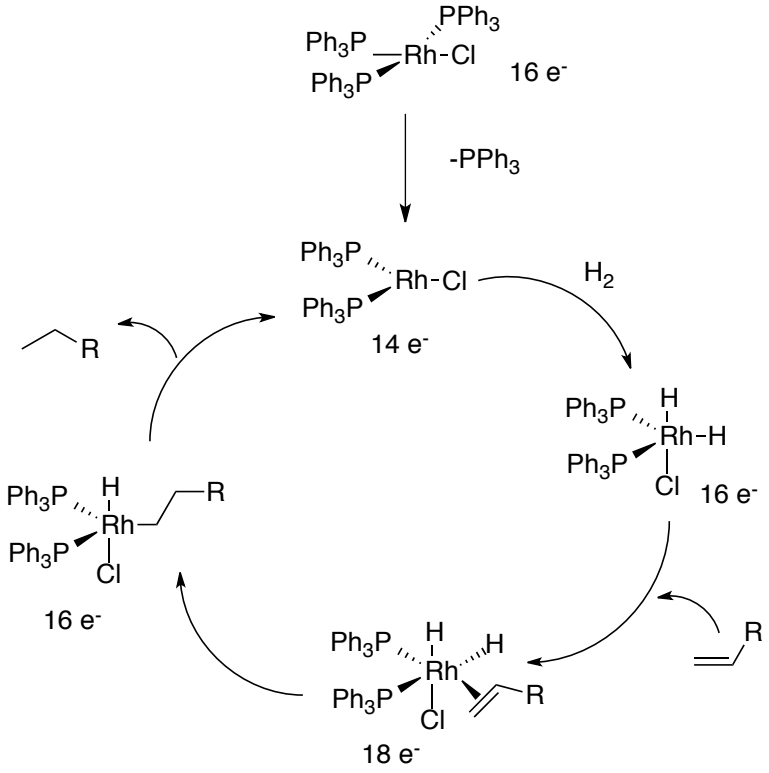

Scheme 5.6: Mechanism for hydrogenation using Wilkinson's catalyst

This mechanism starts with an initial dissociation of a triphenyl phosphine group from the rhodium catalyst forming a $14e^-$ complex. This allows an oxidative addition of H_2 onto the metal followed by formation of the π-complex (between the alkene and the metal). The alkene donates electron density into rhodium's d orbital from the C=C atoms and the metal donates electrons back from a filled d orbital into the alkenes empty π-anti bonding orbital. Both of these motions causes a weaker bond between the C=C atoms. The complex now is in an $18e^-$ state. The final step is the reductive elimination of the desired alkane **97** to give a regenerated $14e^-$ rhodium chloride complex.

5.3.4 Pyrophosphorylation of alcohol 98 to the 8-methyl GDP (100)

Saponification of **97** using potassium carbonate/methanol gave alcohol **98** in 85% yield. This alcohol was converted into the corresponding diphosphate **100** (55%) via bromide **99** following the methodology of Poulter.[182] (See section 5.2).

5.4 Synthesis of (*E*)-7-vinyl GDP (103)

(*E*)-7-vinyl GDP **103** (Scheme 5.7) was prepared from alcohol **101** after saponification of acetate **96** (K_2CO_3/MeOH). This alcohol was then converted to bromide **102** (MsCl/LiBr)[182] and then treatment with tris (tetra-n-butylammonium) hydrogenpyrophosphate in anhydrous acetonitrile to give **103** in 35% overall yield.

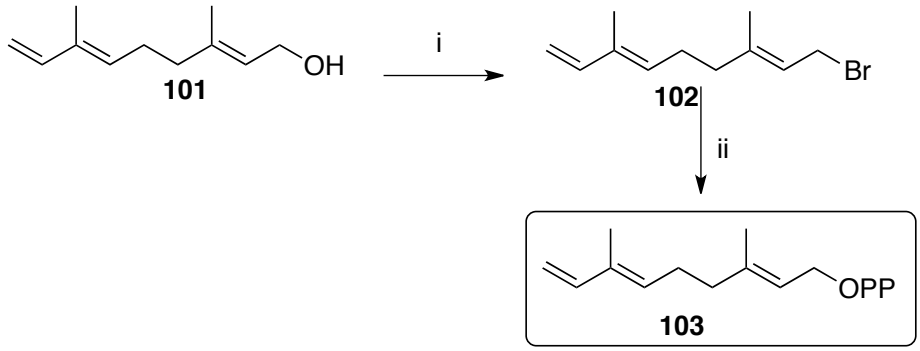

Scheme 5.7: Synthesis of (E)-7-vinyl GDP (**103)** from geranyl acetate (**93**).

Reagents and conditions: i) MsCl, Et_3N, THF, LiBr, -45 °C to 0 °C, 2 hr; ii) $(Bu_4N)_3HP_2O_7$, MeCN, RT, 45% over the last two steps.

5.5 Synthesis of 10-methyl GDP (114)

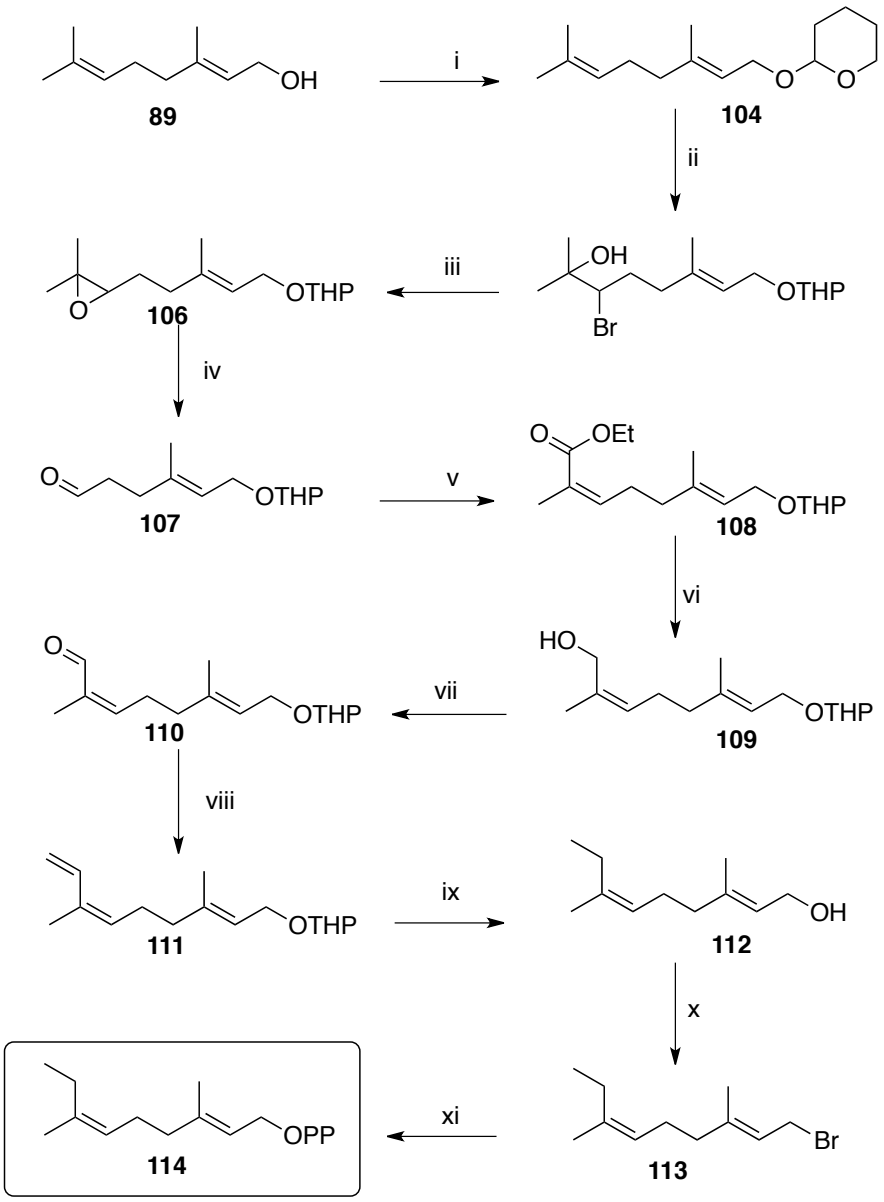

Scheme 5.8: Synthesis of 10-methyl GDP (**114)** from geraniol (**89)**

Reagents and conditions: i) 3,4-DHP, p-TsOH,$(C_2H_5)_2O$, RT, 18 hr, 88%; ii) NBS, THF/H_2O, -5 °C, 4 hr, 71%; iii) DBU,THF, 0 °C to RT , 4hr, 87%; iv) H_5IO_6, 0 °C, 45 min, 57% v) $(CF_3CH_2O)_2P(O)CH(CH_3)CO_2Et$, THF, KHMDS,18-crown-6, -78 °C, 1 hr; vi) DIBAL-H, THF, -20 °C, 3 hr, 87%, vii) MnO_2, C_6H_{14}, 0 °C, 3 hr, 86%; viii) Ph_3PCH_3Br, n-BuLi, THF, -5 °C , 1hr, 55%; ix) $(Ph_3P)_3RhCl$, H_2, $C_6H_6CH_3$, RT, 24 hr, 80% and then PPTS, EtOH, 55 °C , 2 hr, 85%; x) MsCl, Et_3N, THF, LiBr, -45 °C to 0 °C, 2 hr; xi) $(Bu_4N)_3HP_2O_7$, MeCN, RT, 40% over the last two steps

The synthesis of **114** started with protection of geraniol as the tetrahydropyranyl (THP-) ether derivate **104**.[92,93] Subsequent hydrobromination of the terminal double bond with N-bromosuccinimide in water afforded a mixture of bromohydrins **105**. Mechanistically, this reaction involves the electrophilic addition of bromine across the double bond to form a reactive bromonium ion that is further displaced by the nucleophile (water) to yield **105** and succinimide as a by-product.[194] Epoxide **106** is then formed when **105** is exposed to base (eg. 1,8-diazobicycloundec-7-ene (DBU)). The alkoxide intermediate displaces intramolecularly the adjacent bromide affording the epoxide **106**.[195]

Reaction of epoxide **106** with sodium periodate causes an oxidative cleavage between C6 and C7 to forms the shorter aldehyde **107**. The reaction proceeds through the formation of a strained 5 membered ring intermediate that breaks down oxidatively into acetone and the aldehyde **107** required for the next step (Scheme 5.9).

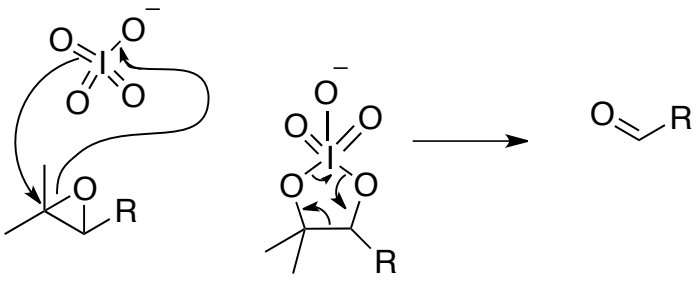

Scheme 5.9: Mechanism of oxidative cleavage with the use of sodium periodate

The *Z*-configured ethyl ester **108** was synthesized following a modification of the Horner-Emmons olefinations.[196, 197] Reduction of the ester **108** with DIBAL-H gave alcohol **109**.[17] The next oxidation of **109** to the aldehyde **110** was carried out using activated manganese (IV) oxide**.** Wittig olefination of the latter using methyl triphenyl phosphonium bromide (Ph_3PCH_3Br), hydrogenation of diene **111** with Wilkinson's catalyst, and THP deprotection (pyridinium p-toluenesulphonate) gives alcohol **112**. This was then converted to the desired 10-methyl GDP analogue **114** (40% from **112**) via bromide **113** as described earlier.[182]

5.6 Synthesis of (*Z*)-7-vinyl GDP (117)

The synthesis of (*Z*)-7-vinyl GDP (**117**) was accomplished by Poulter's method using allylic alcohol **115** (Scheme 5.10), which was synthesized from the corresponding THP ether **111** (See section 5.5), during the synthesis of compound **114.**

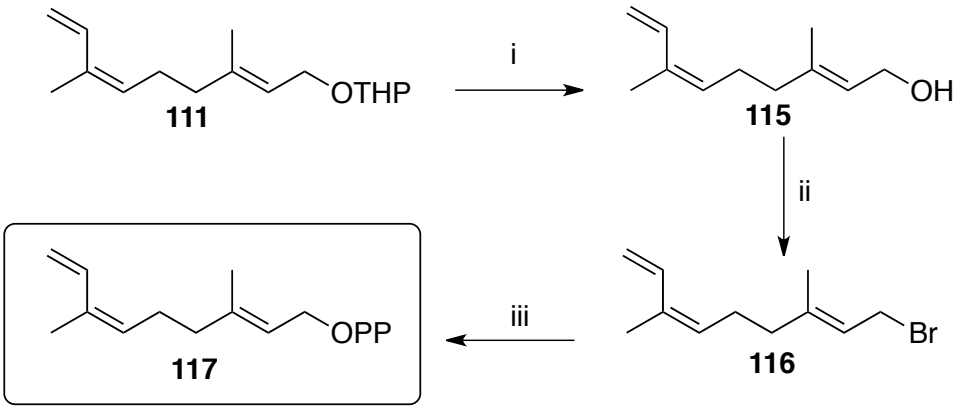

Scheme 5.10: Synthesis of (*Z*)-7-vinyl GDP (**117)** from compound **89**

Reagents and conditions: i) PPTS, EtOH, 55 °C, 2 hr, 92%; ii) MsCl, Et_3N, THF, LiBr, -45 °C to 0 °C, 2 hr; iii) $(Bu_4N)_3HP_2O_7$, MeCN, RT, 43% over the last two steps.

5.7 Incubation of GDP analogues with HAPS

2-Fluoro GDP (**118**), 2,3-dihydroGDP (**119**) and 9-Methyl GDP (**120**) were synthesised by Dr. Juan Faraldos. To check the ability of HAPS to produce α-pinene derivatives with GDP analogues such as 8-methyl GDP (**100**), (*E*)-7-vinyl GDP (**103),** 10-methyl GDP (**114**), (*Z*)-7-vinyl GDP (**117**), 2-Fluoro GDP (**118**), 2,3-dihydroGDP (**119**) and 9-methyl GDP (**120**) was assessed by GC-MS using analytical scale incubations. In brief, HAPS (20 μM) was incubated with GDP analogues (2.0 mM, 25 μL) in buffer (0.5 mL total volume, 100 mM Bis-Tris propane, pH 7.5, 50 mM KCl and 20 mM $MgCl_2$). The aqueous enzymatic medium was overlaid with 0.5 mL pentane to capture volatiles. After gentle shaking overnight at room temperature, the organic layer was removed and the aqueous layer was extracted with additional pentane (0.5 mL). The pooled pentane

extracts were filtered through silica gel column (≈3 g silica) and the eluent was analyzed by GC-MS.

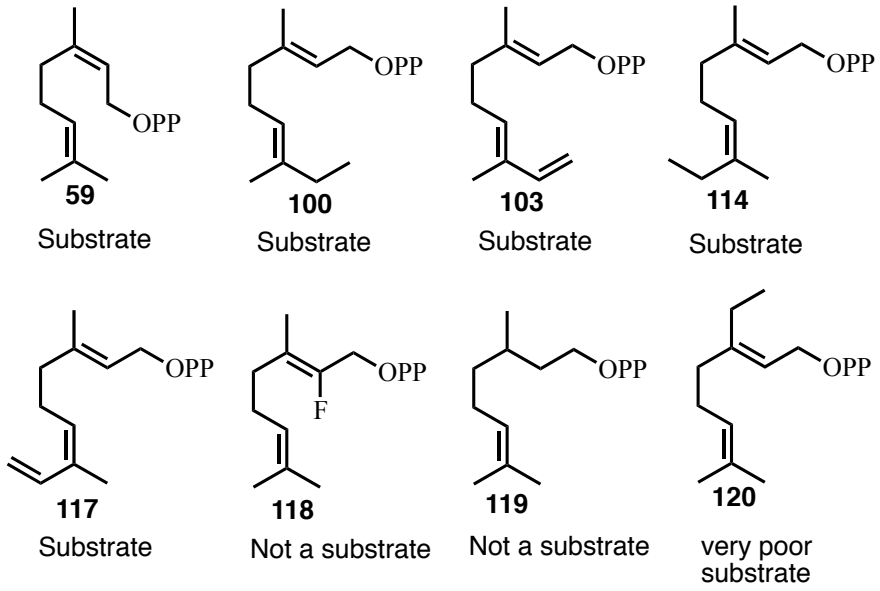

Figure 5.2: Incubation results of GDP analogues with HAPS

Compounds **118** and **119** proved not to be a substrate for HAPS giving no peak on the GC spectra corresponding to the formation of the (+)-α-pinene analogues. All the other GDP analogues, **100**, **103**, **114**, **117** and **120** are substrates for HAPS giving the corresponding (+)-α-pinene analogues. These will be described in more detail in the following paragraphs.

5.7.1 Incubation results for 8-methyl GDP

As described in Scheme 1.6 for GDP (**4**), we can imagine that 8-methyl diphosphate (**100**) may undergo a similar pathway as GDP. Indeed, the extra methyl at the C8 position is not involved at any time in the catalytic pathway of HAPS. The only problem could be steric hindrance in the catalytic active site due to a bigger size of the substrate.

As illustrated in scheme 5.11, 8-methyl GDP could lead to the corresponding 8-methyl linalyl diphosphate (**121**) as for GDP. Then ionization of **121** followed by ring closures and final deprotonation would lead to the formation of the analogue of (+)-α-pinene **124**.

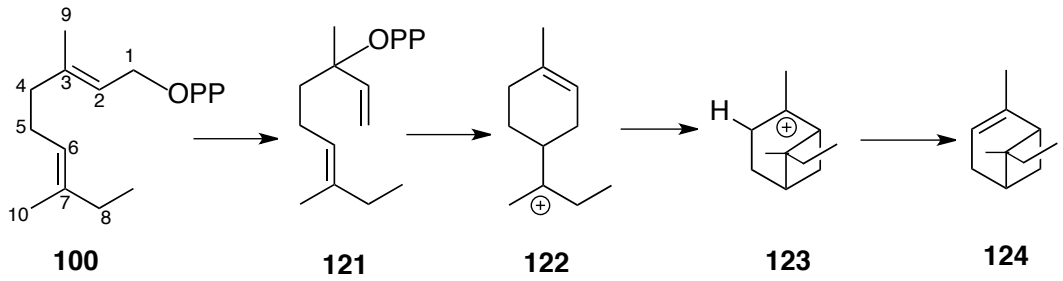

Scheme 5.11: Proposed mechanism for the conversion of 8-methyl GDP (**91**) to (S)-(+)-α-methylpinene (**124**)

GC-MS analysis of the pentane extract layer of incubation of 8Me GDP with HAPS showed the formation of a single peak at t = 11.08 min displaying m/z = 150 corresponding to the m/z of **124** and a mass spectrum similar to the one of (+)-α-pinene. This would suggest the obtaining of the (*S*)-(+)-α-methylpinene **124**.

A

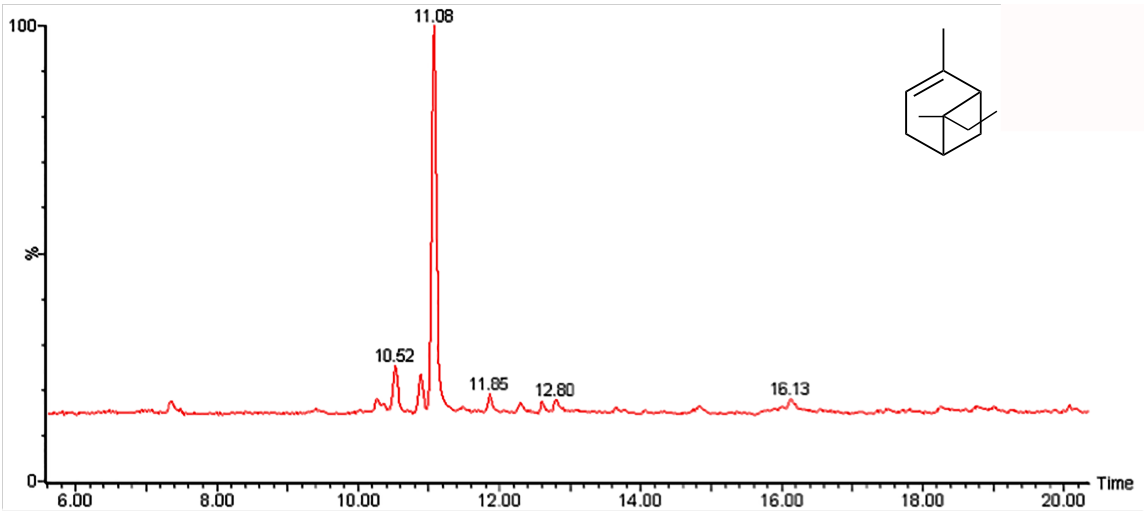

B

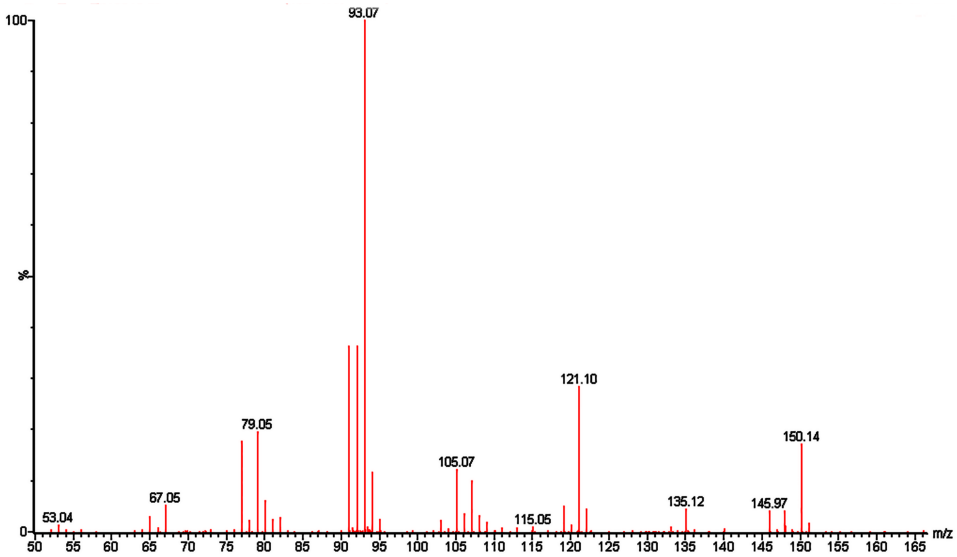

Figure 5.3: A) Gas chromatogram of the novel analogue, (S)-(+)-α-methylpinene **124;** B) MS of the GC peak at retention time 10.52 seconds; C) MS of the peak at retention time 11.06 seconds

5.7.2 Incubation results for (*E*)-7-vinyl GDP (103)

As described for 8-methyl GDP in the previous paragraph, (*E*)-7-vinyl GDP may undergo a similar pathway as GDP and so incubation of (*E*)-7-vinyl GDP could lead to the formation of the corresponding (+)-α-pinene analogue: (*S*)-(+)-α-7-vinylpinene **125**.

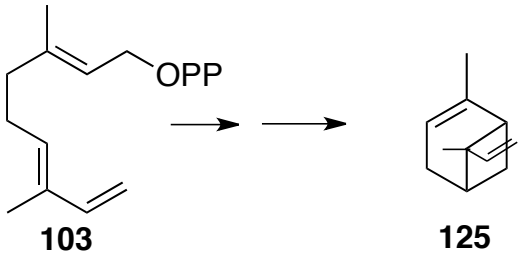

Scheme 5.12: Proposed conversion of (*E*)-7-vinyl GDP (**103**) to (*S*)-(+)-α-7-vinyllpinene (**125**) by HAPS.

GC-MS analysis of the pentane extract layer of incubation of (*E*)-7-vinyl GDP **103** with HAPS showed the formation of a single peak at t = 10.38 min displaying a m/z = 148 corresponding to the m/z of **125** and a mass spectrum similar to the one of (+)-α–pinene. This would suggest that (*S*)-(+)-α-7-vinylpinene **125** was obtained.

A

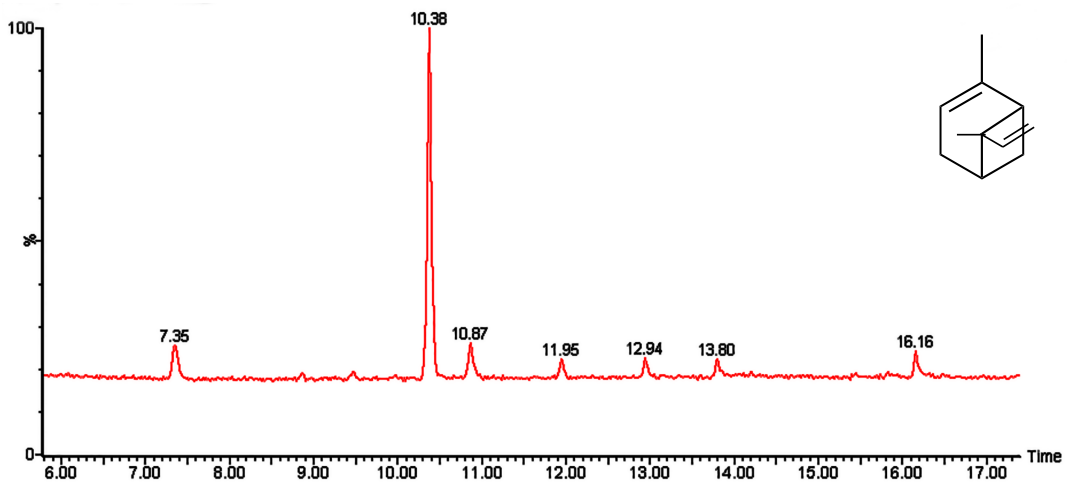

B

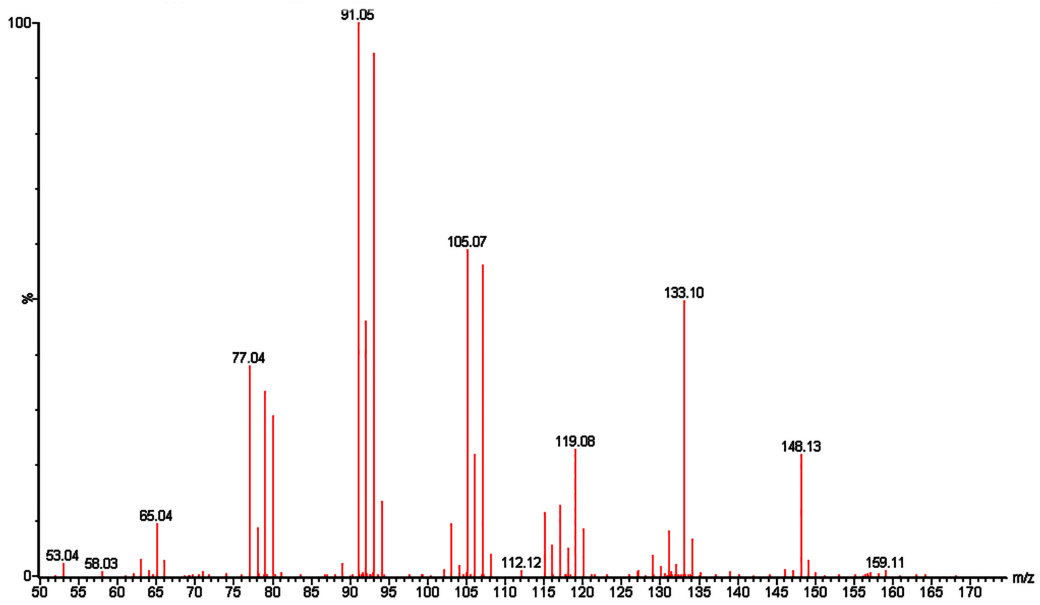

Figure 5.4: A) Gas chromatogram of the novel analogue, (S)-(+)-α-7-vinylpinene**;** B) MS of the peak at retention time 10.38 minutes

5.7.3 Incubation results for 10-methyl GDP (114)

As previously described for 8-methyl GDP (**100**), 10-methyl GDP (**114)** may undergo a similar pathway as GDP and so incubation of 10-methyl GDP could lead to the formation of the corresponding (+)-α–pinene analogue: (*R*)-(+)-α-10-methylpinene **126**.

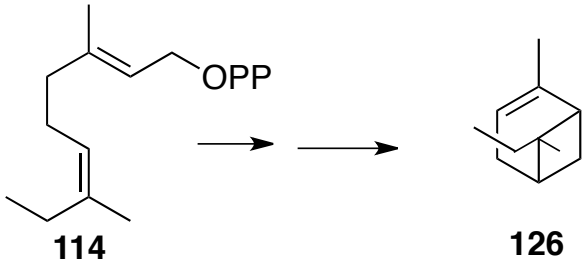

Scheme 5.13: Proposed conversion of 10-methyl GDP (**114**) to (*S*)-(+)-α-10-methylpinene (**126**) by HAPS.

GC-MS analysis of the pentane extract layer of incubation of 10-methyl GDP **114** with HAPS showed the formation of a single peak at t = 10.95 min displaying a m/z = 150 corresponding to the m/z of **126** and a mass spectrum similar to the one of (+)-pinene. This would suggest that (*R*)-(+)-α-10-methylpinene **126** was obtained.

A

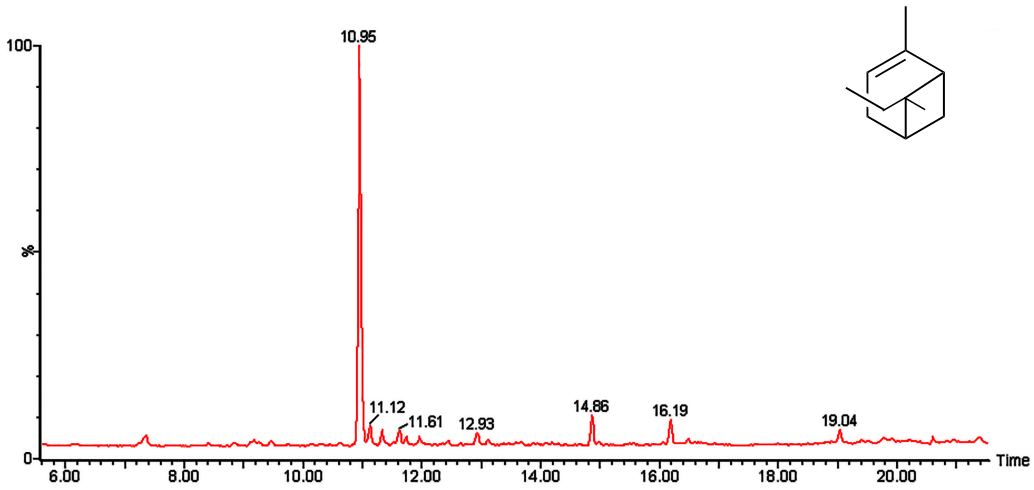

B

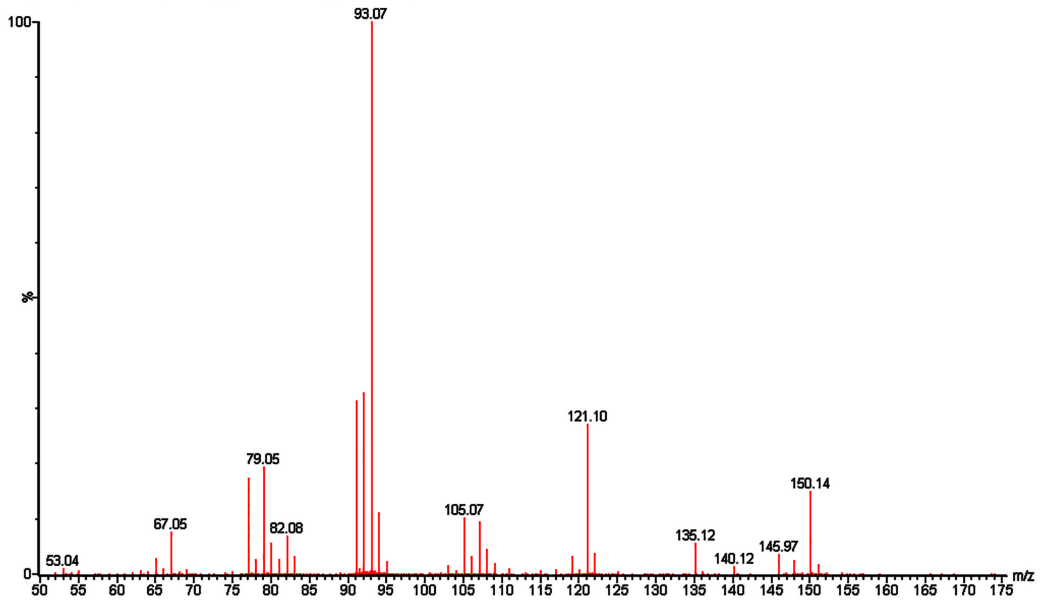

Figure 5.5: A) Gas chromatogram of the novel analogue, (*R*)-(+)-α-methylpinene**;** B) MS of the peak at retention time 10.95 minutes.

5.7.4 Incubation results for (*Z*)-7-vinyl GDP (117)

As previously described for 8-methyl GDP, (*Z*)-7-vinyl GDP may undergo a similar pathway as GDP and so incubation of (*Z*)-7-vinyl GDP could lead to the formation of the corresponding (+)-α–pinene analogue: (*R*)-(+)-α-7-vinylpinene **127**.

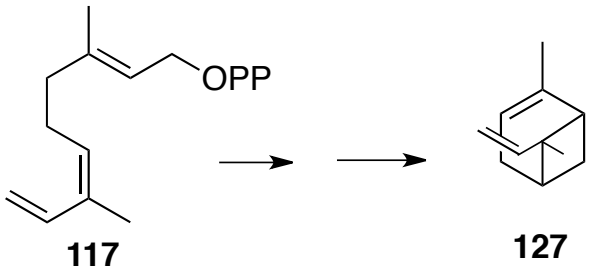

Scheme 5.14: Proposed conversion of (*Z*)-7-vinyl GDP (**117**) to (*R*)-(+)-α-7-vinyllpinene (**127**) by HAPS.

GC-MS analysis of the pentane extract layer of incubation of (*Z*)-7-vinyl GDP **117** with HAPS showed the formation of a major peak at t = 10.33 min displaying a m/z = 148 corresponding to the m/z of **127** and a mass spectrum similar to the one of (+)-α–pinene. This would suggest that (*R*)-(+)-α-7-vinylpinene **127** was obtained.

A

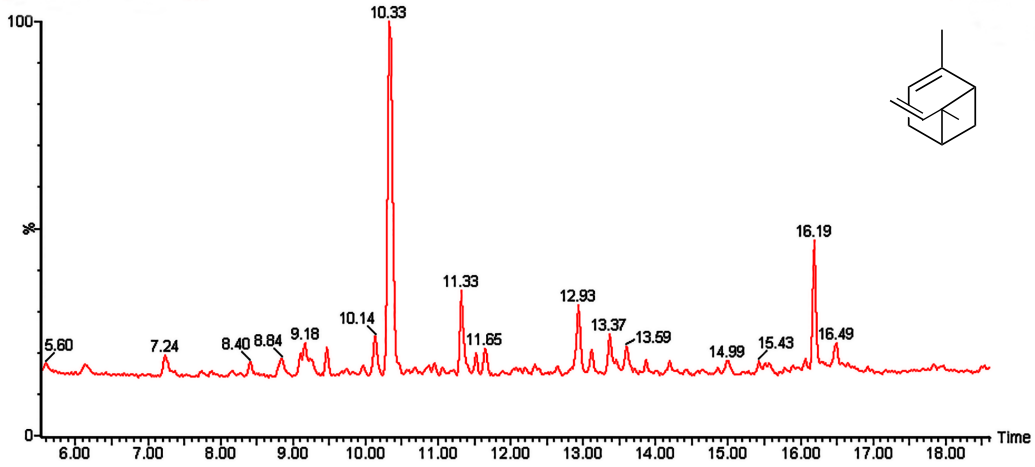

B

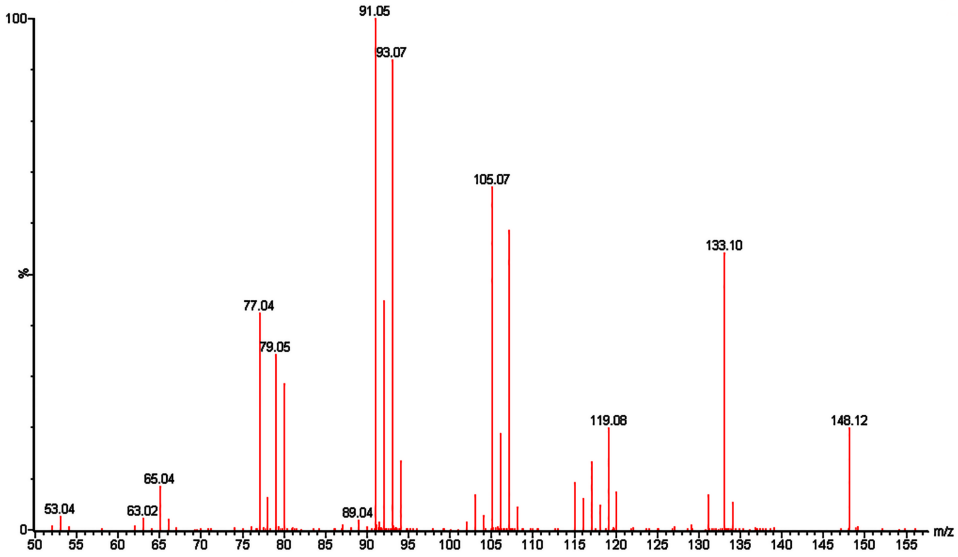

Figure 5.6: A) Gas chromatogram of the novel analogue, (R)-(+)-α-7-vinylpinene**;** B) MS of the peak at retention time 10.33 minutes.

5.8 Conclusions

Modification of the second isoprene unit, at C8 or C10 by a extra methyl or methylene group has no effect on the catalytic process. Indeed, isomerization on trans (geranyl) to cis (neryl) (LDP) needed for cyclization can occur (Scheme 5.10) followed by the carbocation cascade and proton elimination leading to the formation of the corresponding (+)-α-pinene analogues.

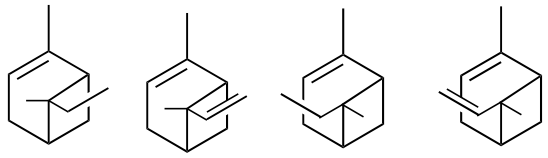

124 **125** **126** **127**

Figure 5.5: (+)-α-pinene analogues obtained by converstion of GDP analogues with HAPS

Modification in the first isoprene unit of GDP by addition of an extra methyl, fluorine or removal of the C2-C3 double bond stops the catalytic process at the first step. Indeed, no formation of any intermediate or final product from the catalytic cascade is observed by GC-MS analysis. So it seems that 2-fluoroGDP (**118**), 2,3-dihydroGDP (**119**) and 9-methyl GDP (**120**) may inhibit conversion of GDP to LDP. For 2,3-dihydroGDP (**119**), the presence of the 2,3-double bond of the substrate is essential for cyclisation to occur in the biosynthesic pathway (Scheme 1.6). For the 2-fluoroGDP (**118**), it is based on electronegativity of the fluorine group. The electron withdrawing fluorine substituent would be expected to retard/inhibit ionisation at the geranyl cation (Scheme 1.6).[107]

For 9-methyl GDP (**120**), it may be difficult to form LDP based on steric hindrance (bulkiness of ethyl group *versus* methyl group). It may be difficult to overcome the topological impediment to direct cyclisation, imposed by the trans geometry of the C2–C3 double bond or due to the steric hindrance, making the compound unable to go into the active site of the enzyme to react.

However, it was not possible to do preparative incubation with GDP analogues in order to obtain a ^{1}H NMR of the final compounds. A long investigation on incubation conditions would be needed.

CHAPTER 6

General conclusions and future work

The monoterpene synthase α-pinene synthase was used as a pilot synthetic platform to produce high-value mono-oxygenated terpenoids. Heterologous expression, purification and characterization of recombinant (+)-α-pinene synthase are performed. Several expression conditions and many purification methods were tried in order to get optimum results. The plant gene was first codon optimised for expression in *E. coli*. Codon optimization can alter both naturally occurring and recombinant gene sequences to achieve the highest possible levels of productivity in any given expression system by increasing the translational efficiency. However, after gene design and expression, (+)-α-pinene synthase was obtained as inactive inclusion bodies and several protein purification techniques were needed in order to get soluble, catalytically active (+)-α-pinene synthase. Several different purification protocols were attempted with this particular synthase, including ion exchange chromatography, ammonium sulphate precipitation, hydrophobic interaction chromatography and size exclusion chromatography before introducing affinity chromatography.

Although His-tagged terpene synthases are catalytically active when expressed, such fusions are, in some cases, inappropriate for detailed crystallographic studies.[88,137-139] A concern however, is that the presence of the his-tag may affect the enzyme activity and so, in addition, it was decided to insert a TEV (Tobacco Etch Virus) cleavage site between the (+)-α-pinene synthase gene and the N-terminal his-tag. After purification by Ni affinity chromatography, the ability of (+)-α-pinene synthase to produce (+)-α-pinene was assessed. The kinetic evaluation (K_M and k_{cat}) of (+)-a-pinene synthase was carried out using radiolabelled [1-^{3}H]-GDP under optimised reaction conditions (*vide supra*). The K_M value was found to be 40 ± 8 μM, and the k_{cat} value 0.001 ± 0.0004 s^{-1}. The K_M value is in good agreement with those previously reported.[15] The N-terminal hexa-histidine tag did not appear to affect the activity of the enzyme and all further experiments were performed with His-tagged (+)-α-pinene synthase (HAPS).

Using monoterpene synthase (α-pinene synthase, HAPS) as a platform to produce important pheromones (verbenone or verbenol) directly from geranyl diphosphate can be used as a novel chemoenzymatic approach. A chemoenzymatic synthesis of (+)-verbenone in 50% yield and >98% optical purity was achieved in two steps starting from geranyl diphosphate. This method favorably compares to previous syntheses as it

avoids the isolation of intermediates (α-pinene/verbenol) and is, for the most part, devoid of undesirable by-products. Although verbenone is a cheap commercially available natural product, this pilot project was intended mostly as a proof of concept using a relatively simple target, and hence accumulate valuable evidence to assess in-depth the suitability of the approach to target more complex terpenoids such as artemisinin and artemisinin derivates in future.

The chemoenzymatic synthesis of (+)-verbenone from geranyl diphosphate demonstrates that terpene synthases are useful catalysts to construct synthetically challenging natural products in only a few chemical steps, with potentially novel biological properties. These engineered (+)-α-pinene analogues may display enhanced biological activities due to the potential improvement of their physical properties. More geranyl diphosphate analogues can be synthesized in future (using phenyl-, fluoro-functional groups).

Finally, a site directed mutagenesis strategy was employed to HAPS to examine the potential catalytic role of four aromatic amino acids, in stabilizing the carbocationic intermediates generated in the active site of HAPS during the natural conversion of geranyl diphosphate to the monoterpene (+)-α-pinene. The replacement by residues of different electrostatic and hydrogen bonding properties drastically changed either the HAPS structure (folding) leading to inactivity or lead to proteins in which the catalytic properties were impaired. Tandem arginine pairs are good target for future mutagenesis studies for HAPS.

CHAPTER 7

Materials and methods

7.1 Materials

Oligonucleotide primers for site directed mutagenesis were purchased from Eurofins MWG|Operon. A synthetic gene for α-pinene synthase from loblolly pine *(Pinus taeda*) was cloned into *Nco*I, *Bam*HI digested pET 21d (*EpochBioLabs*) using methods in previous work within the Allemann group. Chemicals were purchased from Chemodex, Fisher, Fluka, GE Healthcare, Merck, New England Biolabs, NovaBiochem, QIAGEN or Sigma-Aldrich. DNA primers (oligonucleotides) were purchased from Operon or Sigma-Aldrich.

^{1}H-NMR spectra were measured on a Bruker Avance DPX400 NMR spectrometer and are reported as chemical shifts in parts per million downfield from tetramethylsilane, multiplicity (s = singlet, d = doublet, t = triplet, q = quartet, m = multiplet), coupling constant (to the nearest 0.5 Hz) and assignment, respectively. IR spectra were recorded on a Perkin-Elmer 1600 series FTIR spectrometer and samples were prepared as thin films of neat liquid on sodium chloride discs. GC-MS analyses were performed on a Hewlett Packard 6890 GC fitted with a J&W scientific DB-5MS column (30 m x 0.25 mm internal diameter) and a Micromass GCT Premiere mass spectrometer detecting in the range m/z 50-800 in EI+ mode with scanning once a second with a scan time of 0.9 s. Injections (10 **µ**L) were performed in split mode (split ratio 5:1) at 50 °C. Chromatograms were begun with an oven temperature of 49 °C, which was held for 1 min and then increased at 4 °C min-1 for 25.25 min up to 150 °C. Chiral GC analyses were performed on a Perkin Elmer 8700 Gas Chromatograph using a Supelco 23404 beta-Dex L20 column (30 m x 0.25 mm internal diameter) with an FID detector. Chromatograms were performed isothermally at 80 °C for ⟨-pinene and 110 °C for verbenone with the injector at 200 °C.

Centrifuges used were as follows:

Eppendorf 5415 benchtop microcentifuge

Thermo IEC 243 Centra CL3R centrifuge, Thermo Fisher Scientific Inc, USA
Innova 43 shaker (New Brunswick Scientific, UK)

7.1.1 Primers for inserting TEV cleavage site to his-tagged protein

Oligonucleotides for site-directed mutagenesis were purchased from Eurofins MWG|Operon. The primers were as follows (5' to 3') and both primers were phosphorylated at the 5' end.

Forward- CACCACCACCACCACCAC
Reverse- GCCCTGAAAATACAGGTTTTCCAGTGGGACGGTTTCGAC

7.1.2 Primers for site-directed mutagenesis

Oligonucleotides for site-directed mutagenesis were purchased from Eurofins MWG|Operon.
The primers were as follows (5' to 3'), with the changed triplet underlined and the changed bases in italics:

HAPS-Y601A forward:
CGTGTTTCATTACGGC*GCG*AAATACCGTGACGGC
HAPS-Y601A reverse: GCCGTCACGGTATTT*CGC*GCCGTAATGAAACACG

HAPS-F607A forward: CAAATACCGTGACGGC*GCG*AGTGTGGCCAGTATTG
HAPS-F607A reverse: CAATACTGGCCACACT*CGC*GCCGTCACGGTATTTG

HAPS-F597A forward: CTTTGACATTTGCCGCGTG*GCG*CATTACGGCTACAAATAC
HAPS-F597A reverse: GTATTTGTAGCCGTAAT*GCG*CCACGCGGCAAATGTCAAAG

HAPS-F480A forward:
CGGGAAAGTCAGC*GCG*GGCAGCCGCATCAC
HAPS-F480A reverse:
GTGATGCGGCTGCC*CGC*GCTGACTTTCCCG

HAPS-Y601F forward: CGCGTGTTTCATTACGGC*TTT*AAATACCGTGACGGCTTTAG
HAPS-Y601F reverse: CTAAAGCCGTCACGGTATTT*AAA*GCCGTAATGAAACACGCG

HAPS-F607Y forward: CAAATACCGTGACGGC*TAT*AGTGTGGCCAGTATTG
HAPS-F607Y reverse: CAATACTGGCCACACT*ATA*GCCGTCACGGTATTTG

HAPS-F607L forward: CAAATACCGTGACGGC*CTG*AGTGTGGCCAGTATTG
HAPS-F607L reverse: CAATACTGGCCACACT*CAG*GCCGTCACGGTATTTG

HAPS-Y601L forward: CCGCGTGTTTCATTACGGC*CTG*AAATACCGTGACGGCTTTAG

HAPS-Y601L reverse: CTAAAGCCGTCACGGTATTT*CAG*GCCGTAATGAAACACGCGG

HAPS-F597Y forward: CTTTGACATTTGCCGCGTG*TAT*CATTACGGCTACAAATAC
HAPS-F597Y reverse: GTATTTGTAGCCGTAATG*ATA*CACGCGGCAAATGTCAAAG

HAPS-F597L forward: CTTTGACATTTGCCGCGTG*CTG*CATTACGGCTACAAATAC
HAPS-F597L reverse: GTATTTGTAGCCGTAATG*CAG*CACGCGGCAAATGTCAAAG

HAPS-F480Y forward: GGAAAGTCAGC*TAT*GGCAGCCGCATC
HAPS-F480Y reverse: GATGCGGCTGCC*ATA*GCTGACTTTCC

HAPS-F480L forward: GAGAACGGGAAAGTCAGC*CTG*GGCAGCCGCATCACTACTC
HAPS-F480L reverse: GAGTAGTGATGCGGCTGCC*CAG*GCTGACTTTCCCGTTCTC

The oligonucleotides were designed taking the following considerations into account:

1. Both primers should have the desired mutation and must anneal to the same sequence on opposite strands of the parent plasmid.
2. The primers should be 25-45 bases in length and melting temperature, T_m should be 75 to 85 $^{\circ}$C.
3. The primers should contain 40 to 60 % of GC residues and also terminate in one or more C or G bases.
4. The protocol used was that supplied with the Quick-change Site-Directed Mutagenesis Kit from Stratagene and the expression system was *Escherichia coli*.

   All the above parameters were calculated using the following website: www.bioinformatics.org/primerx/index.html.

7.2 Growth media

7.2.1 LB and YT media

LB medium was prepared by dissolving 10 g/L of tryptone, 10 g/L NaCl and 5 g/L bacto-yeast extract, in water and then adjusting the solution to pH 7.5.

YT medium was prepared by dissolving 16 g/L of tryptone, 5g/L NaCl and 10 g/L bacto-yeast extract in water and adjusting the solution to pH 7.5.

7.2.2 LB agar plates

LB agar plates were prepared by adding 7.5 g of agar to 500 mL of LB media. The solution was autoclaved, and then 90 mg of ampicillin-sodium were added to the warm solution once it had cooled to ~40 °C. The mixture was poured into petri dishes and left to solidify, and stored at 4 °C.

7.3 *E. coli* strains

7.3.1 Cloning strains

For sequencing, the XL1-Blue strain was used. This is an excellent host strain for routine cloning because these cells have high transformation efficiency.

7.3.2 Expression strains

For large-scale expressions of HAPS, the *E. coli* strain BL21 Codon plus (DE3)-RIL was used. It carries a T7 RNA polymerase under the control of a lac UV5 promoter. Codon plus RIL cells are codon enriched R, L and I that are mostly used by plants and are often used to express plant genes in bacterial hosts.

7.4 Preparation of Buffers

7.4.1 Lysis buffer

For 1 L of lysis buffer, 6 g of Tris-base (50 mM), 1.85 g EDTA (5 mM), 350 μL β-mercaptoethanol (5 mM) and 100 mL Glycerol (10% v/v) were fully dissolved in deionized water. The pH was adjusted to 8.0.

7.4.2 Dialysis Buffer

For 3 L of dialysis buffer, 3.6 g of Tris-base (10 mM) and 1048 μL β-mercaptoethanol (5 mM) were dissolved in deionized water and the pH was adjusted to 7.5

7.5.1 Insertion of a TEV cleavage site into the hexahistidine-tag protein using PCR

Insertion of the desired primer was performed using *Phusion Site Directed Mutagenesis Kit* (New England Bio Labs).

The reaction mixture contained	μL
H_2O (sterilized)	31.5
5× Phusion HF buffer	10.0
10 mM dNTP's	1.0
Primer A	2.5
Primer B	2.5
Template DNA (1ng)	1
Phusion hot start polymerase	0.5

The PCR reaction was carried out using temperature cycles as follows:

1)	98°C	30 sec	(Initial denaturation)
2)	98°C	10 sec	(Denaturation of template)
3)	67°C	30 sec	(Annealing)
4)	72°C	3.6 min	(Extension at 30 sec per kilobase)
5)	72°C	10 min	(Final extension)
	4°C	hold	

25 cycles were performed for steps (2-4)

7.5.2 Ligation

The PCR product was circularised with quick T4 DNA ligase in a 5 min reaction as follows,

Take 5µl of PCR product. 5µl of 2 × quick ligation buffer was added with mixing. 0.5µl of quick T4 DNA ligase was added with mixing. The final mixture was mixed well for 2-3 sec and incubated at room temperature for 5 min and then chilled on ice. The PCR product was then transformed in to *E. coli* XL1 Blue cells as described below.

7.5.3 Site-directed mutagenesis using PCR

The Promega *Pfu kit* was used for all site directed mutagenesis work.

The reaction mixture contained	µL
Pfu DNA polymerase buffer (10x)	5.0
Primer A	2.0
Primer B	2.0
Template DNA	1.0
10 mM dNTP's	1.0
Pfu DNA polymerase	1.0
H_2O (sterilized)	39.0

The PCR reaction was carried out using temperature cycles as follows:

1) 95°C 3 min (Activation of heat sensitive *Pfu* polymerase)
2) 95°C 1 min (Denaturation of template)
3) 67°C 2 min (Annealing)
4) 72°C 15 min (Extension at 2 min per kilobase)
5) 72°C 10 min (Final extension)
   4°C hold

15 cycles were performed for steps (2-4)

The PCR product was then digested with Dpn 1 (1 µL) endonuclease (target sequence: 5'- GATC – 3' with methylated alanine) to remove all parental DNA. This mixture was incubated at 37 °C for 1hour.

XL1-Blue cells were then transformed with 5 µL of Dpn 1 treated DNA solution. The transformation mixture was incubated on ice for 30 min. After a heat shock at 42° C for 45 s, 1 mL of LB media was added. The resulting mixture was incubated at 37° C for 1 h. The resulting cells were harvested by microcentrifugation at 13000 rpm for 1 min.

The pellet obtained was resuspended in LB media (20 µL) and spread onto LB agar plates containing ampicillin (0.18 mg/mL Agar). The LB agar plates were incubated at 37° C overnight.

7.6 Agarose gel electrophoresis

7.6.1 50 x TAE buffer

Tris base (242 g), acetic acid (57.1 mL) and 100 mL of EDTA (0.5 M) were dissolved in 1 L of water and the solution adjusted to pH 8.

Agarose (0.5 g) was dissolved in 50 mL of TAE (50X) buffer. The mixture was heated in a microwave oven until the agarose was fully dissolved (0.5 -1 min) and then the mixture was poured in to a BioRad Mini-Gel kit fitted with a comb and allowed to set.
5 µL of DNA sample was mixed with 10 µL of DNA dye (30% glycerol, 0.5% bromophenol blue and water) and loaded to the wells. The gel was run at 60 mA for 60 min.

7.6.2 Ethidium bromide

25 µM ethidium bromide stock solutions were prepared by dissolving ethidium bromide (8.1g) in 100 mL of deionised water. This solution was stored in the dark at 4 ˚C. For gel staining, a working concentration of 6 µM was prepared by diluting 48 µL of stock solution to 200 mL with deionised water.

7.7 DNA purification using QIA MiniPrep Kit Protocol

The 10 mL overnight cultures in LB medium containing 0.27 µM ampicillin were centrifuged at 4000 rpm for 10 min.
The pellets were resuspended in 250 µL of buffer P1 and transferred to a micro centrifuge tube following which 250 µL of buffer P2 was added and mixed thoroughly by inverting the tubes 4-6 times. After that 350 µL of Buffer N3 was added and mixed in immediately by inverting the tube 4-6 times. The solution became cloudy upon the addition of N3. This solution was centrifuged for 10 min at 13,000 rpm in an Eppendorf

5415 benchtop microcentifuge. Following centrifugation, supernatants were then transferred from the Eppendorf to the QIAprep spin column by decanting. This solution was again centrifuged for 1 min and the flow through was discarded. The QIAprep spin column was washed with 0.75 mL of Buffer PE and centrifuged for 1 min at 13,000 rpm. The flow through was discarded, and the QIAprep spin column was centrifuged for an additional 1 min to remove residual wash buffer. Finally the QIAprep column was placed in a clean 1.5 mL micro centrifuge tube. At this stage to elute the DNA, the QIAprep spin column was placed on an Eppendorf and 50 µL of Buffer EB passed through the center of QIAprep spin column, This was allowed to stand for 1 min, and centrifuged for 1 min. Finally DNA was collected in the Eppendorf and the spin column was discarded.

7.8 DNA mini prep buffers

Buffer P1 (suspension buffer)
Tris-HCl (157.6 mg, 50 mM), EDTA (58.448 mg, 10 mM) and RNase A (50 µg/ml final concentration) were dissolved in 15 mL of deionised water. The pH was adjusted to 8.0 and the total volume adjusted to 20 mL with deionised water. The solution was stored at 4 ˚C.

Buffer P2 (lysis buffer)
NaOH (4 g, 0.4 M) and SDS (5 g, 2% w/v) were dissolved in separate portions of deionised water (200 mL). The solutions were combined and the total volume was adjusted to 500 mL. The final solution was stored at room temperature.

Buffer N3 (neutralization and binding buffer)

Guanidine hydrochloride (7.6 g, 4M), and potassium acetate (981.4 mg, 0.5 M) were dissolved in 15 mL of deionised water. The pH was adjusted to 4.2 and the total volume was adjusted to 20 mL with deionised water and the solution was stored at room temperature.

Buffer PB (wash buffer)
Guanidine hydrochloride (9.5 g, 5M), Tris-HCl (63.0 mg, 20 mM) and ethanol (7.6 mL, 38% v/v) were added to 8 mL of deionised water. The pH was adjusted to 6.6 and the

total volume was adjusted to 20 mL with deionised water. The solution was stored at room temperature.

Buffer PE (wash buffer)
NaCl (23.4 mg, 20 mM), Tris-HCl (6.3 mg, 2 mM) and ethanol (16 mL, 80% v/v) were added to 2 mL of deionised water. The pH was adjusted to 7.5 and the total volume was adjusted to 20 mL with deionised water. The solution was stored at room temperature.

Buffer EB (Elution buffer)
Tris-HCl (32 mg, 10 mM) was dissolved in 15 mL of deionised water. The pH was adjusted to 8.5 and the total volume was adjusted to 20 mL with deionised water. The solution was stored at room temperature.

7.9 SDS-Polyacrylamide gel electrophoresis

7.9.1 SDS stacking buffer

Tris-base (6 g, 0.5 M) was dissolved in 80 mL of deionised water and the pH adjusted to 6.8 with 6 M HCl. The total volume was adjusted to 100 mL with deionoised water and the resulting solution was stored at room temperature.

7.9.2 SDS resolving buffer

Tris-base (27.23 g, 1.5 M) was dissolved in 100 mL of deionised water and the pH adjusted to 8.8 with 6 M HCl. The total volume was adjusted to 150 mL with de-ionised water and stored at room temperature.

7.9.3 10% (w/v) sodium dodecyl sulfate (SDS)

Sodium dodecyl sulfate (10 g) was dissolved in 90 mL of deionised water. After the solid was fully dissolved, the volume was adjusted to 100 mL and the solution was stored at room temperature.

7.9.4 10% (w/v) Ammonium persulfate

Ammonium persulfate (100 mg) was dissolved in 1 mL of deionised water. The solution was freshly made each time.

7.9.5 SDS electrode running buffer (10x)

Tris-base (30.3 g, 250 mM), glycine (150 g, 2 M) and sodium dodecyl sulfate (10.0 g) were fully dissolved in 900 mL of deionised water. The total volume was adjusted to 1 L and stored at 4 $^{\circ}$C. The concentrated solution was diluted 10 fold before use with deionised water.

7.9.6 SDS staining solution

Coomassie brilliant blue (R-250) (0.25 g), was dissolved in a mixture of methanol,water and glacial acetic acid (45 mL, 45 mL and 10 mL respectively) this solution was stored at room temperature.

7.9.7 SDS destaining solution

Ethanol (40%) and glacial acetic acid (10%) were mixed then the total volume was adjusted to 1 L.

7.9.8 SDS-PAGE protocol

Gel solutions were prepared by mixing the reagents described in the table below. The gel solutions were poured in-between two glass plates. 100 µL of APS and 15 µL of TEMED were added to both the resolving and stacking solutions just prior to pouring the gel. Solutions were mixed gently to initiate polymerization. Firstly, resolving solution was poured into the gap between the glass plates just to reach the bottom line of the wells when the combs were inserted. Once the resolving gel was set, isopropanol was removed using blotting paper and the stacking gel solution was poured until over-flowing and a comb was inserted to create wells for sample loading. For analysis of

HAPS 5% stacking and 12% resolving gels were used. Finally gels were stained with staining solution and then destained.

Gel (%)	dH_2O (mL)	30% Degassed Acrylamide-Bis (mL)	Gel Buffer (mL)
4	6.1	1.3	2.5
5	5.7	1.7	2.5
6	5.4	2.0	2.5
7	5.1	2.3	2.5
8	4.7	2.7	2.5
9	4.4	3.0	2.5
10	4.1	3.3	2.5
11	3.7	3.7	2.5
12	3.4	4.0	2.5
13	3.1	4.3	2.5
14	2.7	4.7	2.5
15	2.4	5.0	2.5
16	2.1	5.3	2.5
17	1.7	5.7	2.5

7.10 Preparation of Competent Cells

Non-competent cells (BL21-CodonPlus (DE3)-RIL cells) from glycerol stocks (2 μL) were used to inoculated LB media (100 mL) and then incubated in a shaker overnight at 37 ˚C. 1 mL of the overnight culture was used to inoculated LB media (100 ml) and incubated at 37 ˚C until an optical density of 0.6 (600 nm) was reached. The cells were centrifuged for 10 min at 4000 rpm (Thermo IEC 243 Centra CL3R centrifuge, Thermo Fisher Scientific Inc, USA) and the supernatant solution was discarded. The pellet was re-suspended in 5 mL of sterilized $CaCl_2$ solution (100 mM) and incubated on ice for 20 min before harvesting the cells through centrifugation as above. The resulting pellet was re-suspended in 6 mL of sterilized $CaCl_2$ and 15 % (v) glycerol as their OD units (1 mL of $CaCl_2$ and 15 % (v) glycerol per 0.1 unit of OD). This mixture was incubated on ice for 20 min and then aliquoted to sterile Eppendorf tubes (100 μL) and flash frozen in liquid nitrogen for storage at -80 ˚C.

7.11 Preparation of Super-Competent Cells

Tfb 1

Potassium acetate (0.59 g, 30 mM), rubidium chloride (2.42 g , 100 mM), calcium chloride (0.29 g , 910 mM), manganese chloride (2.00 g , 50 mM,) were dissolved 15% glycerol 15 % in water (v/v, 80 mL) mixed together and pH adjusted to 5.8 with dilute acetic acid. The solution was then diluted to a final volume of 200 mL with deionised water.

Tfb 11

MOPS (0.21 g, 10 mM), calcium chloride (1.1 g, 75 mM), rubidium chloride (0.121 g, 10 mM) were dissolved 15 % glycerol 15 % in water (v/v) mixed together and pH adjusted to 6.5 with dilute NaOH. The solution was then diluted to a final volume of 100 mL.

Non-competent cells from glycerol stocks (5 μL) were used to inoculate LB medium (100 mL) and the culture was incubated in a shaker overnight at 37 ˚C. 1 mL of overnight culture was used to inoculate LB medium (100 ml) and incubated at 37 ˚C until an optical density of 0.6 (600 nm) was reached then the cells were incubated on ice for 15 min and harvested by centrifugation at 5 °C (4000 g, 10 min) (Thermo IEC 243 Centra CL3R centrifuge, Thermo Fisher Scientific Inc, USA) and the supernatant solution was discarded. The pellets were re-suspended in Tfb 1 buffer (0.4 of original volume of over night culture medium) and incubated on ice for 15 min. Cells were harvested by centifugation as described above and the resulting pellet was re-suspended in Tfb 11 (0.04 of original volume of over night culture medium). The solution was incubated on ice for 20 min and then aliquoted to sterile Eppendorf tubes (100 μL) and flash frozen in liquid nitrogen for storage at -80 ˚C.

7.12 Protein production and purification

7.12.1 Transformation into *E. coli* BL21 codon plus (DE3) – RIL competent cells

1 μL of sequenced DNA was added to 100 μL of competent cells. The transformation mixture was incubated on ice for 30 min. After a heat shock at 42 °C for 45 s 1 mL of LB medium was added. The resulting mixture was incubated at 37 °C for 1 h. The resulting cells were harvested by microcentrifugation at 13000 rpm for 1 min. The pellet obtained was resuspended with in LB medium (20 μL) and spread onto LB agar plates containing ampicillin (0.18 mg/ mL LB-agar). LB agar plates were kept at 37° C overnight.

7.12.2 Large-scale expression

A single colony transformed Pt-DNA was picked and used to inoculate 100 mL of LB medium containing ampicillin (0.27 μM). The culture was incubated overnight at 37 °C with shaking at 150 rpm in an Innova 43 shaker. The 5 mL overnight cultures were used to inoculate 6 x 500 mL of sterile LB medium containing ampicillin (0.27 μM). Cultures were incubated at 37 °C with shaking at 150 rpm. When the optical density (600 nm) reached 0.5-0.8, the cultures were induced with IPTG (0.5 mM) and grown for another 4 h at 37 °C. Cells were harvested by centrifugation at 5 °C (6000 g, 15 min). The supernatant solution was discarded and the pellets were stored at - 80°C.

7.12.3 Base Extraction

Frozen pellets of *E. coli* containing the over expressed enzyme were thawed and resuspended in cell lysis buffer. The resuspended cells were lysed by sonication on an ice bath (5 s pulse on followed by 10 s pulse off, repeated for a total of 4 min). The cell lysate was clarified by centrifugation at 5 °C (17000 g, 30 min: Pellet 1 (P 1) and supernatant solution 1 (SN 1) were obtained. Pellet 1 was resuspended in cell lysis buffer (100 mL). The pH of the solution was slowly adjusted to 12 by dropwise addition of NaOH (5 M) and then the basic solution was stirred for 30 min at 4 °C. βME (5 mM) was added and the pH changed back to pH 8 by dropwise addition of 1 M HCl. This

mixture was stirred for another 1 hour at 4 °C then the suspension was centrifuged (12000 rpm, 30 min). Finally protein was found in the resulting supernatant solution 2.

7.12.4 Ion exchange chromatography

Using buffers at various pH's several attempts at purification of α-PS were attempted by ion exchange chromatography. The resins and pH conditions used were as follows:

Resource S (6ml) at pH 7.0

i. Start buffer: Tris buffer (20 mM Tris base, 5 mM EDTA, 5 mM βME, pH 7.0).
ii. Elution buffer: start buffer + 1M NaCl

Resource Q (8mL): at pH 8.0

i. Start buffer: Tris buffer (20 mM Tris base, 5 mM EDTA, 5 mM βME, pH 8.0).
ii. Elution buffer: start buffer + 1 M NaCl

DEAE sepharose, Q sepharose and SP sepharose resins were also tried at different pH's. For pH 6.2 and 7.0 phosphate buffer was used and for pH 8.0 and 8.8 cell lysis buffer was used. For each attempt a few grams of each resin was placed in an Eppendorf™ tubes then equilibrated with cell lysis buffer. Enzyme solution in cell lysis buffer (Tris-base (50 mM), EDTA (5 mM), β-mercaptoethanol (5 mM) and 100 mL Glycerol (10% v/v), pH 8.0, 500 μL) was added to each sample and shaken gently for 5 min. As it was crude protein the enzyme concentration was not calculated. The mixture was then centrifuged for 1 min at 17,000 g and the flow through (supernatant solution) was decanted. Elution buffer containing 1M NaCl was then added to the resin pellet and mixed gently to elute the bound protein, after centrifugation for 1 min at 13,000 rpm the eluate (supernatant solution) was again decanted. After freeze-drying both the flow through and the eluate were redissolved in 20 μL cell lysis buffer and analysed by SDS-PAGE

For DEAE drip column chromatography a 3 × 1.5 cm diameter drip column was used. The column was pre-equilibrated with buffer. Proteins were eluted using NaCl in a step gradient (200 mM NaCl, 400 mM NaCl, 600 mM NaCl and 1 mM NaCl). Four column volumes (CV) of buffer passed through in each gradient. 1 mL of fractions was

collected. Absorbance was measured at 280nm and plotted against fractions. Aliquots were analysed by SDS PAGE.

7.12.5 Ammonium sulphate precipitation.

A saturated solution of $(NH_4)_2SO_4$ was prepared. Different percentages of saturation were obtained (10% - 90%) by adding different amounts of saturated $(NH_4)_2SO_4$ to 1 mL of supernatant solution 2. For example 1.5 mL of saturated $(NH_4)_2SO_4$ was added to obtain 60% saturation and 3.0 mL of saturated $(NH_4)_2SO_4$ was added to obtain 75%. The mixture was stirred for 1 h and then the resulting precipitate was collected by microcentrifugation at 13000 rpm for 30 min. The pellet obtained was resuspended in Tris buffer (20 mM Tris base, 5 mM EDTA, 5 mM βME, pH 8.0). Resuspended solutions arising from the pellet obtained from the different concentrations of ammonium sulfate used were analysed by SDS-PAGE.

7.12.6 Hydrophobic interaction chromatography (HIC)

Hydrophobic interaction chromatography was performed with the HiTrap Selection Kit (GE healthcare), according to the instruction manual. This Selection Kit includes seven HIC columns with different hydrophobic characteristics were as follows:

- HiTrap phenyl FF (1mL) (high substitution)
- HiTrap phenyl FF (1mL) (low substitution)
- HiTrap phenyl HP (1mL)
- HiTrap butyl FF (1mL)
- HiTrap butyl-S FF (1mL)
- HiTrap Octyl FF (1mL)

1. Start buffer: 50 mM sodium phosphate, 1M NaCl, pH 7.0
2. Elution buffer: 50 mM sodium phosphate, pH 7.0

Each column was pre-equilibrated with start buffer. In each case the SN 2 was added directly to the HIC column. Proteins were eluted with a NaCl gradient (1 M to 0 M) for 15 column volumes using a flow rate of 1 ml/min. 1 mL fractions were collected. Fractions were analyzed by SDS-PAGE.

7.12.7 Size exclusion chromatography (SEC)

Size exclusion chromatography was performed on a 10 × 300 mm bed diameter superdex-200 column (24 mL) (GE healthcare). Tris buffer (20 mM Tris, 5 mM EDTA, 5 mM βME and 0.15 M NaCl at pH 8.0) was used to elute the material from the column. A flow rate of 0.5 ml/min was maintained for each elution. 1 mL of Fractions were collected and were analyzed by SDS-PAGE. A second attempt was carried out following the above protocol but adding 0.1 %(v/v) Tween 20 detergent to the buffer.

7.12.8 Ni^{2+} affinity chromatography

Binding Buffer: 100 mM Tris, 500 mM NaCl, 1mM imidazole, and 5 mM βME.
Elution buffer: 100 mM Tris, 500 mM NaCl, 500 mM imidazole, and 5 mM βME.

The supernatant solution from the base extraction step (SN2) was dialysed against binding buffer and the solution was loaded onto a Ni^{2+}-Sepharose™ 6 Fast Flow drip column (GE Healthcare, 3 mL). After 10 min, the flow-through solution was collected and the column was washed with 10 column volumes (CV) of binding buffer. The protein was eluted with a gradient ranging from 5 to 500 mM imidazole (20 CV) followed by a wash at 500 mM imidazole (10 CV). Protein eluted at approximately 50-150 mM imidazole. Fractions were analysed by SDS-PAGE and those corresponding to the correct molecular weight were pooled and dialysed overnight against 10 mM Tris-Base, 5 mM βME, pH 7.5.

7.13 Concentration of the dialysed protein using Amicon ultrafiltration

The dialysed protein was transferred to an Amicon™ ultrafiltration apparatus containing a 30 kDa cutoff Millipore ultrafiltration membrane. The solution was concentrated at a pressure of 1.5 bar at 4 ˚C, to give a final volume of approximately 5-6 mL. Concentrated protein sample was stored at -20 ˚C with 10 % (v/v) glycerol solution in water.

7.14 Determination of protein concentration

The concentration of protein was measured using the Bradford method.[144] Protein concentrations were measured at OD_{590}/OD_{450} rather than single measurement at OD_{590} to obtain more accurate and sensitive changes in the protein concentrations and thereby to acquire linearity.[198]

7.14.1 Dye Reagent

Coomassie brilliant blue G-250 (20 mg) was dissolved in 10 mL of ethanol and 20 mL of phosphoric acid (85 % w/v) was added. The solution was diluted with double distilled water to make the final volume 200 mL. The solution was filtered and stored at 4 ˚C in the dark to protect it from light.

7.14.2 Protein Determination

1 mg/mL of BSA stock was prepared. The BSA protein diluted to a final concentration of 200 µL. A Calibration curve was obtained in the range of 0-100 µg/mL of BSA and straight line obtained by plotting OD_{590}/OD_{450} as a function of BSA concentration. From the linear equation concentration of the protein was obtained.

7.15 Enzyme characterization

7.15.1 Assay of enzyme activity

Kinetic assays were performed in a manner similar to that previously described within the group for aristolochene synthase.[79] Assays (final volume 250 µL) were initiated by addition of a purified enzyme solution (0.4 µM) to 20-120 µM [1-^{3}H]-geranyl diphosphate in Bis-Tris propane (100 mM), KCl (50 mM) and $MgCl_2$ (100 mM), pH 7.5). The reaction time and enzyme concentrations were optimized to make sure the reaction was in the initial linear phase. After incubation for 15 min, reactions were stopped by addition of 100 µL (100 mM) EDTA and overlaid with hexane (1 mL). The samples were vortexed for 10 s and the hexane layer was removed and the sample

extracted with further hexane (2 x 1 mL). The pooled hexane extracts were filtered through 40 mg of silica gel, emulsified with 15 mL of Ecoscint^{TM} O (National Diagnostics) and analyzed by scintillation counting (Packard 2500 TR^{TM}) in ^{3}H mode for 4 min per sample. Data were fitted to the Michaelis-Menton equation, $V = (V_{max}[S])/(K_M + [S])$ using Systat Sigmaplot 10.

7.16 GC-MS

To test the activity of the purified enzyme and product profiles, the enzyme was incubated with substrate (1.6 mM), buffer (Bis-Tris propane (100 mM), KCl (50 mM) and $MgCl_2$ (20 mM), pH 7.5) in a final volume of 0.5 mL. The assay solution was gently mixed with enzyme (10 μM) the reaction was overlaid with 1 mL of pentane and gently shaken overnight at room temperature. The organic layer was removed and the aqueous layer extracted with additional pentane (500 μL). The pooled pentane extracts were analyzed by GC-MS.

GC-MS analyses were performed on a Hewlett Packard 6890 GC fitted with a J&W scientific DB-5MS column (30 m x 0.25 mm internal diameter) and a Micromass GCT Premiere mass spectrometer detecting in the range *m/z* 50-800 in EI^+ mode with scanning once a second with a scan time of 0.9 s. Injections (10 mm^3) were performed in split mode (split ratio 5:1) at 50 °C. Chromatograms were begun with an oven temperature of 49 °C, which was held for 1 min and then increased at 4 °C min^{-1} for 25.25 min up to 150 °C.

7.17 Experimental

(+)-Verbenone (**13**)

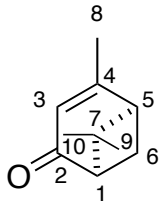

In 27.0 mL assay buffer (Bis-Tris propane (100 mM), KCl (50 mM) and $MgCl_2$ (20 mM), pH 7.5) was added 1.6 mM GDP (16 mg, 40 mmol) and was gently mixed with APS-His6 (4.0 mL, 4 mM). The resulting solution was overlaid with pentane (10 mL) and tightly sealed. The sealed vessel was then gently shaken overnight at room

temperature. The aqueous layer was then carefully removed and then further extracted with pentane (5 x 4 mL). To this enzymatically produced solution of (+)-α-pinene (4.9 mg, 36 μmol) in pentane (30 mL) was added, drop-wise, tert-butyl hydroperoxide (70% wt. aqueous solution, 39.8 μL, 0.29 mmol) and $Cr(CO)_6$ (15.8 mg, 72 μmol). To this mixture was added acetonitrile (4 mL) and the mixture was heated under reflux for 18 h. After cooling in ice the solution was filtered and the residue was washed with additional pentane (2 mL). The filtrate was extracted with 5% NaOH (3 x 5 mL), and the pooled aqueous extracts were back extracted with pentane (5 mL). The pooled fractions were dried with $MgSO_4$, filtered and the solvent was carefully removed under reduced pressure. The residue was dissolved in hexane (1 mL) and (+)-verbenone purified by normal phase HPLC on an Agilent 1100 series system using a Waters Nova-PAK silica HR (3.9 mm x 300 mm) column, eluting with 1% isopropanol in hexane at 1 mL/min. Verbenone eluted at 8.84 min (3.0 mg, 50%).

$\boldsymbol{\delta}_H$ (400 MHz, $CDCl_3$) 1.02 (s, 3 H, H-9); 1.47 (3 H, s, H-10); 2.00 (3H, d, J = 1.5 Hz, H-8); 2.10 - 2.08 (1 H, m, H-6); 2.42 (1 H, m, H-5); 2.70 - 2.62 (1 H, m, H-1); 2.91 - 2.80 (1 H, m, H-6); 5.71(1 H, m, H-3); υ_{max}/cm^{-1} (thin film) 3502, 3039, 2940, 2871, 2360, 2342, 1683 and 1617; m/z (EI^+) 150.1 (90%, M^+), 135.1 (100, $[M\text{-}CH_3]^+$), 122.1 (22), 107.1 (75), 91.1 (40), 71.1 (20), 67.1 (5); $[\alpha]_{20}$ = + 233.3 $°dm^{-1}cm^3g^{-1}$ (c = 0.06, $CHCl_3$). (lit. +258 (c = 1.0 in $CHCl_3$).

(2*E*,6*E*)-8-hydroxy-3,7-dimethylocta-2,6-dien-1-yl acetate (95)

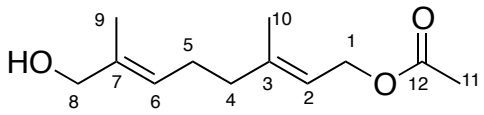

90% tert-butyl hydroperoxide (20.25 ml, 180 mmol) was poured into a magnetically stirred solution of selenium dioxide (0.112 g, 1 mmol) and salicylic acid (0.7 g, 5 mmol) in dichloromethane (17.7 ml). Geranyl acetate (10 g, 50 mmol) was added to the solution and was left to stir at room temperature for 24 hours.

When TLC (Hexane: EtOAc = 4: 1); confirmed the completion of the reaction, hexane (25 ml) was added and the dichloromethane was removed from the solution on the rotary evaporator. Diethyl ether (50 ml) was added and the organic phase was washed with saturated sodium bicarbonate (3 x 20 ml) and brine (20 ml) before being dried with magnesium sulphate, filtered and reduced.

The resulting oil was passed through a column. A ratio of 19:1 hexane:ethyl acetate removed the unused starting material, geranyl acetate. The ratio was then changed to 4:1 to remove the aldehyde fractions, followed by the alcohol fractions. Fractions were analysed by TLC. All fractions were then pooled and concentrated under reduced pressure followed by high vacuum to yield 6.53 g (90.3%) of **95** and 0.51 g (7%) of **94**.

^{1}H NMR of **95** (400 MHz, C_6D_6): δ 1.60 and 1.64 (2x3H, 2xs, 2xCH_3, C^9 and C^{10}), 1.99 (3H, s, CH_3, C^{11}), 1.95-2.15 (4H, m, CH_2CH_2, C^4 and C^5), 3.93 (2H, s, CH_2, C^8), 4.52 (2H, d, $J_{H,H}$=6 Hz, CH_2, C^1), 5.26-5.32 (2H, m, CH, C^2 and C^6).

^{13}C NMR of **95** (125 MHz, C_6D_6): 13.68 (C^9), 16.40 (C^{10}), 21.02 (C^{11}), 25.67 (C^5), 39.05 (C^4), 61.40 (C^1), 68.93 (C^8), 118.75 (C^2), 125.34 (C^6), 135.56 (C^7), 138.20 (C^3), 170.19 (C^{12}).

(2*E*,6*E*)-3,7-dimethyl-8-oxoocta-2,6-dien-1-yl acetate (94)

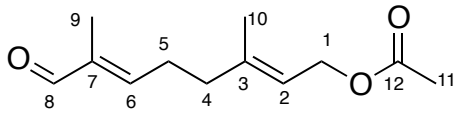

95 (2.5 g, 11.7 mmol) was oxidised to **94** by adding it to a solution of manganese dioxide (20 g, 230 mmol) in hexane (50 ml). The mixture was allowed to stir until TLC plates showed all the starting material had been converted. The solvent was then removed under reduced pressure followed by high vacuum to yield 2.45 g (98%) of colourless oil.

^{1}H NMR (250 MHz, C_6D_6): δ 1.50 and 1.67 (2x3H, 2xs, 2xCH_3, C^9 and C^{10}), 1.81 (3H, s, CH_3, C^{11}), 1.87 (2H, t, $J_{H,H}$=8 Hz, CH_2, C^4), 1.99-2.08 (2H, m, CH_2, C^5), 4.63 (2H, d, $J_{H,H}$=7 Hz, CH_2, C^1), 5.37(1H, t, $J_{H,H}$=5.8 Hz, CH, C^6), 5.93 (1H, t, $J_{H,H}$=7.3 Hz, CH, C^2), 9.35 (1H, s, CH, C^8).

^{13}C NMR (125 MHz, C_6D_6): 9.124 (C^9), 16.06 (C^{10}), 20.50 (C^{11}), 26.78 (C^5), 37.73 (C^4), 60.88 (C^1), 120.21 (C^2), 139.78 (C^7), 140.11 (C^3), 152.00 (C^6), 170.08 (C^{12}), 193.85 (C^8).

(2*E*,6*E*)-3,7-dimethylnona-2,6,8-trien-1-yl acetate (96)

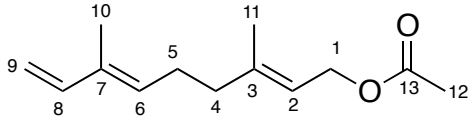

n-Butyl lithium solution (2.5 M in hexanes) (0.94 ml, 2.35 mmol) was added to a stirred solution of methyl triphenyl phosphonium bromide (838 mg, 2.35 mmol) at -10 ^{o}C in dry THF (10 ml) under nitrogen. The resulting yellow solution was stirred for half an hour before a solution of **94** (100 mg, 0.470 mmol) in dry THF (5 ml) was added drop wise over duration of 5 minutes. The solution was then allowed to warm to room temperature and was left to stir for another 48 hours under nitrogen. When TLC (Hexane: EtOAc = 19: 1) confirmed all starting material had been converted, the reaction was quenched with saturated ammonium chloride solution (10 ml).

The quenched mixture was diluted with 10 ml of water and the organic layer was collected. The separated aqueous layer was extracted with diethyl ether until TLC showed the aqueous layer contained no product. The pooled organic layers were washed with brine (20 ml), dried over magnesium sulphate, filtered and concentrated under reduced pressure. The resulting yellow oil was purified by flash chromatography on silica gel (19:1, hexane: ethyl acetate) to yield 52 mg (52%) of colourless oil.

^{1}H NMR (250 MHz, $CDCl_3$): δ 1.65 and 1.67 (2x3H, 2xs, 2xCH_3, C^{10} and C^{11}), 1.99 (3H, s, CH_3, C^{12}), 2.00-2.25 (4H, m, CH_2CH_2, C^4 and C^5), 4.52 (2H, d, $J_{H,H}$=7 Hz, CH_2, C^1), 4.87 (2H, d, $J_{H,H}$=10.75 Hz, CH_{cis}, C^9), 5.02 (2H, d, $J_{H,H}$=17.25 Hz, CH_{trans}, C^9), 5.29 (1H, t, $J_{H,H}$=7.75 Hz, CH, C^6), 5.38(1H, t, $J_{H,H}$=7Hz, CH, C^2), 6.29(1H, dd, $J_{H,Htrans}$=17.25 Hz and $J_{H,Hcis}$=10.75 Hz, CH, C^8).

^{13}C NMR (125 MHz, $CDCl_3$): 12.11(C^{10}), 16.87 (C^{11}), 21.50 (C^{12}), 26.81 (C^5), 39.44 (C^4), 61.75 (C^1), 111.15 (C^9), 118.99 (C^2), 132.51 (C^6), 134.74 (C^7), 141.81 (C^8), 142.20 (C^3), 171.57 (C^{13}).

(2*E*,6*E*)-3,7-dimethylnona-2,6-dien-1-yl acetate (97)

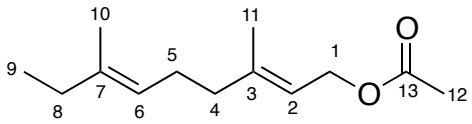

Triphenylphosphinerhodium chloride (43 mg, 0.047 mmol) was added to a solution of **96** (100 mg, 0.473 mmol) in toluene (25 ml) and left to stir. The reaction was left to stir and followed by GC and TLC (Hexane: EtOAc = 19: 1) until all the starting material had been converted. The reaction was then quenched with water (10 ml). The organic layer was separated and the aqueous layer was washed with diethyl ether (3 x 15 ml). The pooled organic layers were then washed with brine (20 ml), dried over magnesium sulphate and concentrated under reduced pressure. The resulting oil was purified by flash chromatography (9:1, hexane: ethyl acetate) to give 62 mg (61.4%) of yellow oil.

^{1}H NMR (400 MHz, $CDCl_3$): δ 0.91 (3H, t, $J_{H,H}$=7.75 Hz, CH_3, C^9), 1.53 and 1.64 (2x3H, 2xs, 2xCH_3, C^{10} and C^{11}), 1.91 (2H, q, $J_{H,H}$=7.6 Hz, CH_2, C^8), 1.99 (3H, s, CH_3, C^{12}), 1.98-2.06 (2H, m, CH_2CH_2, C^4 and C^5), 4.52 (2H, d, $J_{H,H}$=6.8 Hz, CH_2, C^1), 5.01 (1H, t, $J_{H,H}$=6.8 Hz, CH, C^6), 5.28 (1H, t, $J_{H,H}$=5.275 Hz, CH,C^2).
^{13}C NMR (125 MHz, $CDCl_3$): 13.19 (C^9), 16.34 (C^{10}), 16.89 (C^{11}), 21.50 (C^{12}), 26.51 (C^5), 32.74 (C^8), 39.97 (C^4), 61.83 (C^1), 118.62 (C^2), 122.54 (C^6), 133.65 (C^7), 142.76 (C^3), 170.2 (C^{13}).

(2*E*,6*E*)-3,7-dimethylnona-2,6-dien-1-ol (98)

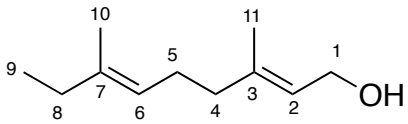

97 (100 mg, 0.47 mmol) was dissolved in a mixture of methanol (9 ml) and distilled water (1 ml). The reaction was stirred at room temperature and lithium hydroxide (56.3 mg, 2.35 mmol) was added. The reaction was monitored by TLC (Hexane: EtOAc = 4: 1). Once all the starting material had been converted the reaction mixture was

neutralised to pH 7 with hydrochloric acid. The organic layer was then separated. The aqueous layer was washed with diethyl ether (3x10 ml) and the pooled organic layers were washed with brine (10 ml), dried over magnesium sulphate and filtered. The solvent was then concentrated under reduced pressure followed by high vacuum. The resulting oil was purified by flash chromatography on silica gel (4:1 hexane to ethyl acetate) to give 76 mg (85%) of colourless oil.

^{1}H NMR (250 MHz, $CDCl_3$): δ 1.00 (3H, t, $J_{H,H}$=7. 5 Hz, CH_3, C^9), 1.63 and 1.72 (2x3H, 2xs, 2xCH_3, C^{10} and C^{11}), 1.96-2.33 (6H, m, 3xCH_2, C^4 and C^5 and C^8), 4.19 (2H, d, $J_{H,H}$=7 Hz, CH_2, C^1), 5.08-5.15 (1H, m, CH, C^6), 5.45 (1H, t, $J_{H,H}$=8.25 Hz, CH, C^2).

(2*E*,6*E*)-1-bromo-3,7-dimethylnona-2,6-diene (99)

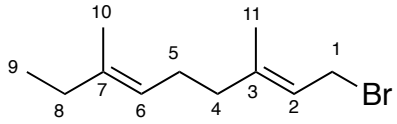

Anhydrous triethylamine (0.72 mg, 0.1ml, 0.7 mmol) was added to a stirred solution of **98** (80 mg, 0.5 mmol) in anhydrous THF (10 ml) at -45 ^{o}C, followed by methane sulfonyl chloride (0.82 mg, 0.08 ml, 0.7 mmol). This mixture was stirred for 15 minutes at -45 ^{0}C and then a solution of lithium bromide (165 mg, 1.9 mmol) in anhydrous THF (5 ml) was added. This mixture was stirred under nitrogen for 2 hours, which after time TLC (Hexane: EtOAc = 9: 1) showed that all the starting material had been used.

The reaction material was partitioned between hexane (20 ml) and water (20 ml). The separated aqueous layer was washed twice more with hexane (2 x 20 ml). The pooled hexane layers were washed with 1 M hydrochloric acid and brine. This was then dried over magnesium sulphate, filtered and then reduced on a rotary evaporator followed by high vacuum. Crude bromide **99** was carried forward for the next reaction.

Synthesis of (2E,6E)-3,7-dimethylnona-2,6-dien-1-yl dihydrogen diphosphate (100)

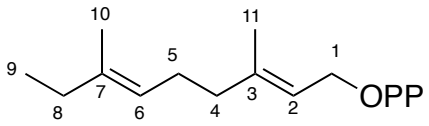

The crude bromide from the reaction **99** was re dissolved in acetonitrile (2 ml) and stirred under nitrogen as tris(tetrabutylammonium) hydrogen pyrophosphate (860 mg, 0.95 mmol) was added. Reaction was followed by TLC (H_2O: NH_4OH:$(CH_3)_2CHOH$ = 2:1:2) and stopped when the bromide spot on the plate had disappeared. The solvent was then removed on the rotary evaporator.

This was then dissolved in an ion exchange buffer (25 mmol NH_4HCO_3 with 2% isopropanol) and run through an ion exchange column to replace the tetrabutylammonium counter ions with ammonium ions. The resulting compound was then run through a HPLC to collect the peaks containing the product. This was then freeze-dried to give 85 mg (55% over the last two steps) of **100**.

^{1}H NMR (500 MHz, D_20): δ 0.82 (3H, t, $J_{H,H}$=8 Hz, CH_3, C^9), 1.49 and 1.58 (2x3H, 2xs, 2xCH_3, C^{10} and C^{11}), 1.82-2.05 (6H, m, 3xCH_2, C^4 and C^5 and C^8), 4.33 (2H, t, $J_{H,H}$=7 Hz, CH_2, C^1), 5.08 (1H, t, $J_{H,H}$=6. 5 Hz, CH, C^6), 5.32 (1H, t, $J_{H,H}$=6 Hz, CH, C^2).

^{13}C NMR (125 MHz, D_2O): 12.10 (C^9), 12.90 (C^{10}), 15.33 (C^{11}), 26.51 (C^5), 31.82 (C^8), 38.88 (C^4), 63.06 (C^1), 122.60 (C^6), 139.45 (C^7), 143.09 (C^3)

^{31}P NMR (202.5 MHz, D_2O): -10.17, -6.45.

m/z (ES^-) 327.1 (100%, $[M+2H]^-$).

(3*E*,7*E*)-9-bromo-3,7-dimethylnona-1,3,7-triene (102)

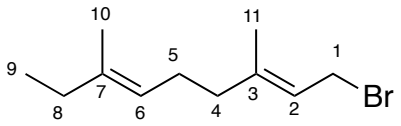

Anhydrous triethylamine (1.44 mg, 0.2 ml, 1.4 mmol) was added to a stirred solution of **101** (160 mg, 1.0 mmol) in anhydrous THF (20 ml) at -45 ^{o}C, followed by methane sulfonyl chloride (1.6 mg, 0.16 ml, 1.4 mmol). This mixture was stirred for 15 minutes at -45 ^{0}C and then a solution of lithium bromide (330 mg, 3.8 mmol) in anhydrous THF (5 ml) was added. This mixture was stirred under nitrogen for 2 hours, which after time TLC (Hexane: EtOAc = 9: 1) showed that all the starting material had been used.

The reaction material was partitioned between hexane (20 ml) and water (20 ml). The separated aqueous layer was washed twice more with hexane (2 x 20 ml). The pooled hexane layers were washed with 1 M hydrochloric acid and brine. This was then dried over magnesium sulphate, filtered and then reduced on a rotary evaporator followed by high vacuum. Crude bromide **102** was carried forward for the next reaction.

Synthesis of (2E,6E,8E)-3,7-dimethylnona-2,6,8-trien-1-yl dihydrogen diphosphate (103)

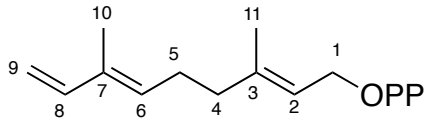

The crude bromide from the reaction **102** was re dissolved in acetonitrile (2 ml) and stirred under nitrogen as tris(tetrabutylammonium) hydrogen pyrophosphate (860 mg, 0.95 mmol) was added. Reaction was followed by TLC (H_2O: NH_4OH:$(CH_3)_2CHOH$ = 2:1:2) and stopped when the bromide spot on the plate had disappeared. The solvent was then removed on the rotary evaporator. The product was then dissolved in an ion exchange buffer (25 mmol NH_4HCO_3 with 2% isopropanol) and run through an ion exchange column to replace the tetrabutylammonium counter ions with ammonium ions. The resulting compound was then run through a HPLC to collect the peaks containing the product. This was then freeze-dried to give 65 mg (45% over the last two steps) of **103**.

^{1}H NMR (500 MHz, D_20): δ 1.63 and 1.66 (2x3H, 2xs, 2xCH_3, C^{10} and C^{11}), 2.05-2.25 (4H, m, CH_2CH_2, C^4 and C^5), 4.38 (2H, t, $J_{H,H}$=6.4 Hz, CH_2, C^1), 4.91 (2H, d, $J_{H,H}$=10.62 Hz, CH_{cis}, C^9), 5.09 (2H, d, $J_{H,H}$=17.4 Hz, CH_{trans}, C^9), 5.38 (1H, t, $J_{H,H}$=6.0 Hz, CH, C^6), 5.51(1H, t, $J_{H,H}$=6.5 Hz, CH, C^2), 6.37(1H, dd, $J_{H,Htrans}$=17.9 Hz and $J_{H,Hcis}$=10.8 Hz, CH, C^8).

^{13}C NMR (125 MHz, D_2O): 10.98 (C^{10}), 15.63 (C^{11}), 25.89 (C^5), 38.37 (C^4), 62.56 (C^1), 111.22 (C^9), 120.31 (C^2), 133.30 (C^6), 134.72 (C^7), 141.63 (C^3), 141.27 (C^8).
m/z (ES^-) 325.1 (100%, $[M+2H]^-$).

(*E*)-2-((3,7-dimethylocta-2,6-dien-1-yl)oxy)tetrahydro-2*H*-pyran (104)

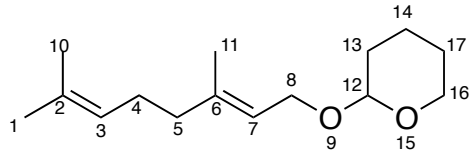

To a stirred solution of **89** (5 g, 32.5 mmol) in dry ether (30 mL) were added DHP (3.0 g, 36 mmol) and TsOH (60 mg). The reaction was stirred under nitrogen for 18 hours. Once TLC (Hexane: EtOAc = 4: 1) showed completion of reaction, the mixture was quenched with Et_3N (15 mL), extracted with a mix of Hexane:EtOAc (1:1) (3 x 20 mL). The organic layer was washed with water (10 mL) and brine (10 mL), dried over $MgSO_4$, and concentrated under reduced pressure to give 6.5 g (88%) of **104**.

^{1}H NMR (250 MHz; $CDCl_3$): 1.5 (3x2H, m, C^{13}, C^{14}, C^{17} OTHP), 1.6 (3x3H, m, C^1, C^{10}, C^{11}), 2.0 (2x2H, m, C^4, C^5), 3.5 (2H, m, C^{16} OTHP), 4.0 (2H, d, $J_{H,H}$= 6.1 Hz, C^8), 4.6 (1H, t, $J_{H,H}$= 7.5 Hz, C^{12} OTHP), 5.1 (1H, t, $J_{H,H}$= 6.6 Hz, C^3), 5.4 (1H, t, $J_{H,H}$= 6.1 Hz, C^7).
^{13}C NMR (125 MHz, $CDCl_3$):17.5 (C^{11}), 19.4 (C^{10}), 20.2 (C^{14}), 25.4 (C^{17}), 26.0 (C^1), 26.7 (C^4), 30.7 (C^{13}), 39.5 (C^5), 59.0 (C^8), 62.6 (C^{16}), 97.6 (C^{12}), 120.7 (C^7), 123.9 (C^3), 131.3 (C^2), 139.8 (C^6).

(*E*)-3-bromo-2,6-dimethyl-8-((tetrahydro-2*H*-pyran-2-yl)oxy)oct-6-en-2-ol (105)

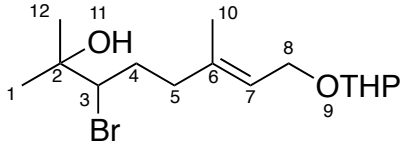

To a stirred solution of **104** (2 g, 8.4 mmol) in THF/H_20 (50/20 mL) at 5 °C was added NBS (1.6 g, 9.2 mmol) in 4 times. After 3 hours, the reaction was quenched with brine (20 mL). The aqueous layer was extracted with hexane (3 x 20 mL). The combined

organic layers were washed with brine (10 mL) and water (10 mL), dried over $MgSO_4$, filtered and concentrated under reduced pressure. The resulting oil was purified by flash chromatography on silica gel (3:1 Hexane:EtOAc) to give 2 g (71%) of **3.**

^{1}H NMR (400 MHz; $CDCl_3$): 1.4 (3H, s, C^{10}), 1.5 (3x2H, m, OTHP), 1.6 (2x3H, s, C^1, C^{12}), 2.0 (2x2H, m, C^4, C^5), 3.5 (2H, m, OTHP), 3.8 (1H, t, $J_{H,H}$= 6.5 Hz, C^3), 3.9 (2H, d, $J_{H,H}$= 6.1 Hz, C^8), 4.6 (1H, t, $J_{H,H}$= 7.4 Hz, OTHP), 5.4 (1H, t, $J_{H,H}$= 6.1 Hz, C^7).
^{13}C NMR (125 MHz, $CDCl_3$):16.3 (C^{11}), 19.5 (C^9), 20.9 (C^9), 25.5 (C^1), 26.4 (C^{12}), 30.2 (C^4), 31.7 (C^9), 38.1 (C^5), 58.9 (C^2), 63.4 (C^8), 69.6 (C^9), 72.4 (C^3), 97.7 (C^9), 122.0 (C^7), 138.2 (C^6).

(*E*)-2-((5-(3,3-dimethyloxiran-2-yl)-3-methylpent-2-en-1-yl)oxy)tetrahydro-2*H*-pyran (106)

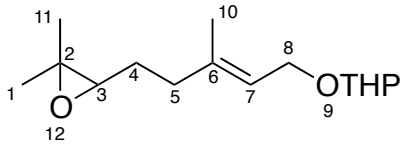

To a solution of **105** (1 g, 3.0 mmol) in THF (20 mL) at 0 °C was added a solution of DBU (0.55 g, 3.6 mmol) in THF (3 mL). The reaction was stirred at 0 °C until the TLC (Hexane: EtOAc = 4: 1) showed completion of the reaction. The THF was removed under reduced pressure and the resulting oil was re-dissolved in hexane (10 mL). This was washed with water (3 x 5 mL) and brine (5 mL) before being dried over $MgSO_4$, filtered and concentrated under reduced pressure to give 660 mg (87%) of **106**.

^{1}H NMR (400 MHz; $CDCl_3$): 1.1 (3H, s, C^{11}), 1.2 (3H, s, C^1), 1.5 (3x2H, m, OTHP), 1.6 (3H, s, C^{10}), 1.7 (2x2H, m, C^4, C^5), 2.5 (1H, t, $J_{H,H}$= 6.8 Hz, C^3), 3.4 (2H, m, OTHP), 3.9 (2H, d, $J_{H,H}$= 6.2 Hz, C^8), 4.6 (1H, t, $J_{H,H}$= 7.0 Hz, OTHP), 5.4 (1H, t, $J_{H,H}$= 6.2 Hz, C^7).
^{13}C NMR (125 MHz, $CDCl_3$): 17.6 (C^{10}), 18.7 (C^9), 19.7 (C^9), 24.7 (C^1), 25.4 (C^{11}), 27.1 (C^4), 30.6 (C^9), 35.2 (C^5), 59.1 (C^2), 62.1 (C^8), 63.4 (C^9), 65.6 (C^3), 97.8 (C^9), 121.3 (C^7), 138.9 (C^6).

(*E*)-4-methyl-6-((tetrahydro-2*H*-pyran-2-yl)oxy)hex-4-enal (107)

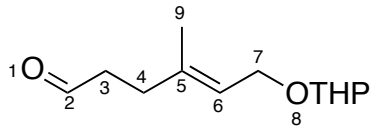

To a solution of **106** (500 mg, 2.0 mmol) in Et_2O (10 mL) at 0°C was added a solution of H_5IO_6 (0.5 g, 2.5 mmol) in THF (2 mL). After 30 minutes, the TLC (Hexane: EtOAc = 4: 1) showed completion of the reaction. The reaction was quenched with $Na_2S_2O_3$ (15 mL), the aqueous layer was extracted with Et_2O (3 x 10 mL). The organic layers were washed with brine (10 mL), dried over $MgSO_4$ and concentrated under reduced pressure to give 240 mg (57%) of **107**.

^{1}H NMR (250 MHz; $CDCl_3$):1.6 (3x2H, m, OTHP), 1.7 (3H, s, C^9), 2.4(2H, t, $J_{H,H}$= 6.8 Hz, C^4), 2.6 (2H, t, $J_{H,H}$= 6.6 Hz, C^3), 3.6 (2H, m, OTHP), 4.0 (2H, d, $J_{H,H}$= 6.0 Hz, C^7), 4.9 (1H, t, $J_{H,H}$= 6.9 Hz, OTHP), 5.4 (1H, t, $J_{H,H}$= 6.0 Hz, C^6), 9.7 (1H, t, $J_{H,H}$= 7.1 Hz, C^2).
^{13}C NMR (125 MHz, $CDCl_3$): 16.5 (C^9), 19.6 (C^8), 25.6 (C^8), 30.7 (C^8), 31.6 (C^4), 41.8 (C^3), 62.3 (C^7), 63.5 (C^8), 98.0 (C^8), 121.8 (C^6), 137.8 (C^5), 201.9 (C^2).

(2*Z*,6*E*)-ethyl 2,6-dimethyl-8-((tetrahydro-2*H*-pyran-2-yl)oxy)octa-2,6-dienoate (108)

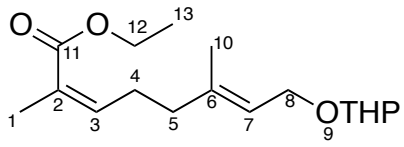

The ylide precursor, $(CF_3CH_2O)_2P(O)CH(CH3)CO_2Et$ (0.45 g, 0.19 mmol, 1.0 equiv), was dissolved in THF (50 mL) and 18-crown-6 (2.5 g, 9.55 mmol, 5.0 equiv) was added. The solution was cooled to -78 °C and KHMDS (1.9 mL of a 1 M solution in THF, 1.91 mmol, 1.0 equiv) was added dropwise over 5 min. The reaction mixture was stirred for 15 min. **107** (0.34 g, 1.91 mmol, 1.0 equiv, dissolved in a small amount of THF) was added dropwise over 5 min. The reaction mixture was stirred for an additional 30 min and quenched with saturated ammonium chloride solution. The mixture was extracted 3x with portions of ethyl acetate, the combined organics were

washed with brine, dried over anhydrous sodium sulfate, and the volatiles were removed under reduced pressure. The residue was purified by column chromatography (10% hexanes/ethyl acetate) to give 0.46 g **108** in 78% yield as only the *Z* isomer, indicated by ^{1}H NMR and NOE.

^{1}H NMR (250 MHz; $CDCl_3$): 1.3 (2H, t, $J_{H,H}$= 5.9 Hz, C^{13}), 1.5 (3x2H, m, OTHP), 1.6 (3H, s, C^{10}), 1.8 (3H, s, C^{1}), 2.1 (2H, t, $J_{H,H}$= 6.6 Hz, C^{5}), 2.5 (2H, t, $J_{H,H}$= 6.8 Hz, C^{4}), 3.8 (2H, m, OTHP), 3.9 (2H, m, C^{12}) 4.0 (2H, d, $J_{H,H}$= 6.1 Hz, C^{8}), 4.9 (1H, t, $J_{H,H}$= 6.9 Hz, OTHP), 5.3 (1H, t, $J_{H,H}$= 6.0 Hz, C^{7}), 5.4 (1H, t, $J_{H,H}$= 6.0 Hz, C^{6}), 5.8 (1H, t, $J_{H,H}$= 6.0 Hz, C^{6}).

(2*Z*,6*E*)-2,6-dimethyl-8-((tetrahydro-2*H*-pyran-2-yl)oxy)octa-2,6-dien-1-ol (109)

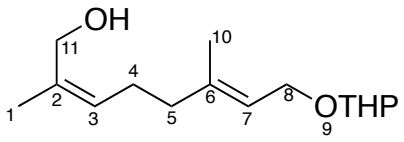

The α,β-unsaturated ester 108 (2.8 g, 9.5 mmol, 1.0 equiv) was dissolved in THF (100 mL) and cooled to -20 °C. DIBALH (5 mL of a 2.5 M solution in toluene, 40 mmol, 2.8 equiv) was added dropwise over 10 min and the reaction mixture was stirred for 3 h. After completion was checked by TLC (Hexane: EtOAc = 3:1), the reaction was quenched by 10% HCl. The aqueous mixture was then extracted 3x with portions of diethyl ether, the combined organics were dried over anhydrous sodium sulfate and the volatiles were removed under reduced pressure. The residue was purified by column chromatography (4:1 hexanes/ethyl acetate) to give the 2.4 g of desired alcohol **109** in 87% yield.

(2*Z*,6*E*)-2,6-dimethyl-8-((tetrahydro-2*H*-pyran-2-yl)oxy)octa-2,6-dienal (110)

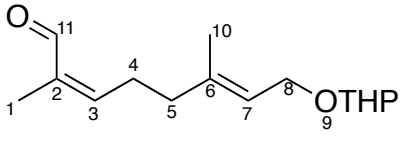

109 (2.2 g, 8.7 mmol) was oxidised to **110** by adding it to a solution of manganese dioxide (30g, 340 mmol) in hexane (150 ml). The mixture was allowed to stir for 3 hours until TLC (Hexane: EtOAc = 4: 1) showed all the starting material had been converted. The mixture was filtered through celite with hexane and the solvent was removed under reduced pressure followed by high vacuum to yield 1.9 g of **110** in 86% yield.

^{1}H NMR (250 MHz; $CDCl_3$): 1.6 (3x2H, m, OTHP), 1.7 (3H, s, C^9), 2.4(2H, t, $J_{H,H}$= 6.5 Hz, C^4), 2.6 (2H, t, $J_{H,H}$= 6.5 Hz C^3), 3.6 (2H, m, OTHP), 4.0 (2H, d, $J_{H,H}$= 6.2 Hz C^7), 4.9 (1H, t, $J_{H,H}$= 7.5 Hz, OTHP), 5.4 (1H, t, $J_{H,H}$= 6.2 Hz, C^6), 9.7 (1H, t ,$J_{H,H}$= 7.4 Hz, C^2)

^{13}C NMR (500 MHz, $CDCl_3$): 16.5 (C^9), 19.6 (C^8), 25.6 (C^8), 30.7 (C^8), 31.6 (C^4), 41.8 (C^3), 62.3 (C^7), 63.5 (C^8), 98.0 (C^8), 121.8 (C^6), 137.8 (C^5), 201.9 (C^2)

2-(((2*E*,6*Z*)-3,7-dimethylnona-2,6,8-trien-1-yl)oxy)tetrahydro-2*H*-pyran (111)

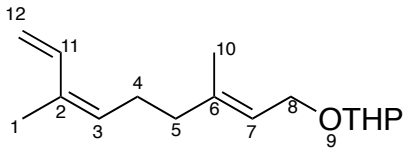

n-Butyl lithium solution (2.5 M in hexanes) (0.8 ml, 2.0 mmol) was added to a stirred solution of methyl triphenyl phosphonium bromide (2.5 g, 7.01 mmol) at -10 ^{o}C in dry THF (30 ml) under nitrogen. The resulting yellow solution was stirred for half an hour before a solution of **110** (1.0 g, 4.7 mmol) in dry THF (15 ml) was added drop wise over duration of 5 minutes. The solution was then allowed to warm to room temperature and was left to stir for another 48 hours under nitrogen. When TLC (Hexane: EtOAc = 9: 1) confirmed all starting material had been converted, the reaction was quenched with saturated ammonium chloride solution (20 ml).

The quenched mixture was diluted with 20 ml of water and the organic layer was collected. The separated aqueous layer was extracted with diethyl ether until TLC showed the aqueous layer contained no product. The pooled organic layers were washed with brine (20 ml), dried over magnesium sulphate, filtered and concentrated under reduced pressure. The resulting yellow oil was purified by flash chromatography on silica gel (19:1, hexane: ethyl acetate) to yield 0.5 g (52%) of **111**.

(2*E*,6*Z*)-3,7-dimethylnona-2,6-dien-1-ol (112)

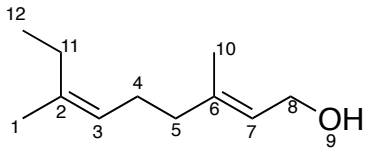

Triphenylphosphinerhodium chloride (130 mg, 0.14 mmol) was added to a solution of **111** (200 mg, 1.19 mmol) in toluene (6 ml) and left to stir. The reaction was left to stir and followed by GC and TLC (Hexane: EtOAc = 4: 1) until all the starting material had been converted. The reaction was then quenched with water (10 ml). The organic layer was separated and the aqueous layer was washed with diethyl ether (3 x 15 ml). The pooled organic layers were then washed with brine (20 ml), dried over magnesium sulphate and concentrated under reduced pressure. This mixture (140 mg, 0.5 mmol) in ethanol (4 mL) was treated with PPTS (14 mg, 0.05 mmol) for 2 hours to gives 68 mg (67.5%) **112** after both reactions.

(2*E*,6*Z*)-1-bromo-3,7-dimethylnona-2,6-diene (113)

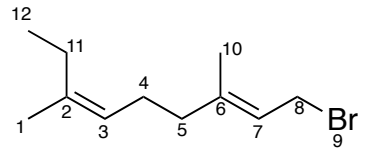

Anhydrous triethylamine (0.48 mg, 0.07 ml, 0.46 mmol) was added to a stirred solution of **101** (53mg, 0.33 mmol) in anhydrous THF (6 ml) at -45 ^{o}C, followed by methane sulfonyl chloride (0.53 mg, 0.05 ml, 0.46 mmol). This mixture was stirred for 15 minutes at -45 ^{0}C and then a solution of lithium bromide (110 mg, 1.26 mmol) in anhydrous THF (3 ml) was added. This mixture was stirred under nitrogen for 2 hours, which after time TLC (Hexane: EtOAc = 9: 1) showed that all the starting material had been used.

The reaction material was partitioned between hexane (20 ml) and water (20 ml). The separated aqueous layer was washed twice more with hexane (2 x 20 ml). The pooled hexane layers were washed with 1 M hydrochloric acid and brine. This was then dried over magnesium sulphate, filtered and then reduced on a rotary evaporator followed by high vacuum. Crude bromide **113** was carried forward for the next reaction.

Synthesis of (2E,6E)-3-methyl-7-ethylocta-2,6-dien-1-yl dihydrogen diphosphate (114)

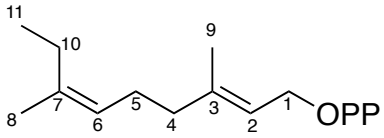

The crude bromide **113** was re dissolved in acetonitrile (2 ml) and stirred under nitrogen as tris (tetrabutylammonium) hydrogen pyrophosphate (860 mg, 0.95 mmol) was added. Reaction was followed by TLC (H_2O: NH_4OH:$(CH_3)_2CHOH$ = 2:1:2) and stopped when the bromide spot on the plate had disappeared. The solvent was then removed on the rotary evaporator.

This was then dissolved in an ion exchange buffer (25 mmol NH_4HCO_3 with 2% isopropanol) and run through an ion exchange column to replace the tetrabutylammonium counter ions with ammonium ions. The resulting compound was then run through a HPLC to collect the peaks containing the product. This was then freeze-dried to gives 21 mg (45%) of **114** over the last two steps.

^{1}H NMR (500 MHz, D_20): δ 0.85 (3H, t, $J_{H,H}$=6 Hz, CH_3, C^{11}), 1.60 and 1.63 (2x3H, 2xs, 2xCH_3, C^8 and C^9), 1.90-2.08 (6H, m, 3xCH_2, C^4 and C^5 and C^8), 4.39 (2H, t, $J_{H,H}$=6 Hz, CH_2, C^1), 5.16 (1H, t, $J_{H,H}$=6. 5 Hz, CH, C^6), 5.38 (1H, bs, CH, C^2).

^{13}C NMR (125 MHz, D_2O): 14.70 (C^{11}), 18.21 (C^9), 24.62 (C^8), 26.95 (C^{10}), 27.87 (C^5), 41.71 (C^4), 65.09 (C^1), 126.32 (C^6), 142.30 (C^7), 145.13 (C^3)

m/z (ES^-) 327.07 (100%, $[M +2H]^-$).

(2*E*,6*Z*)-3,7-dimethylnona-2,6,8-trien-1-ol (115)

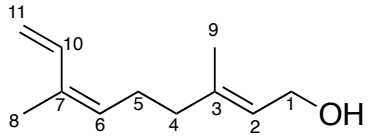

The mixture **111** (200 mg, 0.7 mmol) in ethanol (8 mL) was treated with PPTS (18 mg, 0.07 mmol) for 2 hours and the reaction was then quenched with water (20 ml). The organic layer was separated and the aqueous layer was washed with diethyl ether (3 x 20 ml). The pooled organic layers were then washed with brine (20 ml), dried over

magnesium sulphate and concentrated under reduced pressure to give 92.6 mg (92%) of **115.**

(3*Z*,7*E*)-9-bromo-3,7-dimethylnona-1,3,7-triene (116)

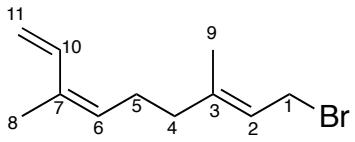

Anhydrous triethylamine (0.96 mg, 0.14 ml, 0.92 mmol) was added to a stirred solution of **115** (90mg, 0.70 mmol) in anhydrous THF (6 ml) at -45 ^{o}C, followed by methane sulfonyl chloride (1.0 mg, 0.1 ml, 0.92 mmol). This mixture was stirred for 15 minutes at -45 ^{0}C and then a solution of lithium bromide (220 mg, 2.52 mmol) in anhydrous THF (3 ml) was added. This mixture was stirred under nitrogen for 2 hours, which after time TLC (Hexane: EtOAc = 9: 1) showed that all the starting material had been used.
The reaction material was partitioned between hexane (20 ml) and water (20 ml). The separated aqueous layer was washed twice more with hexane (2x20 ml). The pooled hexane layers were washed with 1 M hydrochloric acid and brine. This was then dried over magnesium sulphate, filtered and then reduced on a rotary evaporator followed by high vacuum. Crude bromide **116** was carried forward for the next reaction.

Synthesis of (2E,6E)-3-methyl-7ethyl-octa-2,6-dien-1-yl dihydrogen diphosphate (117)

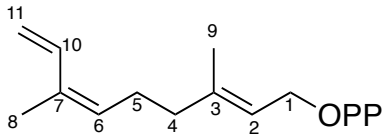

The crude bromide **116** was re dissolved in acetonitrile (4 ml) and stirred under nitrogen as tris(tetrabutylammonium) hydrogen pyrophosphate (1.7 g, 1.90 mmol) was added. The reaction was followed by TLC (H_2O: NH_4OH:$(CH_3)_2CHOH$ = 2:1:2) and stopped when the bromide spot on the plate had disappeared. The solvent was then removed on the rotary evaporator.
This was then dissolved in an ion exchange buffer (25 mmol NH_4HCO_3 with 2% isopropanol) and run through an ion exchange column to replace the

tetrabutylammonium counter ions with ammonium ions. The resulting compound was then run through a HPLC to collect the peaks containing the product. This was then freeze-dried to give 60 mg (43%) of **117**.

^{1}H NMR (500 MHz, D_20): δ 1.72 and 1.79 (2x3H, 2xs, 2xCH_3, C^9 and C^8), 1.99-2.26 (4H, m, CH_2CH_2, C^4 and C^5), 4.39 (2H, m, CH_2, C^1), 5.05 (2H, d, $J_{H,H}$=10.45 Hz, CH_{cis}, C^{11}), 5.24 (2H, d, $J_{H,H}$=16.4 Hz, CH_{trans}, C^9), 5.4-5.6 (2H, m, CH, C^6 and C^2), 6.84(1H, dd, $J_{H,Htrans}$=17.2 Hz and $J_{H,Hcis}$=10.6 Hz, CH, C^{10}).
^{13}C NMR (125 MHz, D_2O): 16.1 (C^9), 18.66 (C^8), 25.89 (C^5), 38.8 (C^4), 65.56 (C^1), 111.22 (C^{11}), 123.4 (C^2), 130.31 (C^6), 134.5 (C^7), 139.72 (C^3), 141.63 (C^3).
m/z (ES^-) 325.1 (100%, $[M +2H]^-$).

References

1. Christianson, D. W. (2008) Unearthing the roots of the terpenome. Curr. Opin. Plant Biol. 12, 141-150.

2. Sacchettini, J. C. and Poulter, C. D. (1997) Creating isoprenoid diversity. Science 277, 1788-1789.

3. Steel, C. L, Crock, J., Bohlmann, J. and Croteau, R. J., (1998) Sesquiterpene Synthases from Grand Fir (Abies grandis). J. Biol. Chem. 273, 2078-2089.

4. Christianson, D.W. (2007) Roots of biosynthetic diversity. Science 316, 60-61.

5. Kellogg, B. A and Poulter, C. D. (1997) Chain elongation in the isoprenoid biosynthetic pathway. Curr. Opin. Plant Biol. 1, 570-578.

6. Poulter, C. D. (1990) Biosynthesis of non-head-to-tail terpenes. Formation of 1'-1 and 1'-3 linkages. Acc. Chem. Res. 23, 70-77.

7. Pandit, J., Danley, D. E., Schulte, G. K., Mazzalupo, S., Pauly, T. A., Hayward, C. M., Hamanaka, E. S., Thompson, J. F. and Harwood, H. J. (2000) Crystal Structure of Human Squalene Synthase. J. Biol. Chem. 275, 30610-30617.

8. Riling, H. C. and Epstein, W. W. (1969) Mechanism of squalene biosynthesis. J. Am. Chem. Soc. 91,1041-1042.

9. Agranoff, B. W., Eggerer, H. U. and Lynen, F. (1958) Isopentenol Diphosphate Isomerase. J. Am. Chem. Soc. 81, 1254-1255.

10. Poulter, C. D. and Rilling, H. C. (1978) The prenyl transfer reaction. Enzymatic and mechanistic studies of the 10–4 coupling reaction in the terpene biosynthetic pathway. Acc. Chem. Res. 11 , 307-313.

11. Ogura, K. and Koyama, T. (1998) Enzymatic Aspects of Isoprenoid Chain Elongation. Chem. Rev. 98, 1263-1276.

12. Grunler, J., Ericsson, J. and Dallner, G. (1994) Branch-point reactions in the biosynthesis of cholesterol, dolichol, ubiquinone and prenylated proteins. Biochim. Biophys. Acta-Lipid Lipid Metab. 1212, 259-277.

13. Gershenzon, J. and Dudareva, N. (2007) The function of terpene natural products in the natural world. Nat. Chem. Biol. 3, 408-414.

14. McGarvey, D. J. and Croteau, R., (1995) Terpenoid Metabolism. Plant Cell, 7 1015-1026.

15. Phillips, M. A., Wildung, M. R., Williams, D. C., Hyatt, D. C., and Croteau, R. (2003) cDNA isolation, functional expression, and characterization of (+)- α-piene synthase and (-)- α-piene synthase from loblolly pine (Pinus taeda): Stereocontrol in pinene biosynthasis. Arch. Biochem. Biophys. 411, 267-276.

16. Dawson, F. A., The amazing terpenes. Naval Stores Rev. March/April, 6-12.

17. Aharoni, A., Jongsma, M. A. and Bouwmeester, H. J. (2005) Volatile science Metabolic engineering of terpenoids in plants. Trends Plant Sci. 10, 594-602.

18. Sharkey, T. D. and Yeh, S. (2001) Isoprene emission from plants. Ann. Rev. Plant Mol. Biol. 52, 407-436.

19. McGarvey, D. J. and Croteau, R. (1995) Terpenoid metabolism. Plant Cell. 7, 1015-1026.

20. Crowell, P. L. (1999) Prevention and therapy of cancer by direct monoterpenes. J. Nutr. 129, 775S-778S.

21. Sun, J (2007). D-Limonene: safety and clinical applications Altern. Med. Rev. 12, 259-264.

22. Pourbafrani, M., Forgacs, G., Niklasson, C. and Taherzadeh, M. J. (2010). Production of biofuels, limonene and pectin from citrus wastes. Bioresource Technol. 101, 4246–4250.

23. Tsuda, H., Ohshima, Y., Nomoto, H., Fujita, K.-I., Matsuda, E., Iigo, M., Takasuka, N. and Moore, M. A. (2004). Cancer Prevention by Natural Compounds. Drug Metab. Pharmacokin. 19, 245-263.

24. Kaufmann, D., Dogra, A. K. and Wink, M. (2001) Myrtenal inhibits acetylcholinesterase, a known Alzheimer target. J. Pharm. Pharmacol. 63, 1368–1371.

25. Miller, D. J., Yu, F. L., Knight, D. W. and Allemann, R. K., (2009) 6- and 14-Fluoro farnesyl diphosphate: mechanistic probes for the reaction catalysed by aristolochene synthase. Org. Biomol. Chem. 7, 962–975.

26. Miller, D. J., Yu, F. L. and Allemann, R. K., (2007) Aristolochene synthase-catalyzed cyclization of 2-fluorofarnesyl-diphosphate to 2-fluorogermacrene A. ChemBioChem 8, 1819–1825.

27. Velickovic, D. T., Randjelovic, N. V., Ristic, M. S. and Smelcerovic, A.A., (2003) Chemical constituents and antimicrobial activity of the ethanol extracts obtained from the flower, leaf, and stem of Salvia officialis L. J. Serb. Chem. Soc. 68, 17-24.

28. Newman, D. J., Cragg, G. M. and Sander, K. M. (2000) The influence of natural products upon drug discovery. Nat. Prod. Rep. 17, 215-234.

29. De Smet, P. A. G. M., (1995) The role of plant derived drugs and herbal medicines in healthcare. Drugs 54, 801-840.

30. Lai, H. and Singh, N., (1995) Selective cancer cell cytotoxicity from exposure to dihydroartemisinin and holotransferrin. Cancer Lett. 91, 41-46.

31. Cane, D. E., Abell, C. and Tillman, A. M. (1984) Pentalenene Biosynthesis and the Enzymatic Cyclisation of Farnesyl Diphosphate: Proof that the Cyclisation is Catalysed by a Single Enzyme. Bioorg. Chemistry 12, 312-328.

32. Wedge, D. E., Galindo, J. C. G. and Macias, F. A. (2000) Fungicidal activity of natural and synthetic sesquiterpenes lactone analogs. Phytochemistry 53, 747-757.

33. Davis, D., Merida, J., Legendre, L., Low, P.S. and Heinstein, P. F. (1993) Independent elicitation of the oxidative burst and phytoalexin formation in cultured plant cells. Phytochemistry 32, 607-611.

34. Carruthers, N. J., Dowd, M. J. and Stemmer, P. M. (2007). Gossypol inhibits calcineurin phosphatase activity at multiple sites. Eur. J. Pharm. 555, 106-114.

35. Cui, G. H., Xu, Z. L., Yang, Y. J., Xu, Y. Y. and Xue, S. P. (2004). A combined regimen of gossypol plus methyltestosterone and ethinylestradiol as a contraceptive induces germ cell apoptosis and expression of its related genes in rats. Contraception. 335-342.

36. Potemski, P. and Pluzanska, A. (1999) Pharmacological action of paclitaxel. Pol Merkur Lekarski. 31, 27-29.

37. Yamazaki, S., Sekine, I. and Saijo, N. (1998) Paclitaxel (taxol): a review of its antitumor activity and toxicity in clinical studies. Cancer and chemotheraphy 4, 605-615.

38. Sitton, D. and West, C. A. (1975) Casbene: an Antifungal Diterpene Produced in Cell-Free Extracts of Ricinus communis seedlings. Phytochemistry 14, 1921-1925.

39. Gershenzon, J. and Dudareva, N. (2007) The function of terpene natural products in the natural world. Nat. Chem. Biol. 3, 408-414.

40. Pandit, J., Dandley, D. E., Schulte, G. K., Mazzalupo, S. M., Pauly, T. A., Hayward, C. M., Hamanaka, E. S., Thompson, J. F. and Harwood, H. J. (2000) Crystal Structure of Human Squalene Synthase. J. Biol. Chem. 275, 30610-30617.

41. Abe, I., Rohmer, M. and Prestwich, G. D. (1993) Enzymatic Cyclisation of Squalene and Oxidosqualene to Sterols and Triterpenes. Chem. Rev. 93, 2189.

42. Ikonen, E. (2006) Mechanisms for cellular cholesterol transport: defects and human disease. Physiol. Rev. 86, 1237-1261.

43. Maxfield, F. R. and Tabas, I. (2005) Role of cholesterol and lipid organization in disease. Nature 438, 612-621.

44. Britton, G. (1995) Structure and properties of carotenoids in relation to function. Fed. Am. Soc. Exp. Biol. 9, 1551-1558.

45. Bauerfind, J. C. and Kläui, H (1981) Carotenoids as Colorants and Vitamin A Precursors. Technological and Nutritional Applications - A volume in Food Science and Technology. 47-317.

46. Fishkin, N., Berova, N., Nakanishi, K. (2004) Primary events in dim light vision: a chemical and spectroscopiv approach toward understanding protein / chromophore interactions in rhodopsin. Chem. Rec. 4, 120-135.

47. Cemek, M., Dede, S., Bayiroglu, F., Hüseyin, C., Cemek, F. and Yuka, K. (2005) Oxidant and antioxidant levels in children with acute otitis media and tonsillitis: a comparatove study. Int. J. Ped. Otorhinolaryno. l69, 823-827.

48. Maggio, D., Barabani, M., Pierandrei, M., Polidori, M. C., Catani, M., P. Mecocci, Senin, U., Pacifici, R. and Cherubini, A. (2003) Marked decrease in plasma antioxidants in aged osteoporotic women: results of a crosssectional study. J. Clin. Endocrin. Metabol. 88, 1523-1527.

49. Uchimiya, M. and Stone, A. T. (2009) Reversible redox chemistry of quinones: impact on biogeochemical cycles. Chemospphere 77, 451-458.

50. Raymond, K., Muller, G. and Matzanke, B. (1984) Complexation of iron by siderophores a review of their solution and structural chemistry and biological function. Top. Curr. Chem. 123, 49-102.

51. Hamilton, J. A. and Cox, G. B. (1971) Ubiquinone biosynthesis in Eschericia coli K-12. Biochem. Lett. 123, 435-443.

52. Patai, S. (1974) The chemistry of the quinoid compounds. The chemistry of the functional groups (Patai, S., Ed.). Wiley, New York.

53. Roberts, C. (1938), The chemistry of natural rubber. Part 1. J. Rub. Res. 7, 215-219.

54. Wallach, O. (1887) Zur Kenntnis der Terpene und Ätherischen Oele. Justus Lieb. Ann. Chem. 238, 78-89.

55. Ruzicka, L. (1953) The isoprene rule and the biogenesis of terpenic compounds. Experientia 9, 357-367.

56. Dewick, P. M. (1997) Medicinal Natural Products: A Biosynthetic Approach. Chap. 5, pp. 186. John Wiley & Sons, UK.

57. Eschenmoser, A., Ruzicka, L., Jeger, O. and Arigoni, D. (1955) Zur Kenntnis der Triterpene. Eine stereochemische Interpretation der biogenetischen Isoprenregel bei den Triterpenen. Helv. Chim. Acta. 38, 1890-1894.

58. Eisenreich, W., Bacher, A., Arigoni, D. and Rohdich, F. (2004) Biosynthesis of isoprenoids via the non-mevalonate pathway. Cell. Mol. Life Sci. 61, 1401-1409

59. Poulter, C. D. and Rilling, H. C. (1981) Prenyl transferases and isomerases, John Wiley & sons, New York.

60. Bach, T. J., Rogers, D. H. and Rudney, H. (1986) Detergent-solubilization, Purification, and Characterization of Membrane-bound 3-hydroxy-3-methylglutaryl-coenzyme A Reductase from Radish Seedlings. Eur. J. Biochem. 154, 103-105.

61. Qureshi, N. and Porter, J. W. (1981) Conversion of Acetyl-CoA to Isopentenyl Diphosphate in Biosynthesis of Isoprenoid Compounds, John Wiley and Sons, New York.

62. Rohmer, M. (1993) The Biosynthesis of Triterpenoids of the Hopane Series in the Eubacteria: A Mine of New Enzyme Reactions. Pure Appl. Chem. 65, 1293.

63. Rohmer, M., Knani, M., Simonin, P., Sutter, B. and Sahm, H. (1993) Isoprenoid Biosynthesis in Bacteria: a Novel Pathway for the Early Steps Leading to Isopentenyl Diphosphate. Biochem. J. 295, 517-524.

64. Schwender, J., Seemann, M., Lichtenthaler, H. K., and Rohmer, M. (1996) Biosynthesis of isoprenoids via a novel pyruvate/glyceraldehyde 3-phosphate non-mevalonate pathway in the green alga scenedesmus obliquus. Biochem. J. 316, 73-80.

65. Rohmer, M. (1999) The Discovery of a Mevalonate-Independent Pathway for Isoprenoid Biosynthesis in Bacteria, Algae and Higher Plants. Nat. Prod. Rep. 16, 565-574.

66. Rohmer, M., (2003) mevalonate-independent methylerythritol phosphate pathway for isoprenoid biosynthesis. Elucidation and distribution. Pure Appl. Chem. 75, 375-387.

67. Jomma, H., Wiesner, J., Sanderband, S., Altincicek, B., Weidemeyer, C., Hintz, M., Turbachova, I., Eberl, M., Zeidler, J., Lichtenthaler, H. K., Soldati, D. and Beck, E. (1999) Inhibitors of the Nonmevalonate Pathway of Isoprenoid Biosynthesis as Antimalarial Drugs. Science 285, 1573-1576.

68. Holloway, P. W. and Popjak, G. (1967) The Purification of 3,3-Dimethylallyl- and Geranyl- Transferase and Isopentenyl Diphosphate Isomerase from Pig Liver. Biochem. J. 104, 57-70.

69. Prisic, S., Xu, J., Coates, R.M., and Peters, R. J. (2007) Probing the role of the DXDD motif in class 11 diterpene cyclases. Chembiochem 8, 869-874.

70. Christianson, D.W. (2006) Structural biology and chemistry of the terpenoid cyclases. Chem. Rev. 106, 3412-3442.

71. Forcat, S. and Allemann, R. K. (2004) Dual role for a phenylalanine 178 during catalysis by aristolochene synthase. Chem. Comm. 2094-2095.

72. Forcat, S. and Allemann, R. K. (2006) Stabilisation of transition states prior to and following eudesmane cation in aristolocene synthase. Org. Biomol. Chem. 4, 2563-2567.

73. Calvert, M. J., Taylor, S. E. and Allemann, R. K. (2002) Tyrosine 92 of Aristolochene Synthase Directs Cyclisation of Farnesyl Diphosphate. Chem. Commun. 2384-2385.

74. Lesburg, C. A., Zhai, G., Cane, D. E. and Christianson, D. W. (1997) Crystal structure of pentalene synthase: mechanistic insights on terpenoid cyclisation reactions in biology. Science 277, 1820-1824.

75. Rynkiewicz, M. J., Cane, D. E. and Christianson, D. W. (2001) Structure of trichodine synthase from *Fusarium sporotrichioides* provides mechanistic inferences on the terpene cyclisation cascade. Proc. Chem. Soc. 98, 13543-13548.

76. Bohlmann, J., Meyer-Gauen, G. and Croteau, R. (1998) Plant terpenoid synthases: molecular biology and phylogenetic analysis. Proc. Natl. Acad. Sci. U.S.A. 95, 4126-4133.

77. Steele, C. L., Crock, J., Bohlmann, J. and Croteau, R. (1998) Sesquiterpene Synthases from Grand Fir (Abies grandis). J. Biol. Chem. 273, 2078-2089.

78. Davis, G. D. and Essenberg, M. (1995) (+)- δ -cadinene is a product of sesquiterpene cyclase activity in cotton. Phytochem. 39, 553-567.

79. Calvert, M. J., Ashton, P. R. and Allemann, R. K. (2002) Germacrene A is a product of the Aristolochene Syntase-Mediated Conversion of Farnesyldiposphate to Aristolochene. J. Am. Chem. Soc. 124, 11636-11641.

80. Colby, S., Alonso, W., Katahira, E., McGarvey, D. and Croteau, R. (1993) 4S-limonene synthase from the oil glands of spearmint (Mentha spicata). cDNA isolation, characterization, and bacterial expression of the catalytically active monoterpene cyclase. J. Biol. Chem. 268, 23016-23024.

81. Bohlmann, J., Steele, C. L. and Croteau, R. (1997) Monoterpene synthases from grand fir (Abies grandis) - cDNA isolation, characterization, and functional expression of myrcene synthase, (-)(4S)-limonene synthase, and (-)-(1S,5S)-pinene synthase. J. Biol. Chem. 272, 21784-21792.

82. Chen, X. Y., Chen, Y., Heinstein, P. and Davisson, V. J. (1995) Cloning, expression, and characterization of (+)-delta-cadinene synthase: a catalyst for cotton phytoalexin biosynthesis. Arch. Biochem. Biophys. 324, 255-266.

83. Steele, C. L., Crock, J, Bohlmann J. and Croteau, R. (1998) Sesquiterpene synthases from grand fir (Abies grandis). Comparison of constitutive and wound-induced activities, and cDNA isolation, characterization, and bacterial expression of delta-selinene synthase and gamma-humulene synthase. J. Biol. Chem. 273, 2078-2089.

84. Crock, J., Wildung, M. and Croteau, R. (1997) Isolation and bacterial expression of a sesquiterpene synthase cDNA clone from peppermint (Mentha x piperita) that produces the aphid alarm pheromone (E)- β -farnesene. Proc. Natl. Acad. Sci. U.S.A. 94, 12833-12838.

85. Cane, D. E. and Kang, I. (2000) Aristolochene synthase: purification, molecular cloning, high-level expression in *E. coli* and characterisation of the *Aspergillus terreus* cyclase. Arch. Biochem. Biophys. 376, 354-364.

86. Wendt, K. U. and Schultz, G. E. (1998) Isoprenoid Biosynthesis: Manifold Chemistry Catalyzed by Similar Enzymes. Structure 6, 127-133.

87. Sun, T. P. and Kamiya, Y. (1994) The Arabidopsis GA1 locus encodes the cyclase ent-kaurene synthetase A of gibberellin biosynthesis. Plant Cell 6, 1509-1518.

88. Whittington, D. A., Wise, M. L., Urbansky, M., Coates, R. M., Croteau, R. and Christianson, D. W. (2002) Bornyl Diphosphate Synthase: Structure and Strategy for Carbocation Manipulation by a Terpenoid Cyclase. Proc. Natl. Acad. Sci. U.S.A. 99, 15375-15380.

89. Caruthers, J. M., Kang, I., Rynkiewicz, M. J., Cane, D. E. and Christianson, D. W. (2000) Crystal Structure Determination of Aristolochene Synthase from the Blue Cheese Mold, *Penicillium roqueforti*. J. Biol. Chem. 275, 25533-25539.

90. Shishova, E. Y., Di Costanzo, L., Cane, D. E. and Christianson, D. W. (2007) X-ray Crystal Structure of Aristolochene Synthase from Aspergillus terreus and Evolution of Templates for the Cyclization of Farnesyl Diphosphate. Biochemistry 46, 1941-1951.

91. Starks, C. M., Back, K., Chappell, J. and Noel, J. P. (1997) Structural Basis for Cyclic Terpene Biosynthesis by Tobacco 5-epi-Aristolochene Synthase. Science 277, 1815-1820.

92. Hyatt, D. C., Youn, B., Zhao, Y., Santhamma, B., Coates, R. M., Croteau, R. B. and Kang, C. (2007) Structure of limonene synthase, a simple model for terpenoid cyclase catalysis. Proc. Natl. Acad. of Sci. U.S.A. 104, 5360-5365.

93. Trapp, S. C. and Croteau, R. B. (2001) Genomic organization of plant terpene synthases and molecular evolutionary implications. Genetics 158, 811-832.

94. Wheeler, C. J. and Croteau, R. (1987) Monoterpene cyclases. Stereoelectronic requirements for substrate binding and ionization. J. Biol. Chem. 262, 8213–8219.

95. Wheeler, C. J. and Croteau, R. (1988) Monoterpene cyclases: physicochemical features required for diphosphate binding determined from inhibition by structural analogs. Arch. Biochem. Biophys. 260, 250–256.

96. Degenhardt, J., Kollner, T. G. and Gershenzon, J. (2009) Monoterpene and sesquiterpene synthases and the origin of terpene skeletal diversity in plants. Phytochemistry 70, 1621-1637.

97. Croteau, R. (1987) Biosynthesis and catabolism of monoterpenoids. Chem. Rev. 87, 929-954.

98. Wise, M. L., and Croteau, R. (1999) Monoterpene Biosynthesis. In Comprehensive Natural Products Chemistry: Isoprenoids Including Steroids and Carotenoids; D. E. Cane, Ed.; Elsevier Science: Oxford, 2, 97.

99. Davis, E. M. and Croteau, R. (2000) Cyclization Enzymes in the Biosynthesis of Monoterpenes, Sesquiterpenes and Diterpenes. In Topics in Current Chemistry: Biosynthesis – Aromatic Polyketides, Isoprenoids. Alkaloids; F. Leeper, J. C. Vederas, Eds; Springer-Verlag: Heidelberg, Germany; 209, 53.

100. Schilmiller, A. L., Schauvinhold, I., Larson, M., Xu, R., Charbonneau, A. L., Schmidt, A., Wilkerson, C., Last, R. L. and Pichersky, E. (2009) Monoterpenes in the glandular trichomes of tomato are synthesized from a neryl diphosphate precursor rather than geranyl diphosphate. Proc. Natl. Acad. Sci. U.S.A. 106, 10865-10870.

101. Adams, K. P., and Croteau, R. (1998) Monoterpene biosynthesis in the liverwort *Conocephalum conicum*: demonstration of sabinene synthase and bornyl diphosphate synthase. Phytochemistry 49, 475-480.

102. Adams, K. P., Crock, J. E. and Croteau, R. (1996) Partial purification and characterization of a monoterpene cyclase, limonene synthase, from the liverwort *Ricciocarpos natans*. Arch. Biochem. Biophys. 332, 352-356.

103. Hyatt, D. C. and Croteau R. (2005) Mutantional analysis of monoterpene synthase reaction: altered catalysis through direct mutagenesis of (-)-pinene synthase from *Abies grandis*. Arch. Biochem. Biophys. 439, 222-223.

104. Peters, R. J., Flory, J. E., Jetter, R., Ravn, M. M., Lee, H. J., Coates, R. M. and Croteau, R. B. (2000) Abietadiene synthase from grand fir (*Abies grandis*): Characterization and mechanism of action of the "pseudomature" recombinant enzyme. Biochemistry 39, 15592-15602.

105. Bohlmann, J, Steele, C. L. and Croteau R. (1997) Monoterpene synthases from grand fir (*Abies grandis*). cDNA isolation, characterization, and functional expression of myrcene synthase, (-)-(4S)-limonene synthase, and (-)-(1S,5S)-pinene synthase. J. Biol. Chem. 272, 21784-21792.

106. Wise, M. L. and Croteau R. (1999) Comprehensive Natural Products Chemistry: Isoprenoids Including Carotenoids and Steroids. D.E. Cane, editor. 2. Elsevier Science; Oxford 155-200.

107. Croteau, R. (1986) Evidence for the ionization steps in monoterpene cyclization reactions using 2-fluorogeranyl and 2-fluorolinalyl diphosphates as substrates. Arch. Biochem. Biophys. 251, 777-782.

108. Croteau, R., Alonso, W. R., Koepp, A. E. and Johnson, M. A. (1994) Biosynthesis of monoterpenes: partial purification, characterization, and mechanism of action of 1,8-cineole synthase. Arch. Biochem. Biophys. 309, 184-192.

109. Karp, F., Zhao, Y., Santhamma, B., Assink, B., Coates, R. M. and Croteau, R. B. (2007) Inhibition of monoterpene cyclases by inert analogues of geranyl diphosphate and linalyl diphosphate. Arch. Biochem. Biophys. 468, 140-146.

110. Chen, F., Tholl, D., D'Auria, J. C., Faroog, A., Pichersky, E. and Gershenzon, J. (2003). Biosynthesis and emission of terpenoid volatiles from Arabidopsis flowers. Plant Cell 15, 481–494.

111. Iijima, Y., Davidovich-Rikanati, R., Fridman, E., Gang, D. R., Bar, E., Lewinsohn, E. and Pichersky, E. (2004) The biochemical and molecular basis for the divergent patterns in the biosynthesis of terpenes and phenylpropenes in the peltate glands of three cultivars of basil. Plant Physiol. 136, 3724-3736.

112. Martin, D. M. and Bohlmann, J. (2004) Identification of *Vitis vinifera* (-)-alpha-terpineol synthase by in silico screening of full-length cDNA ESTs and functional characterization of recombinant terpene synthase. Phytochemistry 65, 1223-1229.

113. Rajaonarivony, J. I. M., Gershenzon, J. and Croteau, R. (1992) Characterization and mechanism of (4S)-limonene synthase, a monoterpene cyclase from the glandular trichomes of peppermint (*Mentha x piperita*). Arch. Biochem. Biophys. 296, 49–57.

114. Bohlmann, J., Phillips, M., Ramachandiran, V., Katoh, S. and Croteau, R. (1999) cDNA cloning, characterization, and functional expression of four new monoterpene synthase members of the Tpsd gene family from grand fir (*Abies grandis*). Arch. Biochem. Biophys. 368, 232–243.

115. Shimada, T., Endo, T., Fujii, H., Hara, M., Ueda, T., Kita, M. and Omura, M. (2004) Molecular cloning and functional characterization of four monoterpene synthase genes from *Citrus unshiu Marc*. Plant Sci. 166, 49–58.

116. McKay, S. A. B., Hunter, W. L., Godard, K. A., Wang, S. X., Martin, D. M., Bohlmann, J. and Plant, A. L. (2003) Insect attack and wounding induce traumatic resin duct development and gene expression of pinene synthase in Sitka spruce. Plant Physiol. 133, 368–378.

117. Croteau, R., Satterwhite, D. M., Wheeler, C. J. and Felton, N. M. (1989) Biosynthesis of monoterpenes – stereochemistry of the enzymatic cyclizations of

geranyl diphosphate to (+)-alpha-pinene and beta-pinene. J. Biol. Chem. 264, 2075–2080.

118. Croteau, R., Gershenzon, J., Wheeler, C. J. and Satterwhite, D. M. (1990) Biosynthesis of monoterpenes – stereochemistry of the coupled isomerization and cyclization of geranyl diphosphate to camphane and isocamphane monoterpenes. Arch. Biochem. Biophys. 277, 374–381.

119. Croteau, R. and Karp, F. (1977) Demonstration of a cyclic diphosphate intermediate in enzymatic conversion of neryl diphosphate to borneol. Arch. Biochem. Biophys. 184, 77–86.

120. Hoelscher, D. J., Williams, D. C., Wildung, M. R. and Croteau, R. (2003) A cDNA clone for 3- carene synthase from *Salvia stenophylla*. Phytochemistry 62, 1081–1086.

121. Phillips, M. A., Wildung, M. R., Williams, D. C., Hyatt, D. C. and Croteau, R. (2003) cDNA isolation, functional expression, and characterization of (+)- α -pinene synthase and (-)- α -pinene synthase from loblolly pine (*Pinus taeda*): stereocontrol in pinene biosynthesis. Arch. Biochem. Biophys. 411, 267-276.

122. Johnson, M. A. and Croteau, R. (1987) Biochemistry of conifer resistance to bark beetles and their fungal symbionts in Ecology and Metabolism of Plant Lipids. ACS Symp. Ser. 325, 76–92.

123. Petkewich, R. (2008), Beetle Epidemic Escalates. Chem. Eng. News 86, 36–37.

124. Blomquist, G. J., Figueroa-Teran, R. M., Song, M. M., Gorzalski, A., Abbott, N. L. Chang, E. and Tittiger, C. (2010) Pheromone production in bark beetles. Insect Biochem. Mol. Biol. 40, 699–712.

125. Etxebeste, I. and Pajares, J. A. (2011) Verbenone protects pine trees from colonization by the six-toothed pine bark beetle. Ips sexdentatus Boern. (Col.: Scolytinae), J. Appl. Entomol. 135, 258-268.

126. Phillips, M. A., and Croteau, R. B. (1999) Resin-based defenses in conifers, Trends Plant Sci. 5, 184-190.

127. Wender, P. A., and Mucciaro, T. P. (1992) A new and practical approach to the synthesis of taxol and taxol analogs: the pinene path. J. Am. Chem. Soc. 114, 5878–5879.

128. Kaufmann, D., Dogra, A. K. and Wink, M. J. (2001) Myrtenal inhibits acetylcholinesterase, a known Alzheimer target. Pharm. Pharmacol. 63, 1368–1371.

129. Selvaraj, M., Kandaswamy, M, Park, D. W. and Ha, C. S. (2010) Highly efficient and clean synthesis of verbenone over well ordered two-dimensional mesoporous chromium silicate catalysts. Catal. Today 158, 286–295.

130. Alonso, W. R., Rajaonarivony, J. I. M., Gershenzon, J. and Croteau, R. (1992) Purification of 4S-limonene synthasee, a monoterpene cyclase from the glandular trichomes of peppermint (*Mentha x piperita*) and spearmint (*Mentha spicata*). J Biol Chem. 267, 7582-7587.

131. McGeady, P. and Croteau, R. (1995) Isolation and characterization of an active-site peptide from a monoterpene cyclase labeled with a mechanism-based inhibitor. Arch. Biochem. Biophys. 317, 149-155.

132. McGeady, P., Pyun, H. J., Coates, R. M. and Croteau, R. (1992) Biosynthesis of monoterpenes: inhibition of (+)-pinene and (-)-pinene cyclases by thia and aza analogs of the 4R- and 4S-alpha-terpinyl carbocation. Arch. Biochem. Biophys. 299, 63-72.

133. Dudareva, N., Cseke, L., Blanc V. M. and Pichersky, E. (1996) Evolution of floral scent in Clarkia: novel patterns of S-linalool synthase gene expression in the *C. breweri* flower. Plant Cell 8, 1137-1148.

134. Bohlmann, J., Steele, C. L., and Croteau, R. (1997) Monoterpene synthases from grand fir (*Abies grandis*). cDNA isolation, characterization, and functional expression of myrcene synthase, (-)-(4S)-limonene synthase, and (-)-(1S,5S)-pinene synthase. J. Biol. Chem. 272, 21784-21792.

135. Williams, D. C., McGarvey, D. J., Katahira E. J. and Croteau, R. (1998) Truncation of limonene synthase preprotein provides a fully active 'pseudomature' form of this monoterpene cyclase and reveals the function of the amino-terminal arginine pair. Biochemistry 37, 12213-12220.

136. Phillips, M. A., Savage T. J. and Croteau, R. (1999) Monoterpene synthases of loblolly pine (*Pinus taeda*) produce pinene isomers and enantiomers. Arch. Biochem. Biophys, 372, 197-199.

137. Williams, D. C., Wildung, M. R., Jin, A. Q., Dalal, D., Oliver, J. S., Coates R. M., and Croteau, R. (2000) Heterologous expression and characterization of a "Pseudomature" form of taxadiene synthase involved in paclitaxel (Taxol) biosynthesis and evaluation of a potential intermediate and inhibitors of the multistep diterpene cyclization reaction. Arch. Biochem. Biophys. 379, 137-146.

138. Gunnewich, N., Page, J. E., Kollner, T. G., Degenhardt, J. and Kutchan, T. M. (2007) Functional expression and characterization of trichome-specific (-)-limonene synthase and (+)-alpha-pinene synthase from *Cannabis sativa*. Nat. Prod. Commun. 2, 223-232.

139. Colby, S. M., Alonso, W R., Katahira, E. J., McGarvey, D. J. and Croteau, R. (1993) 4S-limonene synthase from the oil glands of spearmint (*Mentha spicata*). cDNA isolation, characterization, and bacterial expression of the catalytically active monoterpene cyclase. J. Biol. Chem. 268, 23016-23024.

140. Agilent Technologies, Genomics, Agilent BL21-Codonplus Competent cells, Data sheet.

141. Burgess, R. R. (2009) Protein precipitation techniques. Methods in Enzymology (Guide to Protein Purification) 463, 331-342.

142. SAFC Biosciences, Technical Bulletin, Protein Purification Techniques, Volume 1.

143. Wise, M. L., Savage, T. J., Katahira, E. and Croteau, R. (1998) Monoterpene synthases from common sage (*Salvia officinalis*). cDNA isolation, characterization, and functional expression of (+)-sabinene synthase, 1,8-cineole synthase, and (+)-bornyl diphosphate synthase. J. Biol. Chem. 273, 14891-14899.

144. Bradford, M. M. (1976) A Rapid and Sensitive Method for the Quantitation of Microgram Quantities of protein Utilizing the Principle of protein-Dye Binding. Anal. Biochem. 72, 248-254.

145. Felicetti, B. and Cane, D. E. (2004) Aristolochene synthase: mechanistic analysis of active site residues by site-directed mutagenesis. J. Am. Chem. Soc. 126, 7212-7221.

146. Karp, F., Zhao, Y., Santhamma, B., Assink, B., Coates, R. M. and Croteau, R. B. (2007) Inhibition of monoterpene cyclases by inert analogues of geranyl diphosphate and linalyl diphosphate. Arch. Biochem. Biophys. 468, 140-146.

147. Stéphanie Heuskin, (2011) PhD thesis, Contribution to the study of semiochemical slow-release formulations as biological control devices. Academmie universitaire wallone-Europe universite de liege- Gembloux Agro Bio.

148. Zwenger, S. and Basu, C. (2008) Plant Terpenoids: Applications And Future Potentials. Biotechnol. Mol. Biol. Rev. 3, 1–7.

149. Schnee, C., Köllner, T. G., Held, T. C., Turlings, J., Gershenzon, J. and Degenhardt, J. (2006) The products of a single maize sesquiterpene synthase form a volatile defense signal that attracts natural enemies of maize herbivores. Proc. Natl. Acad. Sci. 103, 1129-1134.

150. Kessler, A. and Bladwin, I. T. (2002) Plant responses to insect herbivory: the emerging molecular analysis. Annu. Rev. Plant Biol. 53, 299-328.

151. Mann, R. S., Kaufman, P. E and Butler, J. F. (2010) Evaluation of semiochemical toxicity to houseflies and stable flies (Diptera: Muscidae). Pest. Manag. Sci. 66, 816-824.

152. Faraldos, J. A., Coates, R. B. and Giner, J. (2013) Alternative synthesis of the Colorado potato beetle pheromone. J. Org. Chem. 78, 10548-10554.

153. Kaufman, P. E., Mann R. S. and Butler, J. F. (2010) Evaluation of semiochemical toxicity to *Aedes aegypti*, *Ae. albopictus* and *Anopheles quadrimaculatus* (Diptera: Culicidae). Pest. Manag. Sci. 66, 497-504.

154. Raffa, K. F., Phillips, T. W., Salom S. M. In: Schowalter, T. D., Filip, G. (1993) Mechanisms and strategies of host colonization by bark beetles. Beetle pathogen interaction in conifer forests. Academic Press Ltd, London. 103-128.

155. Suh, Y. W., Kim, N. K., Ahn, W. S and Rhee, H. K. (2003) One-pot synthesis of campholenic aldehyde from α-pinene over Ti-HMS catalyst II: effects of reaction conditions. J. Mol. Catal. A: Chem. 198, 309–316.

156. Lajunen, M. K., Maunula, T. and Koskinen, A. M. P. (2000) Co(II) Catalysed Oxidation of α-Pinene by Molecular Oxygen. Part 2. Tetrahedron 56, 8167–8171.

157. Canepa, A. L., Herrero, E. R., Crivello, M. E., Eimer, G. A. and Casuscelli, S. G. (2011) H_2O_2 based ⟨-pinene oxidation over Ti-MCM-41. A kinetic study. J. Mol. Catal. A: Chem. 347, 1–7.

158. Selvaraj, M., Kandaswamy, M., Park, D. W. and Ha, C. S. (2010) Highly efficient and clean synthesis of verbenone over well ordered two-dimensional mesoporous chromium silicate catalysts. Catal. Today 158, 286–295.

159. Sivik, M. R., Stanton, K. J. and Paquette, L. A. (1995) (1R,5R)-(+)-verbenone of high optical purity [Bicyclo[3.1.1]hept-3-en-2-one-,4,6,6-trimethyl-,(1R)-]. Org. Synth. 72, 57–61.

160. Limberger, R. P., Aleixo, A. M., Fett-Neto, A. G. and Henriques, A. T. (2007) Bioconversion of (+)- and (-)-alpha-pinene to (+)- and (-)-verbenone by plant cell cultures of Psychotria brachyceras and Rauvolfia sellowii. Electron. J. Biotechno. 10, 500–507.

161. Pearson, A. J., Chen, Y. S., Han, G. R., Hsu, S. Y. and Ray, T. (1985) A new method for the oxidation of alkenes to enones. An efficient synthesis of Δ5-7-oxo steroids. J. Chem. Soc., Perkin Trans. 1, 267–273.

162. Christianson, D. W. (2006) Structural Biology and Chemistry of the Terpenoid Cyclases. Chem. Rev. 106, 3412–3442.

163. Wheeler, C. J. and Croteau, R. (1986) Terpene cyclase catalysis in organic solvent/minimal water media: demonstration and optimization of (+)-alpha-pinene cyclase activity. Arch. Biochem. Biophys. 248, 429-434.

164. Dunleavy, J. K. (2006) Sulfur as a Catalyst Poison. Platinum metal Rev. 50, 110-110.

165. Muzart, J. (1992) Chromium-catalyzed oxidations in organic synthesis. Chem. Rev. 92, 113–140.

166. Ling, M. M. and Robinson, B.H. (1997) Approaches to DNA mutagenesis: an overview. Anal Biochem. 254,157-178.

167. Antikainen, N. M. and Martin, S. F. (2005) Altering protein specificity: techniques and applications. Bioorg. Med. Chem. 13, 2701-2716.

168. Felicetti, B. and Cane, D. E. (2014) Aristolochene synthase: mechanistic analysis of active site residues by site-directed mutagenesis. J. Am. Chem. Soc. 126, 7212-7221.

169. Marrero, P. F., Poulter, C. D. and Edwards, P. A. (1992) Effects of site-directed mutagenesis of the highly conserved aspartate residues in domain II of farnesyl diphosphate synthase activity. J. Biol. Chem. 267, 21873-21878.

170. Hyatt, D. C. and Croteau, R. B. (2005) Mutational analysis of a monoterpene synthase reaction: altered catalysis through directed mutagenesis of (-)-pinene synthase from Abies grandis. Arch. Biochem. Biophys. 439, 222-233.

171. Kampranis, S. C., Ioannidis, D., Purvis, A., Mahrez, W., Ninga, E., Katerelos, N. A., Anssour, S., Dunwell, J. M., Degenhardt, J., Makris, A. M., Goodenough, P. W. and Johnson, C. B. (2007) Rational conversion of substrate and product specificity in a Salvia monoterpene synthase: structural insights into the evolution of terpene synthase function. Plant Cell 19, 1994,

172. Yu, F., Miller, D. J. and Allemann, R. K. (2007) Probing the reaction mechanism of aristolochene synthase with 12,13-difluorofarnesyl diphosphate. Chem. Commun. 4155-4157.

173. Allemann, R. K. (2008) Chemical wizardry? The generation of diversity in terpenoid biosynthesis. Pure Appl. Chem. 80, 1791.

174. Faraldos, J. A., Antonczak, A. K., Gonzalez, V., Fullerton, R., Tippmann E. M. and Allemann, R. K. (2011) Probing eudesmane cation-π interactions in catalysis by aristolochene synthase with non-canonical amino acids. J. Am. Chem. Soc. 133, 13906-13909.

175. Deligeorgopoulou, A., Taylor, S. E., Forcat, S. and Allemann, R. K. (2003) Stabilisation of eudesmane cation by tryptophan 334 during aristolochene synthase catalysis. Chem. Commun. 2162-2163.

176. Deligeorgopoulou, A. and Allemann, R. K. (2003) Evidence for differential folding of farnesyl pyrophosphate in the active site of aristolochene synthase: a single-

point mutation converts aristolochene synthase into an (E)-beta-farnesene synthase. Biochemistry 42, 7741-7747.

177. I-Tasser Online, Version 4.1, Zhang Lab, University of Michigan.

178. Theoretical and computational Biophysics group, VMD 1.9, University of Illinois at Urbana-Champaign.

179. Gennadios, H. A., Gonzalez, V., Costanzo, L. Di., Li, A., Yu, F. L., Miller, D. J., Allemann, R. K. and Christianson, D. W. (2009) Crystal structure of (+)-delta-cadinene synthase from *Gossypium arboreum* and evolutionary divergence of metal binding motifs for catalysis. Biochemistry 48, 6175-6183.

180. Bradford, M. M. A. (1976) Rapid and sensitive method for the quantitation of microgram quantities of protein utilizing the principle of protein-dye binding. Anal. Biochem. 72, 248-254.

181. Cramer, F. and Böhm, W. (1959) Synthese von Geranyl- und Farnesyl-pyrophosphat. Angew. Chem. 71, 775-776.

182. Davisson, V. J., Woodside, A. B., Neal, T. R., Stremler, K. E., Muehlbacher, M. and Poulter, C. D. (1986) Phosphorylation of Isoprenoid Alcohols. J. Org. Chem. 51, 4768-4779.

183. Jin, Y., Roberts, F. G. and Coates, R. M. (2007) Stereoselective Isoprenoid Chain Extension With Acetoacetate Dianion: (E, E, E) Geranylgeraniol from (E, E)-Farnesol. Synthesis 84, 43-57.

184. Turek, T. C., Gaon, I. and Distefano, M. D. (2001) Synthesis of Farnesyl Diphosphate Analogues Containing Ether-Linked Photoactive Benzophenones and Their Application in Studies of Protein Prenyltransferases, J. Org. Chem. 66, 3253-3264.

185. Barrero, A. F. and Herrador, M. M. (2007) Mild TiIII- and Mn/ZrIV-catalytic reductive coupling of allylic halides: efficient synthesis of symmetric terpenes. J. Org. Chem. 72, 2988-2995.

186. Acelrod, E. H. and Milne, G. M. (1970) J. Am. Chem. Soc. 92, 2139-2141.

187. Chehade, K. A., Andres, D. A., Morimoto, H. and Spielmann, H. P. (2000) Design and synthesis of a transferable farnesyl pyrophosphate analogue to Ras by protein farnesyltransferase. J. Org. Chem. 65, 3027-3033.

188. Omura, K. and Swern, D. (1978) Oxidation of alcohols by "activated" dimethyl sulfoxide. A preparative, steric and mechanistic study. Tetrahedron 34,1654-1660.

189. Maryanoff, B. E. and Reitz, A. B. (1989) The Wittig olefination reaction and modifications involving phosphoryl-stabilised carbanions. Chem. Rev. 89, 863-927.

190. Halpern, J. and Wong, C. S. (1973) Hydrogenation of tris (triphenylphosphine) chlororhodium (I). J. Chem. Soc., Chem. Commun. 629-632.

191. Mague, J. T. and Wilkinson, G. (1966) Tris(triphenylarsine)- and tris(triphenylstibine)-chlororhodium(I) complexes and their reactions with hydrogen, olefins, and other reagents, J. Chem. Soc. A. 1736-1740.

192. Miyashita, N., Yoshikoshi, A. and Grieco, P. A. (1977) Pyridinium p-Toluenesulfonate. A Mild and Efficient Catalyst for the Tetrahydropyranylation of Alcohols. J. Org. Chem. 42, 3772-3774.

193. Sum, F. W. and Weiler, L. (1979) Stereoselective Synthesis of β-Substituted α, β-Unsaturated Esters by Dialkylcuprate Coupling to The Enol Phosphate of β-Keto Esters. Can. J. Chem. 57, 1431-1441.

194. Guss, C. O. and Rosenthal, R. (1955) Bromohydrins from olefins N-bromosuccinimide in water. J. Am. Chem. Soc. 77, 2549–2549.

195. Jerry. M. (1985) Advanced Organic Chemistry: Reactions, Mechanisms, and Structure (3rd ed.), New York: Wiley.

196. Still, W. and Gennari, C. (1983) Direct synthesis of Z-unsaturated esters. A useful modification of the horner-emmons olefination. Tetrahedron Letters 24, 4405-4408.

197. Schomaker, J. M. and Borhan, B. (1955) Total Synthesis of Haterumalides NA and NC via a Chromium-Mediated Macrocyclization. J. Am. Chem. Soc. 77, 2549–2549.